A review on the current status of various hydrothermal technologies on biomass feedstock

Mayank Kumar, Adetoyese Olajire Oyedun, Amit Kumar[1]

Department of Mechanical Engineering, 10-263 Donadeo Innovation Centre for Engineering, University of Alberta, Edmonton,

Alberta T6G 1H9, Canada

Abstract

Hydrothermal processing, a thermochemical approach, is an excellent method of converting energy-rich biomass into useful products. This approach offers the advantage of handling biomass with relatively high moisture content by precluding an energy-intensive pretreatment step. Hydrothermal processing is of world-wide interest in view of depleting fossil-fuel reserves and increased environmental greenhouse gas emissions. There is potential to develop this novel technology at demonstration scale. This paper reviews the three hydrothermal technologies, namely hydrothermal liquefaction, gasification and carbonization, to provide insight into the likelihood of commercialization. The study discusses the role of different process parameters that have key impacts on the quality and yield of the desired products. This study also identifies the gaps in the literature including the need to establish a baseline to develop key process models and to perform a techno-economic assessment to get a better sense of the viability of the technology in future.

---

[1] Corresponding author. Tel.: +1-780-492-7797
E-mail address: Amit.Kumar@ualberta.ca (A. Kumar).

Keywords: Hydrothermal conversion; hydrothermal liquefaction; hydrothermal gasification; hydrothermal processing; biomass.

1. Introduction

Increasing energy demands related to increasing population, rapid industrialization, and stringent environmental regulations call for alternative routes of energy production, as conventional energy derived from fossil fuels cause severe environmental harm through the release of greenhouse gas emissions. Moreover, the imbalance in supply and demand makes it inevitable that substitutes for conventional energy sources are needed [1]. Biomass refers to biological matter or waste obtained from living organisms that has solar energy stored in it. It is deemed to be a potential energy source [2, 3] and is considered to be inexpensive, clean, and environmentally friendly. Biomass wastes include plants or plant-based wastes, municipal wastes, industrial wastes, animal wastes, and household wastes. Due to its renewability and sustainability, biomass waste could become a viable alternative source of energy and, moreover, is expected to provide 25 % of the world's energy demand [4]. Biomass with high moisture content is not economical to process by conventional technologies, as a significant amount of energy goes into the drying process. Hydrothermal processing is efficient as it eliminates the costly drying step, thereby making it attractive. The energy required for drying exceeds that used for hydrothermal processing at supercritical conditions for biomass with a moisture content of 30 % or greater [5].

Hydrothermal processing is a thermochemical process that involves thermal disintegration of biomass in hot compressed water, wherein a series of complex reactions causes changes in the water's physical properties (i.e., its density, solubility, and dielectric constant) [6]. The process converts biomass into a solid (bio-char), a liquid (bio-oil or bio-crude), or a gas (e.g., hydrogen, methane). The process also leads to byproducts that can be used for power generation and the recovery of useful nutrients [7]. The desired products are obtained by manipulating variables such as temperature, pressure, catalyst, and time [8]. Of late, hydrothermal processing technologies have been the subject of major research for a range of biomass types including agricultural wastes and algae [9, 10]. There are many challenges facing the commercialization of these technologies, including expensive and complex reactors [11] that require high capacity water handling equipment [9]. Overall poor understanding of mass balance further make it difficult to accurately measure product yields during the hydrothermal run [12]. The hydrothermal processes (carbonization, liquefaction, and gasification) illustrated in Figure 1 are based on data from Kruse et al. and Toor et al. [13, 14].

Thermochemical processing technologies have been used since 1788 to convert biomass to bio-crude [15]. They are gaining widespread interest as a means of catering to energy demands and tackling growing environmental concerns related to increasing global warming and decreasing fossil fuel reserves.

Hydrothermal processing can produce energy-dense fuels and valuable chemicals. The process allows efficient heat integration and thus takes into account the energy penalty due to water valorization from hydrothermal media [16]. The hydrothermal processing such as liquefaction and gasification produces an aqueous phase. The residual carbon of the aqueous phase can be used to produce biogas through anaerobic digestion. The gas thus produced can be used for heat and to generate electricity through a combined heat and power generation system and, therefore, the hydrothermal process coupled with anaerobic digestion allows a useful use of energy, thereby reducing energy requirements in the process [17, 18]. With that said, the use of organics in the aqueous phase is also a way to reduce the operating costs of the hydrothermal technology, as using organics helps reduce wastewater treatment costs. In the case of algal feedstocks, the aqueous phase has biogenic carbon, phosphorous, nitrogen, and micronutrients that can be recycled for algal cultivation purposes. In addition, high value chemicals such as ethanol, acetone, and acetic acid can be obtained through extraction and catalytic processes [19]. Furthermore, a pinch analysis can be used to optimize the process by identifying intensive heat streams, i.e., heat can be recovered and used in the process to make hydrothermal technology more economical [20, 21]. Considerable improvements in homogeneous and heterogeneous catalysts, including metallic catalysts, have led to major advancements in hydrothermal processing technologies [22].

Figure 1

Hydrothermal processing operates in one of two states: subcritical and supercritical. The states are defined with respect to the critical point of water (T_c = 373 °C, p_c = 22.1 MPa). The hydrothermal process commences with the dispersion of the water-soluble part of biomass into water at 100 °C followed by subsequent hydrolysis above 150 °C, causing the disintegration of the cellulosic and hemicellulosic fractions of biomass into its monomeric chains. Then, slurry forms at 200 °C under 1 MPa and proceeds towards either liquefaction or gasification depending on the desired product [8]. The first study on supercritical water gasification was published by Modell [23], who used maple wood sawdust as a feedstock. Research efforts have been underway in this promising field for a long time, and hydrothermal technology research has had a sudden upsurge in publications that show the technology's potential for biomass conversion. However, existing knowledge is disconnected, and this review aims at collecting and analyzing the existing experimental studies on hydrothermal technologies. It is challenging to establish the research findings due to the variations that arise from different types of feedstock and reaction environments. Hydrothermal technology processes, along with process parameters needs, need to be understood. Hence, the overall objective of this paper is to conduct a review of the hydrothermal processing of biomass feedstocks. The specific objectives are:

- To review and summarize hydrothermal liquefaction processes and discuss operating parameters that have a major impact on the processes
- To review and detail the experimental studies on the catalytic hydrothermal liquefaction process of different biomass feedstocks
- To review and analyze the reaction mechanisms of the hydrothermal gasification process and study the operating parameters
- To review and illustrate the experimental studies on the catalytic hydrothermal gasification process of different biomass feedstocks
- To study and provide a brief account of experimental studies on the hydrothermal carbonization of biomass feedstock
- To identify the gaps in knowledge and economic bottlenecks relevant to the large-scale commercialization of hydrothermal technologies

1.1 History of hydrothermal processing

There is great potential in continuous process hydrothermal technology for large-scale commercial conversion of wet biomass to energy-rich fuels and chemicals [24, 25]. When biomass is subjected to hydrothermal conditions, water molecules cause the degradation of the larger molecules in biomass into smaller fragments. During the 1970s and 1980s, early research efforts on hydrothermal processing were undertaken at the Pittsburgh Energy Research Center; there, the technology was based on the process of lignite coal liquefaction [26]. Then it was discovered by researchers at the Lawrence Berkeley Laboratory [27] and Biomass Liquefaction in Albany [28]. The processes developed at the Pittsburgh Research Center and the Lawrence Berkeley Laboratory varied with respect to pre-treatment methods and post-conversion processes; that is, the former used drying and grinding whereas the latter used acid hydrolysis [29]. In the Netherlands, Shell developed a hydrothermal upgrading unit for biomass liquefaction [30]. NextFuels in Asia is in the process of developing a commercial hydrothermal liquefaction facility based on a daily production scale of 1000 barrels of oil from palm oil wastes [31]. A Danish company developed CatLiq, which processes sewage sludge including algae and manure [32]. All of these initiatives led to the formation of companies like Steeper Energy, which, in collaboration with Aalborg University, is developing a commercial technology [33]. Changing World Technologies was being known to be developing a commercial HTL plant to convert turkey waste to oil through thermal de-polymerization [34]. Unfortunately, Changing World Technologies suffered from bankruptcy and was purchased by Ridgeline Energy Services in Canada [35, 36]. Early investigations into hydrothermal liquefaction were carried out at the University of Toronto (Canada), the University of Arizona (USA), and the Royal Institute of Technology (Sweden) [26]. This research focused mainly on terrestrial biomass feedstock and later on algal feedstocks. The interest in HTL-based technologies remains a key driver for the production of fuels and chemicals towards an HTL bio-refinery concept.

The concept of hydrothermal gasification was initially proposed by Modell's group in a report published by the Massachusetts Institute of Technology (USA) [37]. Modell and coworkers performed supercritical water decomposition of glucose and then applied this novel technology to test hazardous organic wastes in supercritical water. They also studied oxidation in supercritical water, referred to as supercritical water oxidation (SCWO), to gain an understanding of the technology [38]. Following Modell's research, the Pacific Northwest National Laboratory (USA) developed a technology featuring the application of metal catalysts at low temperatures (400 ˚C) [39, 40]. Later, a research group at the University of Hawaii developed a technology based on high temperatures (600 ˚C) using a carbonaceous catalyst [41, 42]. This led teams of scientists and researchers from other research centers and universities such as the Karlsruhe Research Center [43], Hiroshima University [44], the University of Michigan [45], the University of Leeds [46] and elsewhere to contribute to research efforts.

The concept of hydrothermal carbonization, initially suggested by Friedrich Bergius as early as 1913, simulated a natural coalification technique [47]. The process later became known as the hydrothermal degradation of organics for the production of fuels and chemicals [48, 49]. The burgeoning number of publications in hydrothermal processing technology shows the interest world-wide in research in this area.

1.2 Biomass: a possible future energy source

Biomass, an abundant source of renewable energy, is often composed of organic substances derived from carbon, hydrogen, and oxygen. The substances are categorized based on a range of sources such as trees, algae, grass, urban wastes, agricultural wastes, forestry wastes, domestic wastes, municipal wastes, and industrial wastes [50-52]. Biomass contributes 10-14 % of world-wide energy demand [53]. It is usually a heterogeneous mixture of organic substances together with a small amount of inorganic substances. On a dry basis, biomass has typically 30-40 % oxygen, 30-60 % carbon, and 5-6 % hydrogen, depending on ash content. Other inorganic elements include nitrogen, chlorine, and sulfur, which together make up < 1 % of the biomass. Broadly, biomass is composed of cellulose, hemicellulose, lignin, and extractives including proteins, ash, and pectin [54, 55]. The carbohydrate portion of the biomass is the cellulose and the hemicellulose, and the non-carbohydrate portion is made up of lignin [1]. Cellulose, $(C_6H_{10}O_5)_n$, is an abundant natural polymer formed by β-1,4 glycosidic linkage of D-glucopyranose units that are held together by strong intra and inter molecular hydrogen bonds [56]. Cellulose, being crystalline, is insoluble in water and resistant to enzymatic attack. However, it rapidly decomposes and dissolves under subcritical and supercritical conditions of water. Hemicellulose, a hetero-polysaccharide, is an amorphous polymer formed by the branching of a straight chain skeleton of xylan and gulucomannan [57]. It is composed of monomers of D-glucopyranose, D-mannopyranose, D-galactopyranose, D-xylopyranose, and L-arabinofuranose [58] and constitutes 20-40 % of biomass. It is linked to cellulose and lignin via hydrogen and covalent bonding, respectively. It is less crystalline because of its non-uniformity and the presence of side groups. It is easily hydrolyzed by an acid or a base at temperatures above 180 °C [48]. The third component, lignin, is an aromatic compound of *p*-hydroxyphenylpropanoid units in which hydroxyl and methoxy bonds are linked through ether bonds [5]. Lignin is composed of basic building blocks of molecules such as trans *p*-coumaryl alcohol, coniferyl alcohol, and sinapyl alcohol [48]. It is hydrophobic and resistant to biological degradation. It has a higher heating value than cellulose and hemicellulose [59]. Extractives in biomass are made up of other heterogeneous materials including inorganic and organic compounds, proteins, fatty acids, phenols, resins, and terpenes [58, 60]. Extractives make up < 2% of the dry matter and accounts for its color, odor, and durability [57, 58] and can be extracted by various polar or non-polar solvents [57]. Biomass is widely used as a source of fuel, energy, and chemicals [2]. The selection of biomass for a particular energy conversion technology depends on the nature and composition of the biomass [2].

2. Water: a boon for hydrothermal processing

Water is regarded as an environmentally innocuous medium for most organic reactions. It exists in three phases: solid, liquid, and gas. Below water's critical point, the vapor pressure curve separating the liquid and vapor phase ends at the critical point ($T_c = 373$ °C, $p_c = 22.1$ MPa). Beyond the critical point, the properties of water can be changed without any phase transition. The supercritical state (SC) refers to the zone of high temperature and pressure at the critical point at which water acts as both a reactant and a catalyst. At this condition, properties such as the ionic product, density, viscosity, and dielectric constant of water show quick variations. Supercritical water (SCW) is an excellent solvent for most homogeneous organic reactions owing to high miscibility and the absence of any phase boundaries. It acts as a "nonpolar" solvent and has a dipole moment of 1.85 D. The dipole moment is a measure of the ability of the solvent to form dipoles. Water in the supercritical state is able to react with different compounds. As shown in Figure 2, the dielectric constant, a gauge of hydrogen bond effectiveness is 80 at normal temperature and pressure and reduces substantially to 5 at the critical point, which is typical of a non-polar solvent [36]. This is usually due to the reduction in ordered hydrogen bonds per molecule of water with the increase in temperature. As a result, the affinity of water towards hydrophilic molecules increases [61]. This change in the dielectric constant of water makes water a suitable medium for solvating organic molecules, which causes reactions to occur in a single phase, leading to higher reaction rates due to improved nucleophilic substitutions and eliminations [62], and subsequent hydrolysis reactions [63]. However, the phase transition of water to its organic form causes the precipitation of salts due to its decreased solubility, which often results in clogging issues. The organic reactions that take place in acidic/alkaline pH occur in a neutral condition in sub-critical water [64]. Similarly, water viscosity tends to decrease with an increase in temperature, leading to a higher diffusion coefficient and mass transfer.

The ionic product of water (K_w) initially increases from 10^{-14} mol^2 L^{-2} at 25 °C to ~ 10^{-11} mol^2 L^{-2} at 300 °C, beyond which it drops sharply below 10^{-20} mol^2 L^{-2} at the supercritical point [65, 66]. The initial increase in K_w proliferates [H^+] and [OH^-]. This promotes heterolytic cleavage of aromatics and catalyzes acid/base reactions [67]. Delocalization of p-electrons, owing to the substitution of hydroxyl groups, causes instability and benzene ring cleavage [68]. The further decline in K_w is attributed to the decrease in density that leads to accelerated free radical reactions [69].

Figure 2

The role of water in hydrothermal processing cannot be underestimated. At high temperature, free-radical mechanism proceeds via two phases. The first phase is an induction period wherein a radical pool is generated. The second phase involves free-radicals reactions. Both phases depend on process variables [68]. Low water density supports the free-radical reaction; however, high water density dictates the ionic reaction mechanism [69]. Hydrolysis releases catalytic acid or alkali from water and salt [70, 71]. The protons released at high temperature and pressure generate alkyl and C–N radicals and cause ring opening of heterocyclic compounds [72]. Water at a supercritical state shows the intermediate behavior of a liquid and a gas. The physico-chemical properties of water with respect to temperature, summarized in Table 1, are obtained from Tekin et al. and Onwudili and Williams [53, 73].

Table 1

3. Effects of hydrothermal processing on biomass

Many studies focus on simple model compounds rather than real biomass to circumvent problems associated with the heterogeneity and complexity of biomass. Glucose and xylose used as a model for cellulose and hemicellulose, respectively, while phenol is used to model lignin, as cellulose, hemicellulose and lignin are the main constituents of lignocellulose fractions. A few studies have used methanol in models for alcohol and others have used 5-hydroxymethylfurfural (5-HMF), an intermediate for glucose gasification. Cellulose is the main component in lignocellulosic biomass fractions and mostly yields glucose [74]. The hemicellulosic fraction is made up of five-membered carbons such as xylose and arabinose and six-membered sugar units like glucose, mannose, and galactose, which may be substituted with phenolics, uronics, and acetyl groups [75]. Hemicellulose easily undergoes hydrolysis into oligosaccharides, monosaccharides, and other products like furfural, hydroxymethylfurfural, and acetic acid via hydrothermal processing [76]. Similarly, xylan, a building block of hemicellulose, can be broken into xylose oligosaccharides and intermediates that can be used as prebiotics, making them a highly valuable nutritive [77-80]. The xylose oligosaccharides do not act as a direct source of nutrients for microorganisms and thus require further breakdown into simple monosaccharides, by a chemical or enzymatic approach, to be used as a medium for the production of xylitol [81-83], a reduced precursor of xylose.

Hydrothermal processing has also been used for the production of lactic acid [84] and xylanases [85]. Improvements in the recovery and purification of xylose oligosaccharides through hydrothermal processing have been achieved by using active carbons [86] and ultra or nano filtration membranes [87] and reactor configurations [88-90]. As discussed above, lignin and other heterogenic polymers of phenolics are made up of p-coumaryl, coniferyl, and sinapyl alcohols with the aromatic groups p-hydroxyphenyl, guaiacyl and syringyl [91, 92]. Hydrothermal processing is supposed to re-localize lignin on the surface of biomass, thereby improving the accessibility of enzymes for hydrolysis [93-95]. Lignin components are usually depolymerized through a series of reactions involving degradation and re-localization, the degree of which depends on process conditions [96, 97]. The mechanism of lignin breakdown involves the fast cleavage of lignin-carbohydrate bonds into low molecular weight and highly reactive lignin fragments that undergo gradual re-condensation and re-polymerization in the presence of organic acids [96, 98]. The release of soluble lignin is quantitatively determined at an ultraviolet (UV) absorbance of either 205 or 280 nm, due to its aromaticity [99, 100]. Phenolics, byproducts of lignin degradation, are natural antioxidants and food additives [101, 102]. Guaiacol (G) units of lignin are known to produce vanillin, vanillic acid, dihydroconiferyl alcohol, and guaiacol [103]; syringaldehyde, syringic acid and sinapaldehyde are usually obtained from syringyl (S) units of lignin [104].

4. Hydrothermal liquefaction

Hydrothermal liquefaction (HTL) involves the thermochemical conversion of a broad range of biomass types in the presence of hot compressed water at subcritical conditions into a liquid product known as bio-oil [14, 105-124]. HTL requires an operating temperature of 300-350 °C at 5-20 MPa for 5-60 min, wherein water is in the liquid phase [125]. The process begins with solvolysis of biomass in micellar forms, the disintegration of biomass fractions (cellulose, hemicellulose, and lignin), and thermal depolymerization into smaller fragments [126, 127]. HTL, which mimics the processing of fossil fuels buried deep inside the earth, occurs in minutes or hours [128]. HTL produces oil with low oxygen content as opposed to other processes like fast pyrolysis. HTL proves to be very energy efficient as it entails temperatures lower than those reached during pyrolysis [129, 130].

The process is driven by a complex set of reactions and transformations in subcritical water. The process mechanism involves the hydrolysis of biopolymers into water-soluble oligomers followed by the breakup of intramolecular and intermolecular hydrogen bonds into simple monomers like glucose and other products such as acetaldehyde, acetic acid, and furfural compounds [129]. Hemicellulose is easily susceptible to hydrolysis around 180 °C [48]. Xylose, a component of hemicellulose, may exist either in pyranose, furanose, or open chain form. The furfural is believed to form a pyranose ring structure while formic acid and glyceraldehyde form an open structure [129]. Lignin decomposes to phenolics in hydrothermal media [131]. During the hydrothermal run, the oxygen content of the organics decreases from about 40 % to 10-15 % [132]. Oxygen is removed in the form of a gas such as CO_2, CO, CH_4, and H_2. Along with gases, an aqueous fraction of water and other small organics are formed. The products from liquefaction processes have fewer process conditions and the resulting products can be safely stored and transported [133]. Srokol and coworkers observed that the acid-catalyzed reactions result in a 5-hydroxymethylfurfural via dehydration while base-catalyzed reactions produce glyeraldehyde, which could further break down into lactic acid, formic acid, acetic acid, etc.

Figure 3 (A) depicts plausible pathways of bio-oil via hydrothermal liquefaction from polysaccharides [134]. Polysaccharides are made of pentoses and hexoses bound together by glycosidic bonds [135]. The degradation products of polysaccharides comprises of low molecular weight compounds such as phenols, ketones, aldehydes and acids out of which cyclic ketones constitute nearly 50%

[134]. During hydrothermal liquefaction, polysaccharides undergo hydrolysis into monosaccharides, which further undergoes isomerization, cyclization and dehydration to produce phenols or cyclic ketones. Carbohydrates are known to form aromatics through ring opening and subsequent reactions involving cyclization and condensation [136]. Similarly, the plausible decomposition of proteins into bio-oil are summarized in Figure 3 (B) [134]. The nitrogen-containing compounds are the major ones which consist of pyrroles, pyrazines, and amines. Proteins undergoes hydrolysis into amino acids which then either proceeds decarboxylation to produce carbonic acid and amines or deamination reaction into ammonia and organic acids [16]. The resulting molecules results in pyrazine, pyrrole, indoles and aromatic amides molecules via cyclization and condensation [137].

Figure 3

As shown in Figure 4, the formation of polycyclic nitrogenous compounds involves Maillard reactions between reducing sugars and amino acids, obtained from carbohydrates and proteins hydrolysis, respectively [138]. The formation of Melanoidin-like polymers in Maillard reactions occurs at low temperature of 260 °C, which does not favor the formation of bio-oil [118, 138]. With an increase in temperature, the Melanoidin-like polymers decompose and turn into monocyclic compounds like pyrazines and pyrroles, thereby improving bio-oil yield [138].

Figure 4

Conditions such as temperature [21, 139-153], pressure [154-157], particle size [158], and reaction times [21, 159-171] influence the conversion of biomass into bio-oil. Temperature improves fragmentation and lignocellulosic fraction cleavage and has a considerable effect on product yield. It is imperative to overcome the energy barrier and use sufficient activation energy for biomass breakup to achieve higher concentrations of free radicals. Biomass liquefaction is usually endothermic at low temperatures and becomes exothermic at high temperatures [172]. As a result, bio-oil yield increases with temperature and reaches a point where a further rise in temperature suppresses liquefaction. Reduced bio-oil yield could also be due to the dominating secondary decomposition and Bourdard gas reactions [173] along with the recombination effects of high concentrations of free radicals into char. At moderately low temperatures (< 275 °C), bio-oil yield also shows a decline due to the partial breakdown of biomass components. Thus, it is believed that an intermediate temperature range of 300-350 °C will likely result in a higher bio-oil yield [174-176].

Pressure is another crucial factor in the hydrothermal liquefaction process as it helps maintain water in the liquid state and thus incur savings by avoiding the high energy costs of a two-phase system [30]. An increase in pressure results in the effective penetration and extraction of biomass. However, pressure becomes insignificant and has little impact on liquid oil near or at supercritical water liquefaction reaction conditions [155, 156, 177]. It should to be noted that a further elevation of pressure under supercritical conditions results in higher local solvent density, which prevents C-C bond fragmentation. Residence time affects product composition and hydrothermal liquefaction conversion efficiency [161, 178]. As degradation under supercritical conditions occurs rapidly, it is often desirable to have short residence times [179]. This is because the dominating secondary and tertiary reactions in a temperature reaction medium form liquids or gases from heavy intermediates and thus decrease bio-oil yield [172]. So, bio-oil attains maximum yield, after which it declines with further increases in residence times [180].

The nature of biomass feedstock affects bio-oil yield due to differing biomass compositions. Hemicellulose and cellulose increase bio-oil yield while lignin goes into the residue fraction [181] because hemicellulose, being amorphous, is easily susceptible to degradation, and cellulose, with a relatively intermediate degree of polymerization, also tends to degrade; however, lignin's decomposition is limited by its high degree of polymerization and complex interlinkage [129].

The biomass type also affects the nature of the bio-oil. Loosely packed biomass liquefaction results in bio-oil with high oxygen and moisture content that is undesirable as it lowers the quality and HHV of the fuel [172]. Small particle size improves accessibility and penetration of heat, thereby improving conversion rate and bio-oil efficiency. As grinding to the smallest possible size may increase costs, it is better to have a standard particle size of 4-10 mm for the hydrothermal run [172]. A summary of the factors influencing the hydrothermal liquefaction of biomass is presented in Table 2.

Table 2

4.1 Catalytic hydrothermal liquefaction

4.1.1 Homogeneous catalysts

The use of catalysts in hydrothermal liquefaction processes is intended to improve process efficiency by reducing char and tar formation. Two types of catalysts, homogeneous and heterogeneous, are reported in the literature and are summarized here.

Homogeneous catalysts comprise alkali salts such as Na_2CO_3, K_2CO_3 and $KHCO_3$ [140, 142, 182-203]. Alkali salts reduce char/tar formation and improve product yield by accelerating the water–gas shift reaction. They are economical to use for hydrothermal technologies. The working mechanism involves the formation of esters through the decarboxylation reaction between the hydroxyl groups in biomass and the formate ions in alkali carbonates. Ester formation is followed by a series of reactions, i.e., dehydration, deoxygenation, decarboxylation, and the dehydrogenation of micellar-like fragments into smaller ones. This is followed by a cycle of rearrangements through cyclization, polymerization, and condensation [204]. Karagöz et al. [205] suggested that potassium salts are more catalytically active than other salts ($K_2CO_3 > KOH > Na_2CO_3 > NaOH$). Along with these salts, other catalysts in the form of acids and gases have been used [206]. With homogeneous catalysts, there are some advantages: decreased solids production, increased bio-crude yield, and improved bio-crude properties. Moreover, the incorporation of alkali salts in the hydrothermal media elevates pH, thereby decreasing dehydration reactions, which usually lead to unstable unsaturated molecules [207]. With NaOH, less char is produced [198]. This is because the OH^- neutralizes the molecules causing polymerization in char formation. The polymerization reaction between the hydroxyl groups at the residue surface and the carboxylic groups in the aqueous stream produces ester bonds, which form char. Hence, NaOH cannot cause polymerization, due to the neutralization of carboxylic acids. As a result, NaOH's participation is restricted in condensation reactions [176].

A recent publication discussed the use of catalysts such as colemanite and borax for the hydrothermal processing of biomass [208]. According to the study, a borax catalyst is effective to 300 ˚C, and colemanite is much more effective than borax.

Table 3

4.1.2 Heterogeneous catalysts

As discussed, homogenous catalysts such as NaOH, Na_2CO_3, and KOH have been widely used for the catalytic HTL of biomass. Homogenous catalyst recovery is expensive due to the cost-intensive separation process and is energy intensive. Although heterogeneous catalysts are used mostly in hydrothermal gasification, a few reports have discussed the hydrothermal liquefaction of lignocellulosic biomass to improve bio-crude quality. Some gasification is needed to remove oxygen; however, prolonging it could reduce bio-oil yield.

Heterogeneous catalysts include platinum, nickel, and palladium. As these metals are rare, there has been shift of focus to metallic oxides, i.e., zirconium dioxide (ZrO_2) [158, 209-211]. Apart from these catalysts, studies on catalytic hydrothermal liquefaction have used alkali catalysts, which improve bio-oil yield. Other known metal oxide catalysts include MnO, MgO, NiO, ZnO, CeO_2, La_2O_3, etc. [212-214]. Nanocatalysts involving use of Ni have been tested as they have the potential to improve bio-oil yield at low temperatures, which could help in the commercialization of HTL [215]. Reductive noble metal catalysts such as Pt and Ru are expensive; therefore, an attempt has been made to use a CuZnAl catalyst, which has the potential to covert furfural into cyclopentanone via hydrogenation and hydrogenolysis [216]. Moreover, the activity of such catalysts can be modified by varying Cu or Zn oxide and allows recycling through reactivation in H_2 gas environment. Zeolite has been cited as a catalyst for the hydrothermal liquefaction of biomass [194].

The transition metal improves the quality of bio-oil [217]. However, in order to avoid the deactivation of catalysts during a hydrothermal run, catalysts showing high hydrothermal stability are important. Keeping in mind industrial applications, carbonaceous materials such as carbon nanotubes (CNTs) using activated carbon as a support for metallic catalysts are suitable because they can provide a large surface area and recycle noble metals [218, 219].

The use of carbon nanotubes (CNT)-supported transition metals for the catalytic HTL of biomass into bio-oil has also been studied [220]. Apart from catalysts, studies have considered co-solvents, which scavenge unsaturated molecules that form through dehydration and that may otherwise be re-polymerized. The most commonly used organic solvents are methanol, butanol, phenol, acetone, and propylene glycol [221-225]. Another study on the use of transition metal chlorides ($ZnCl_2$, $CuCl_2$, and $NiCl_2$) for subcritical hydrothermal liquefaction has also been performed [226].

Table 4

5. Hydrothermal gasification

Hydrothermal gasification is a process that involves a reaction temperature above 350 °C in the absence of oxidants and produces a flue gas rich in either H_2 or CH_4, depending on reaction conditions [227]. HTG is done in either batch or continuous mode. The batch process offers the advantage of carrying out experiments at different concentrations and catalysts, while the continuous system allows for studies of reaction kinetics. Hydrothermal gasification has three main types: aqueous phase refining, catalytic gasification in a near-critical state, and supercritical water gasification. Aqueous phase refining occurs at low concentrations at ~ 215-265 °C to produce H_2 and CO_2 in the presence of a heterogeneous catalyst [228, 229]. The process is not desired unless hydrogen is used *in situ* for the hydrogenation of biomass [230]. Catalytic gasification of biomass in a near-critical state occurs at 350–400 °C and produces CH_4 and CO_2 in the presence of a heterogeneous catalyst wherein CO undergoes hydrogenation to CH_4 [231-234]. This process was first performed in a batch reactor at Battelle Memorial Institute [235, 236] and later realized in a bench-scale continuous system [237]. Supercritical water gasification (SCWG) uses water at a supercritical state in the range of 600–700 °C to generate mainly H_2 and CO_2 with/without a catalyst. SCWG is preferred for biomass with a moisture content above 30 % [238]. Even biomass with a moisture content as high as 90 % (w/w) can be gasified. SCWG uses high energy to raise the temperature of water to 600 °C, and the energy content in the product can be easily recovered by passing it through a heat exchanger. Heat exchangers operate at high pressures, which makes heat recovery possible [239]. Moreover, reactors at supercritical conditions operate at high pressure that do not require gas pressurization afterwards and thus the compressed medium allows gasification to occur with minimal heat loss [240-242]. The further dissolution of reaction intermediates in the reaction medium minimizes coke and tar formation [239]. When process conditions and the nature of the catalyst are varied, the desired products are obtained [241, 243]. Hydrothermal gasification has significant advantages over traditional processes. The traditional method produces low-quality syngas with impurities such as char/tar that lead to clogging issues. This low-quality syngas needs to be purified, which increases costs [244, 245].

The products from hydrothermal gasification include CO_2, H_2, CO and CH_4, with small amounts of C_2H_4 and C_2H_6. Figure 5 depicts the simplified process flow for the conversion of biomass to gaseous products via aqueous intermediate compounds under hydrothermal conditions [246]. At low temperatures, cellulose undergoes hydrolysis into glucose, which is isomerized into mannose and fructose [247]. At subcritical temperatures, the saccharides thus generated undergo dehydration into furans and furfural compounds [248]. However, above critical temperature and pressure, saccharides undergo hydration through free radical reaction to produce carboxylic acids [248].

Lignin, a complex compound, consists of *p*-coumaryl, sinapyl, or coniferyl alcohols that hydrolyze to produce phenols, cresols, syringols, guaiacols, and catechols. At subcritical conditions, these phenolics can undergo dehydrogenation and dehydration into coke. Above critical conditions, these phenolics degrade to form gases through the generation of intermediates such as aldehydes, alcohols, ketones, and carboxylic acids [246].

Lignin alkali initially undergoes hydrolysis to form phenol and formaldehyde, which gets converted into gaseous products [249]. In other pathway, compounds such as formaldehyde and phenol may also undergo cross-linking to form resins through reactions with reactive sites in supercritical water conditions. Hence, lignin, not only produces low-molecular molecules, but also produces high molecular weight char or tar [250]. The product composition and yield are influenced by a number of design and operation parameters. Key parameters include temperature, pressure, time, heating rate, reactor type, and the nature of the catalyst.

Figure 5

As SCWG proceeds to the critical point of water, the gasification of biomass into H_2 and CH_4 occurs through reactions (a) and (b):

$$C_6H_{12}O_6 + 6\ H_2O \rightarrow 6\ CO_2 + 14\ H_2 \qquad (a)$$

$C_6H_{12}O_6 \rightarrow 3\ CH_4 + 3\ CO_2$ (b)

The H_2 formation is endothermic while CH_4 is somewhat exothermic. As per Le Chatelier's principle, H_2 would dominate CH_4 at elevated temperatures; however, CH_4 would be favorable at high pressures. Thus, free radical reactions are favored at high temperatures and low pressures during gas formation [251]. Higher temperatures lead to higher conversion but reduce SCWG's energy efficiency. Hence, it is desirable to achieve gasification at lower temperatures with the help of catalysts. The types of catalysts used for SCWG are discussed in detail in the next section.

SCWG involves methanation (c), steam reforming (d) and water gas shift (e) reactions.

$CO + 3H_2 \rightarrow CH_4 + H_2O$ (c)

$C_6H_{10}O_5 + H_2O \rightarrow 6\ CO + 6\ H_2$ (d)

$CO + H_2O \rightarrow CO_2 + H_2$ (e)

The extent of gasification is expressed in terms of gasification efficiency, which is a measure of the fraction of H_2 or C in the gaseous product to that in the feeding stream. Carbon gasification efficiency (CGE) increases with temperature, reaching ~100 % at 700 °C, while H_2 efficiency exceeds 100 % and reaches ~158 % efficiency at 740 °C. The enormous increase in H_2 efficiency is attributed to the abstraction of H from H_2O, which depicts the role of water as a reactant and medium. In a continuous reactor, gas yields are presumed to be unaffected by the reaction time after complete biomass conversion into gases [242, 252]. In batch reactors, reaction time has a profound effect on yield [253]. When reaction time increases from 30 to 120 min, the gaseous yield falls. Heating rates also affect yield in batch reactors. High heating rates tend to have high gaseous yields [254]. The percentage of biomass in the input stream also changes the product yield [255-257]. As biomass concentration increases, a high temperature is required to achieve complete gasification [255]. In general, CGE ranges from 92 - 100 % for lower feed concentrations and drops to 68 - 80 % above 10 %. CH_4 yields increase with biomass concentration, and a gas mixture of CO_2 and H_2 tends to form at low biomass concentrations [256]. Experiments involving hydrothermal gasification technology without catalysts are summarized in Table 5 using references [258-268].

Table 5

5.1 Catalytic hydrothermal gasification

Effective degradation of biomass into low-molecular weight gaseous compounds requires high operating temperatures (up to 600 °C). High temperatures result in a high yield; however, the high temperature lowers process energy efficiency. Hence, gasification at a lower temperature is desirable and is often carried out by catalyst. The use of catalysts improves the yield and quality of fuels. It is also known to enhance gasification performance at mild conditions, thereby showing huge promise as a suitable candidate for supercritical hydrothermal gasification. As for hydrothermal liquefaction, the literature highlights two types of catalysts, homogeneous and heterogeneous, and they are discussed below.

5.1.1 Homogeneous catalysts

The use of homogeneous catalysts such as alkali metals (NaOH, Na_2CO_3, K_2CO_3, $KHCO_3$, etc.) on sub- and supercritical gasification of biomass has been widely reported in the literature [43, 177, 269-280]. Such catalysts are often used to improve the water-gas shift reaction. The catalytic effect of K_2CO_3 was reported in a number of studies for the catalytic SCWG of a broad range of model compounds and biomass types [246, 269, 281-285]. K_2CO_3 shows activity through the formation of $HCOO^-K^+$ [254, 286, 287]. The process involves the release of CO_2 and H_2 via formic acid as an intermediate through reactions (f-j):

$$CO + H_2O \rightarrow HCOOH \leftrightarrow CO_2 + H_2 \quad \text{(f)}$$

$$2KHCO_3 \rightarrow H_2O + K_2CO_3 + CO_2 \quad \text{(g)}$$

$$K_2CO_3 + H_2 \rightarrow KHCO_3 + KOH \quad \text{(h)}$$

$$KOH + CO \rightarrow HCOOK \quad \text{(i)}$$

$$HCOOK + H_2O \rightarrow KHCO_3 + H_2 \quad \text{(j)}$$

NaOH has also been found to enhance the water-gas shift reaction and favor H_2 formation and gasification efficiency [270, 288-294]. Hydrogen gas was believed to form through the release of CO and carboxylic acids through the decarbonylation of hydroxylated carbonyl compounds, followed by the generation of hydrogen gas through the water–gas shift reaction. Another H_2 production route was believed to occur through the reaction of sodium salts of simple carboxylic acids with water. In addition, the catalytic effect of

KOH is due to the enhanced water-gas shift reaction through formic acid as an intermediate [43, 271]. Despite the potential of alkali catalysts for high hydrogen yield, they cause plugging, fouling, and corrosion [295]. An experiment with a SCW fluidized bed system for biomass gasification at 923 K and 30 MPa showed no reactor plugging up to 30 wt. % glucose and 18 wt. % corn cob [296]. In addition, the positive effects of natural mineral catalysts such as trona, dolomite, and borax have been realized with SCWG [297]. The rapid dissemination of knowledge of this technology provides future possibilities for scale-up operations. Onwudili et al. [293] predicted the possibility of scale-up for H_2 in a semi-continuous mode through the elimination of CO_2 as Na_2CO_3. Thus, Na_2CO_3 acted as both catalyst and C sequestration agent. A study by Lin et al. [291] involved the integration of a water-hydrocarbon reaction, a water-gas shift reaction, CO_2 absorption, and various pollutants in a single process, HyPr-RING (Hydrogen Production by Reaction Integrated Novel Gasification).

Table 6

5.1.2 Heterogeneous catalysts

Though homogeneous catalysts can accelerate water-gas shift reactions, they cause problems related to plugging, corrosion, and fouling [254]. Heterogeneous catalysts, however, have high hydrogen selectivity, recyclability, and CGE [287]. The literature reports three types of heterogeneous catalysts used for SCWG: activated carbon, transition metals, and oxides. The carbon derived from plants, shells, and wood has been used as a heterogeneous catalyst for supercritical water gasification due to its high stability in reducing environments along with a high degree of dispersion [41, 298-300]. These carbons include activated carbons like charcoal, coconut shells, and coal-activated carbon. The catalytic effect of activated carbon is thought to be due to the adsorption of the reacting species onto the carbon surface [301]. Although carbon forms a good catalyst support with no solid acid-base properties, the lack of metallic support results in reduced metal dispersion on the carbon surface.

Several studies have described the application of transition metal catalysts (supported/unsupported) in SCWG reactions, i.e., Raney nickel [44, 302-306], ruthenium [307, 308], and other noble metals. According to Huo et al. [309], the activity and selectivity of a porous Ni catalyst for cellulosic conversion to methane is believed to occur through pyrolysis, hydrogenation, and methanation. Nickel supports, with the aim of improving CGE, have been reported in the literature [288, 310-316]. de Vlieger et al. [311] showed that a high dehydrogenation activity of Pt–Ni catalysts resulted in high H_2 through the suppression of CH_4 and acetic acid. Another study used a fixed bed Ni/Ru catalyst to develop a wastewater clean-up facility [317].

Ni/Ni supports, though economical, are usually unstable and suffer from the effects of sintering in both batch and continuous mode [40]. The combined effect of catalyst structural changes and limited life performance of Ni deactivate it in hydrothermal media [318]. A study on the supercritical water gasification of wood at 300 – 410 °C and 12-34 MPa for 90 min resulted in complete gasification, though the Raney Ni surface was found to have carbon deposits [319]. Elliott et al. [320] performed experiments to improve an Ni catalyst by adding Ag, Ru, Sn, and Cu. Also, the effect of Ce loading to inhibit carbon deposition during the SCWG of glucose was studied in an autoclave reactor at 673 K and 24.5 MPa. With the Ce loading content of 8.46 wt.%, the maximum H_2 yield and selectivity were recorded [321]. Ni has shown activities with other compounds such as lignin and cellulose [183, 322-324].

Another known transition metal, Ruthenium (Ru), is known to be a highly active catalyst for low temperature catalytic gasification reactions [325-331]. Catalytic gasification involves the dehydrogenation of reacting species onto a catalyst surface and the scission of C-C or C-O bonds. Further breakdown of C-C produces synthesis gas, which proceeds through water-gas shift and methanation, whereas C-O breaks down into alcohols and organic acids [287]. Ruthenium is also known for high metal dispersion due to reduced metal loadings. Ni or Ru supported on zirconia, titania, γ-alumina, or activated carbon are highly stable at severe oxidizing and corrosive reaction environments [40, 325, 332-344]. Nonetheless, a few reports highlight the poisoning effect of Ru/C, presumed to be from the presence of S in the form of S^{2-} and SO_4^{2-} [345-347].

Other works have studied Pt as a catalyst on aqueous phase reforming reactions [348] and ZrO_2 for SCWG [272, 349]. Finally, oxides of Cu, Mn, Co, Al, Ca, Zr, Ce, and Ru have been shown to be effective for catalytic SCWG [350-354]. It is interesting to note that the reactor materials, made of alloys, affects the reaction. The designs of the "new" Hastelloy [42, 252] and Inconel [355, 356] reactors use heavy metals, which show catalytic activity towards water-gas shift reactions and methanol reforming. Yu et al. [357] studied the SCWG of glucose at 600 °C and 34.5 MPa in reactors made up of the new Hastelloy and Inconel. The gasification efficiency in the new Hastelloy reactor and the Inconel reactor dropped to ~ 85 % and ~ 68 %, respectively, with a 0.8 M increase in glucose concentration, and Inconel was found to catalyze the water-gas shift reaction.

Heterogeneous catalysts tend to undergo sintering, which deactivates catalysts. A recent study discussed the use of a bimetallic catalyst in hydrothermal processes [358]. The use of a dual metal-support catalyst was reported for supercritical water gasification with the aim of improving H_2 yield [359]. Table 7 illustrates the use of heterogeneous catalysts for the hydrothermal gasification of various biomass compounds.

Table 7

6. Hydrothermal carbonization

Hydrothermal carbonization (HTC) converts biomass into a value-added product (solid fuel) at a comparatively low temperature (180 – 250 °C) and saturated pressure (2-10 MPa) [360-363]. The resulting product has carbon content similar to lignite with mass yields varying from 35 to 60% [364-368]. The obtained aqueous phase has most of the dissolved organics in the form of carbon with a minimal amount of gas [364, 369, 370]. The process is influenced by the nature of its feedstock as well as loading and process conditions [360, 366, 367, 369]. The carbonization improves the heating value and dewatering capability of the feedstock [371]. Process efficiency and dewatering capacity are improved by boosting the solid yield and recycling, respectively [371]. In addition, solid loading has a positive effect on product distribution [366, 367], and the process design is positively affected by internal heat recovery [372-374] as the HTC reaction heat is usually low [375]. Carbonaceous materials from hydrothermal carbonization are used in super capacitors and fuel cells for energy storage. The application of hydrothermal carbonization material in energy storage, conversion, and fuel cells is presented in Table 8 [376-390].

Hydrothermal carbonization (HTC) is widely used to convert lignocellulosics into solid hydrochars, which have better physico-chemical characteristics than raw feedstock [391]. HTC technology uses batch and semi-continuous systems, both of which have rendered it less economically viable.

Figure 6 provides insight into the reaction pathways with key products for hydrothermal carbonization [13]. The blend of phenols, organic acids, and ketones make up bio-crude through hydrothermal liquefaction. At critical conditions of water, reactions pertaining to free radicals become prevalent and gasification becomes favored, leading to the formation of CH_4 and H_2 [229]. To facilitate the formation of a solid product such as char, the process temperature must be controlled to avoid liquefaction and gasification. The glucose dehydration to form 2,5-hydroxy-methylfurfuraldehyde followed by aldol condensation outlines the formation of substances like carbon spheres [360, 364, 392]. The chemistry involving reactions such as oxidation, esterification and etherification on the hydroxymethyl group and reactions such as oxidation, reduction and aldol on the formyl group have been reported [393]. Also, solid-solid interactions, as in the case of torrefaction, have been investigated [394]. The composition of HTC is also supported by reaction pathways through liquid and solid state to form coke and char, respectively [364, 395].

Figure 6

HTC is also used in char production as it has high energy content, good grindability, and high hydrophobicity [396]. Using spectroscopic methods, a hydrochar microspheres based chemical model microspheres reflecting the discernible core and the shell of hydrochar particles, which is shown in Figure 7 [397]. In the formation of hydrochar microspheres via hydrothermal carbonization of saccharides, sucrose and starch hydrolyzes to form corresponding monosaccharides such as glucose and or fructose, as the case may be [135]. Starch also produces maltose and the fructose is obtained by glucose isomerization [135]. The monosaccharides such as glucose and fructose breaks down into lower molecular weight compounds like organic acids, thereby decreasing pH [398]. The hydronium ions produced acts as a catalyst for oligosaccharides degradation into the corresponding monosaccharides which further undergoes a series of reactions involving ring C-C bond breaking, and dehydration into furfural compounds [399]. These compounds thus generated undergoes further decomposition to form aldehydes, acids and phenols [399]. Following the series of reactions, the monomers and the decomposition molecules undergo condensation and polymerization into polymers [400]. Such polymerization reactions are enhanced by aldol condensation or intermolecular dehydration [397]. This reaction phenomenon also causes polymer aromatization. As their concentration approaches critical supersaturation point, nucleation occurs which further grows through diffusion at the surface of the chemical species which are linked to the microspheres via hydroxyl, carboxylic and carbonyl groups [401]. Owing to this interaction and linkage, As a result of these reactions, carbonaceous microspheres having stable oxygen groups in the form of pyrone or ether are produced [397].

Figure 7

HTC produces char which has high energy content. The HTC process leaves the char less dusty, which improves pelletization characteristics [402, 403]. The commercial realization of HTC has suffered because of its high temperature and pressure requirements, which increase costs. Pellet quality is measured in terms of mechanical durability, that is, its ability to remain intact during handling or storage [404]. Reza et al. [405] reported that pellet durability improved when HTC temperature increased. Hoekman et al. [403] reported that pellets obtained from hydrochar show good durability at temperatures as low as 200 ˚C. Durability can further be enhanced at higher temperatures, but high temperatures produce pellets that are more brittle. Similarly, a temperature below 200 ˚C produces less durable pellets, as the pellets swell when immersed in water. Nonetheless, hydrochar from HTC produces highly stable, water-resistant pellets [403].

The high cost of commercial HTC technology comes from the need for hydrochar to bind torrefied or raw biomass. Hydrochar is as an effective binder because of the furan and phenolic resins obtained from the degradation of hemicellulosics and cellulosics [403]. Hence, hydrochar improves the durability and pelletization characteristics of other biomass feedstocks. Liu et al. [406] studied the durability and combustion characteristics of hydrochar/lignite pellets. They concluded that hydrochar, along with lignite, improved the tensile strength of blended pellets, especially with a hydrochar fraction of > 50%.

There are logistics associated with the large-scale commercial use of HTC pellets. Commercial HTC technology should have applications that include technical and economic benefits beyond commercial biomass. HTC biochar can be used as a solid biofuel. The industrial application of HTC biochar uses pelletization technology and thus the transportation, handling, and storage of pellets affecting its mechanical durability are important from an economical point of view in industry [407]. Pellet crumbling leads to problems that reduce combustion efficiency and increase emissions [407]. Another logistic problem originates from HTC’s hydrophobicity, which influences the mechanical durability of pellets. Also, with the aim of making HTC technology more environmental friendly in order to develop it commercially, the treatment of spent liquor through anaerobic digestion [408-413] and the influence of the recirculation of spent liquor have been investigated in literature [414-417]. Recirculation helps increase the mass and energy yields of the hydrochar product, which further affects the economy of the process.

Recently, a pilot-scale study was proposed for the HTC of lignocellulosics into solid fuels, which shows the relevance of solid fuel production from wet biomass [418]. More than 80% of energy yields are obtainable through the HTC of woody biomass at the pilot-scale, which indicates how much energy content from the feed is converted into solid fuel [419]. Hence, the future of HTC is promising in terms the conversion of wet biomass to solid fuels [420, 421]. Hydrochar has several applications such as fuel source, catalysts, soil amendment, adsorbent, and energy storage [422]. However, recent research interests are oriented towards the production of hydrochars that have application in industry [49, 423]. The application of HTC for biochar production, as provided in Table 8, is obtained from the references [420, 422, 424-433].

Table 8

7. Issues with hydrothermal technologies

7.1 Economic considerations

Economic considerations are important, both with respect to a novel technology itself and with implementation. The economic viability of a plant helps determine the profitability of a technology and the costs associated with optimizing it.

Based on an economic assessment, the competitiveness and feasibility of a process can be compared to known conventional technologies. Though several techno-economic assessments have been done for thermochemical-based conversion processes such as fast pyrolysis and conventional gasification [434-451], cost analyses are available for biomass-based hydrothermal-based HTL [30, 452-455] or HTG [456-458] processes. The Pacific Northwest National Laboratory (PNNL), under the sponsorship of the National Advanced Biofuels Consortium (NABC), performed bench-scale HTL and upgrading experiments for woody biomass. The techno-economic study included the development of a large-scale commercial HTL and upgrading platform for bio-oil production for two cases, a state-of-technology (SOT) case with experimental results from the HTL process and a goal case that assumed plausible future improvements for mature HTL technology [454]. The results showed that production costs were lower for the goal case, which assumed decreasing organics loss to the aqueous phase that led to higher product yields and reduced wastewater treatment costs. The cost results from the SOT case highlighted that the bio-oil production cost, based on the current HTL process, is not competitive compared to petroleum-based gasoline. Although the results from the goal case look promising for bio-oil production from woody biomass through HTL, the lack of process knowledge and concepts has financial risks. The main factors influencing the bio-oil production cost are feedstock cost, product yield, and upgrading equipment cost. The identification of key parameters will be necessary in a future research study.

Techno-economic studies on bench-scale experiments for lipid-extracted microalgae (LEA) liquid fuels through hydrothermal liquefaction (HTL) and upgrading processes have also been undertaken [459]. The results highlighted that the HTL process is promising for the production of liquid fuel compared with conventional gasoline and diesel. However, the uncertainties in the feedstock cost had a major influence on production cost. Other key factors influencing production cost were product yield and equipment cost for upgrading. Faeth et al. [460] reported that costs for a continuous HTL process can be reduced through lower residence times. In another study, catalytic hydrothermal gasification was performed for the conversion of wet LEA to methane together with wastewater treatment through HTL [461]. The coupled HTL and CHG improved bio-crude yield and overall economics. Jones et al. [462] evaluated the economics of hydrothermal liquefaction (HTL) and catalytic upgrading of whole algal biomass to obtain renewable diesel fuel. In their study, the feedstock cost had the most significant impact on diesel fuel cost. The economic study highlights the need to look for improved cultivation, harvesting, and dewatering methods to reduce feedstock costs.

The feasibility of SCWG has setbacks due to current hydrogen costs. It costs around three times as much to obtain H_2 through direct biomass gasification than through the steam methane reforming (SMR) of natural gas [463]. The cost of obtaining H_2 from natural gas via SMR is 1.5–3.7 US $/kg (assuming a 7 US$/GJ natural gas price) and 10–14 US$/GJ from biomass [464]. The high operating and capital costs for high-pressure supercritical water systems poses economic challenges. The lack of understanding of SCWG technology, together with net positive energy and economic considerations, limits the ability to obtain hydrogen from commercial SMR. However, there have been a few techno-economic studies on supercritical water gasification technology for biomass and algae. In 1997, General Atomics came up with first cost estimate for an SCWG using sewage sludge with dry matter contents of 20% and 40%; however, their estimate was based on a supercritical water oxidation (SCWO) plant because there is relatively little known about the novel SCWG technology [465]. In 1999, Amos calculated cost estimates for starch waste with a 15% dry matter content and product gas cleaned by expensive membrane technology [466]. The membrane alone made up more than 35% of the purchased equipment costs. In 2002, Matsumura et al. [456] estimated the costs for supercritical gasification using water hyacinths with a 5% dry matter content . Their estimate included only the investment costs for bulk plant components and left out the costs of piping, engineering, services, etc. Including these costs raises the total investment costs fourfold. Gasafi et al. [457] studied the economics of SCWG using sewage sludge as feedstock with the aim of producing hydrogen. According to their findings, the hydrogen cost production was about 35.2 € GJ^{-1} if no revenues from sewage sludge disposal, which were significantly higher than the cost of hydrogen obtained through electrolysis (26.82 € GJ^{-1}), are considered. In 2013, Brandenberger et al. [467] estimated costs for microalgae cultivated in ponds and photo-bioreactors for synthetic natural gas (SNG) production using SCWG and reported that the economic challenges are due to the cost of algal biomass production, which are 94% of the required capital investment. In 2014, the results from a techno-economic analysis of glucose and sewage sludge for hydrogen production via SCWG were studied [458]. The authors of that study identified that there were no profits associated with a glucose feed concentration of 15% until the price of hydrogen goes beyond \$ 5 kg^{-1}. The SCWG technology still needs to be optimized through a proper understanding of process concepts and plant components to improve economic efficiency. More research is needed on hydrothermal processing technology to make it economically feasible.

7.2 Gaps in Knowledge

The reactor configuration and design have a crucial role in the process run and affect process reaction kinetics. The main challenges in reactor design are related to enhancing heat integration, handling plausible poor heat transfer due to contact between the incoming reactor effluent with the reactor feed owing to its high viscosity, and decreasing costs of the reactor system itself when operating at high pressures [468]. These challenges require an experimental analysis of required heat transfer coefficients at various locations in the process to determine proper heat integration. Moreover, the type of material for the HTL reactor design needs to be evaluated by taking into account harsh reaction conditions and possible corrosive effects. Considerable research is needed to improve the suitable liquid hourly space velocity (LHSV) in the HTL reactor system. The pump needs to be able to handle high solids content. The feasibility of separating bio-oil and water at the reactor temperature and pressure is yet to be determined. This is important because efficient bio-oil separation from an aqueous phase will increase the yield of bio-oil.

A study of prevailing reaction rates and products from biomass processing through hydrothermal technologies will help us understand how to optimize reactor design. HTL bio-oil yield is influenced by factors such as temperature, feed solid content, the nature of the biomass, and residence time. A detailed characterization of all the products obtained from hydrothermal processing (i.e., bio-oil, aqueous, gaseous, and solid products) is required. Considerable effort is needed to comprehend bio-oil stability and quality and thereby better understand ongoing process reactions and upgrading needs. This effort would also be important when options for transporting bio-oil offsite (when an upgrading plant is not co-located with HTL plant) are identified. The characterization methods, which use equipment such as GC/MS, NMR, and HPLC for product analysis, are critical to understanding the nature of the reactive species influencing product quality and yield. However, analytical techniques such as chromatography cannot accurately predict high molecular weight compounds due to the technique's low resolution and limited selectivity.

A study on the continuous flow system is needed to understand process development for commercial applications. The catalyst has an important role in determining process yield and performance. There are research gaps with respect to catalyst maintenance, stability, plausible regeneration, and subsequent lifetimes. Improving the long-term use of catalysts is essential both to improve their performance and to minimize deactivation during reactions.

Supercritical water gasification, another hydrothermal processing technology, is a promising approach for handling wet biomass. However, an analysis of SCWG design suggests that the feasibility of the process depends on feed type and concentration. Clogging, plugging, and char formation are major problems in the SCWG of biomass. In addition, the limited dissolution of inorganic salts in biomass under supercritical water conditions causes precipitation during SCWG and these salts combine with char and plug the reactor. Though continuous stirred reactors and fluidized beds can handle plugging problems, there are underlying issues with the complex design and the high energy demands in the process. Thus, an efficient SCWG reactor system design is still in progress. Another technical challenge is in selecting material to avoid corrosion in the reactor. The extreme environments in the SCWG process require materials capable of preventing corrosion. In addition, pumping biomass at high concentrations is an issue. In order to optimize the process, efficient and better energy recovery equipment is needed. The wide use of metal catalysts such as Ni and Ru in the SCWG of biomass are aimed at improving H_2 production; however, they are known to cause a methanation reaction and produce CH_4. The selectivity towards H_2 production and, in turn, the stability of the catalyst at supercritical conditions, presents a challenge. Catalyst poisoning, loss, and deactivation during SCWG pose technical challenges and suggest the need for catalyst supports to prevent unwanted side reactions and enhance H_2 yields.

Process optimization and research in the areas of hydrothermal processing will likely improve product yield and thus profitability.

8. Conclusion

Hydrothermal processing technologies have significant potential for biomass with high moisture content. We performed an extensive literature review to understand the status quo of various hydrothermal processing technologies. Studies differ with respect to their analysis of experimental results and provide in-depth understanding for future process development. In general, hydrothermal processing precludes an energy-intensive pretreatment step for bioconversion to useful products. This review focused on different hydrothermal processing technologies, namely the liquefaction, gasification, and carbonization of individual biomass fractions/whole biomass, and their effects on process conditions. The nature and yield of products from hydrothermal technologies depends on factors such as catalyst, feedstock type, the nature of the solvent, and process conditions. The nature of biomass in terms of protein, carbohydrates, and lipid fractions determines the compositional yield of the product type. The effect of a catalyst on product yield cannot be dismissed, as it change the compositional characteristics of the product obtained. Thus, choice and selection of catalyst for a particular application is important in view of its major influence on the yield and desired properties of the final product.

Hydroprocessing technologies have not yet been commercialized due to a number of technological gaps and economic constraints.

- Technological gaps with respect to various plant components including reactor design for process development and optimization in order to achieve a thermal efficiency high enough to attain an economic process. A synergistic effect of the individual components in the process design is crucial for efficient operation.

- Considerable challenges remain in the area of catalyst recycling and regeneration in order to improve the lifetime and efficiency of the hydrothermal process.
- Along with technological constraints, there are economic bottlenecks. As the technology uses high pressure equipment, the process has high capital investments.

If economically feasible, a process can be practically achievable. However, cost studies are not enough to support the development of large-scale processes. Commercialization requires testing with different feedstocks to understand the process. In addition, integrating a techno-economic analysis with energy tools helps understand energy flow and consumption, which have a direct impact on cost. Internal recovery of heat and power in an integrated system would reduce external energy demands and costs, thereby improving technology costs. A sensitivity analysis combined with Monte Carlo simulations for risk analysis would help evaluate the technology properly.

Although hydrothermal technologies have several challenges, such as environmental concerns, depletion of fossil-fuel reserves, etc., research towards specific fuels targeted for the transportation sector and as raw materials for the chemical industry continues. In view of this, hydrothermal technologies hold significant promise, and research and development continues to overcome the barriers associated with the technology for plausible market integration in future.

Acknowledgements

The authors are grateful to Alberta Innovates – Bio Solutions (AI-BIO), Emissions Reduction Alberta (earlier called as Climate Change and Emissions Management Corporation (CCEMC)), the Natural Sciences and Engineering Research Council of Canada (NSERC) and Symbiotic EnviroTek Inc. for providing financial support to do this research. Astrid Blodgett is thanked for her editorial assistance.

References:

[1] Tekin K, Karagöz S. Non-catalytic and catalytic hydrothermal liquefaction of biomass. Res Chem Intermed 2013;39:485-98.

[2] McKendry P. Energy production from biomass (part 1): overview of biomass. Bioresour Technol 2002;83:37-46.

[3] Tekin K, Karagöz S. t-BuOK catalyzed bio-oil production from woody biomass under sub-critical water conditions. Environmental Chemistry Letters 2013;11:25-31.

[4] Briens C, Piskorz J, Berruti F. Biomass Valorization for Fuel and Chemicals Production--A Review. International Journal of Chemical Reactor Engineering 2008;6.

[5] Savage PE, Levine RB, Huelsman CM. Chapter 8 Hydrothermal Processing of Biomass. Thermochemical Conversion of Biomass to Liquid Fuels and Chemicals: The Royal Society of Chemistry; 2010. p. 192-221.

[6] Brunner G. Near critical and supercritical water. Part I. Hydrolytic and hydrothermal processes. The Journal of Supercritical Fluids 2009;47:373-81.

[7] Gao X, Yu Y, Wu H. Life Cycle Energy and Carbon Footprints of Microalgal Biodiesel Production in Western Australia: A Comparison of Byproducts Utilization Strategies. ACS Sustainable Chemistry & Engineering 2013;1:1371-80.

[8] Yokoyama S, Matsumura Y. The Asian biomass handbook: a guide for biomass production and utilization. The Japan Institute of Energy 2008:61-2.

[9] Elliott DC. Hydrothermal Processing. Thermochemical Processing of Biomass: Conversion into Fuels, Chemicals and Power2011. p. 200-31.

[10] Chiaramonti D, Prussi M, Buffi M, Rizzo AM, Pari L. Review and experimental study on pyrolysis and hydrothermal liquefaction of microalgae for biofuel production. Applied Energy 2017;185, Part 2:963-72.

[11] Zhang L, Xu C, Champagne P. Overview of recent advances in thermo-chemical conversion of biomass. Energy Convers Manage 2010;51:969-82.

[12] Karagöz S, Bhaskar T, Muto A, Sakata Y, Uddin MA. Low-Temperature Hydrothermal Treatment of Biomass: Effect of Reaction Parameters on Products and Boiling Point Distributions. Energy & Fuels 2003;18:234-41.

[13] Kruse A, Funke A, Titirici M-M. Hydrothermal conversion of biomass to fuels and energetic materials. Curr Opin Chem Biol 2013;17:515-21.

[14] Toor SS, Rosendahl L, Rudolf A. Hydrothermal liquefaction of biomass: a review of subcritical water technologies. Energy 2011;36:2328-42.

[15] Dimitriadis A, Bezergianni S. Hydrothermal liquefaction of various biomass and waste feedstocks for biocrude production: A state of the art review. Renew Sustain Energy Rev 2017;68, Part 1:113-25.

[16] Peterson AA, Vogel F, Lachance RP, Fröling M, Antal Jr MJ, Tester JW. Thermochemical biofuel production in hydrothermal media: a review of sub-and supercritical water technologies. Energy & Environmental Science 2008;1:32-65.

[17] Luterbacher JS, Fröling M, Vogel F, Maréchal F, Tester JW. Hydrothermal gasification of waste biomass: Process design and life cycle asessment. Environmental science & technology 2009;43:1578-83.

[18] Steubing B, Zah R, Ludwig C. Heat, electricity, or transportation? The optimal use of residual and waste biomass in Europe from an environmental perspective. Environmental science & technology 2011;46:164-71.

[19] Maddi B, Panisko EA, Wietsma T, Lemmon T, Swita M, Albrecht K, et al. Quantitative Characterization of Aqueous Byproducts from Hydrothermal Liquefaction of Municipal Wastes, Food Industry Wastes, and Biomass Grown on Waste. ACS Sustainable Chemistry & Engineering 2017.

[20] Chen Y, Ren X, Wei Q, Guo J. Hydrothermal liquefaction of Undaria pinnatifida residues to organic acids with recyclable trimethylamine. Bioresour Technol 2016;221:477-84.

[21] Hadhoum L, Balistrou M, Burnens G, Loubar K, Tazerout M. Hydrothermal liquefaction of oil mill wastewater for bio-oil production in subcritical conditions. Bioresour Technol 2016;218:9-17.

[22] Kumar G, Shobana S, Chen W-H, Bach Q-V, Kim S-H, Atabani A, et al. A review of thermochemical conversion of microalgal biomass for biofuels: chemistry and processes. Green Chemistry 2017;19:44-67.

[23] Modell M. Gasification and liquefaction of forest products in supercritical water. Fundamentals of thermochemical biomass conversion: Springer; 1985. p. 95-119.

[24] Elliott DC, Biller P, Ross AB, Schmidt AJ, Jones SB. Hydrothermal liquefaction of biomass: developments from batch to continuous process. Bioresour Technol 2015;178:147-56.

[25] Matsumura Y, Minowa T, Potic B, Kersten SR, Prins W, van Swaaij WP, et al. Biomass gasification in near-and super-critical water: status and prospects. Biomass Bioenergy 2005;29:269-92.

[26] Biller P, Ross AB. Hydrothermal processing of algal biomass for the production of biofuels and chemicals. Biofuels 2012;3:603-23.

[27] Schaleger L, Figueroa C, Davis H. Direct liquefaction of biomass: results from operation of continuous bench-scale unit in liquefaction of water slurries of Douglas fir wood. Biotechnol Bioeng Symp;(United States): Lawrence Berkeley Lab., CA; 1982.

[28] Thigpen P. Final Report: An Investigation of Liquefaction of Wood at the Biomass Liquefaction Facility, Albany, Oregon, Battelle Pacific Northwest Laboratories, Department of Energy, Wheelabrator Cleanfuel Corporation. Technical Information Center, Office of Scientific and Technical Information, US Department of Energy, contract 1982.

[29] Elliott DC. Process development for biomass liquefaction. Am Chem Soc, Div Fuel Chem, Prepr;(United States) 1980;25.

[30] Goudnaan F, Van de Beld B, Boerefijn F, Bos G, Naber J, Van der Wal S, et al. Thermal efficiency of the HTU® process for biomass liquefaction. Progress in thermochemical biomass conversion 2008:1312-25.

[31] Green Car Congress. NextFuels introduces hydrothermal process to produce biofuels from wet uwsfpprF, 2017]. Available from: http://www.greencarcongress.com/2013/08/20130819-next.html.

[32] Nielsen RP, Olofsson G, Søgaard EG. CatLiq–High pressure and temperature catalytic conversion of biomass: The CatLiq technology in relation to other thermochemical conversion technologies. Biomass Bioenergy 2012;39:399-402.

[33] Steeper Energy. Hydrofaction^{TM} Oil. Available from: http://steeperenergy.com/technology/hydrofaction-oil.

[34] Adams T, Appel B, Samson P, Roberts M. Converting turkey offal into bio-derived hydrocarbon oil with the CWT thermal process. Power-Gen Renewable Energy Conference2004.

[35] The Carthage Press. Canadian firm acquires Carthage RES plant; 2013 [February 14 AfhwccaNNrt.

[36] Tran K-Q. Fast hydrothermal liquefaction for production of chemicals and biofuels from wet biomass – The need to develop a plug-flow reactor. Bioresour Technol 2016;213:327-32.

[37] Matsumura Y. Chapter 9 - Hydrothermal Gasification of Biomass A2 - Pandey, Ashok. In: Bhaskar T, Stöcker M, Sukumaran RK, editors. Recent Advances in Thermo-Chemical Conversion of Biomass. Boston: Elsevier; 2015. p. 251-67.

[38] Bermejo M, Cocero M. Supercritical water oxidation: a technical review. AlChE J 2006;52:3933-51.

[39] Sealock Jr LJ, Elliott DC, Baker EG, Butner RS. Chemical processing in high-pressure aqueous environments. 1. Historical perspective and continuing developments. Industrial & engineering chemistry research 1993;32:1535-41.

[40] Elliott DC, Sealock Jr LJ, Baker EG. Chemical processing in high-pressure aqueous environments. 2. Development of catalysts for gasification. Industrial & Engineering Chemistry Research 1993;32:1542-8.

[41] Xu X, Matsumura Y, Stenberg J, Antal MJ. Carbon-catalyzed gasification of organic feedstocks in supercritical water. Industrial & Engineering Chemistry Research 1996;35:2522-30.

[42] Yu D, Aihara M, Antal Jr MJ. Hydrogen production by steam reforming glucose in supercritical water. Energy & Fuels 1993;7:574-7.

[43] Kruse A, Meier D, Rimbrecht P, Schacht M. Gasification of pyrocatechol in supercritical water in the presence of potassium hydroxide. Industrial & Engineering Chemistry Research 2000;39:4842-8.

[44] Yoshida T, Matsumura Y. Gasification of cellulose, xylan, and lignin mixtures in supercritical water. Industrial & Engineering Chemistry Research 2001;40:5469-74.

[45] Savage PE. A perspective on catalysis in sub-and supercritical water. The Journal of Supercritical Fluids 2009;47:407-14.

[46] Onwudili JA, Williams PT. Reaction of different carbonaceous materials in alkaline hydrothermal media for hydrogen gas production. Green Chemistry 2011;13:2837-43.

[47] 1–33. BFCruhpNFLNp.

[48] Bobleter O. Hydrothermal degradation of polymers derived from plants. Prog Polym Sci 1994;19:797-841.

[49] Kambo HS, Dutta A. A comparative review of biochar and hydrochar in terms of production, physico-chemical properties and applications. Renew Sustain Energy Rev 2015;45:359-78.

[50] Wörmeyer K, Ingram T, Saake B, Brunner G, Smirnova I. Comparison of different pretreatment methods for lignocellulosic materials. Part II: Influence of pretreatment on the properties of rye straw lignin. Bioresour Technol 2011;102:4157-64.

[51] Takata E, Tsutsumi K, Tsutsumi Y, Tabata K. Production of monosaccharides from napier grass by hydrothermal process with phosphoric acid. Bioresour Technol 2013;143:53-8.

[52] Tian C, Liu Z, Zhang Y, Li B, Cao W, Lu H, et al. Hydrothermal liquefaction of harvested high-ash low-lipid algal biomass from Dianchi Lake: Effects of operational parameters and relations of products. Bioresour Technol 2015;184:336-43.

[53] Tekin K, Karagöz S, Bektaş S. A review of hydrothermal biomass processing. Renew Sustain Energy Rev 2014;40:673-87.

[54] Mtui GY. Recent advances in pretreatment of lignocellulosic wastes and production of value added products. African Journal of Biotechnology 2009;8.

[55] Sánchez C. Lignocellulosic residues: biodegradation and bioconversion by fungi. Biotechnol Adv 2009;27:185-94.

[56] Delmer DP, Amor Y. Cellulose biosynthesis. The Plant Cell 1995;7:987.

[57] Rowell RM, Pettersen R, Han JS, Rowell JS, Tshabalala MA. Cell wall chemistry. Handbook of wood chemistry and wood composites 2005:35-74.

[58] Sun R. Cereal straw as a resource for sustainable biomaterials and biofuels: chemistry, extractives, lignins, hemicelluloses and cellulose: Elsevier; 2010.

[59] Vassilev SV, Baxter D, Andersen LK, Vassileva CG, Morgan TJ. An overview of the organic and inorganic phase composition of biomass. Fuel 2012;94:1-33.

[60] Telmo C, Lousada J. The explained variation by lignin and extractive contents on higher heating value of wood. Biomass Bioenergy 2011;35:1663-7.

[61] Weingärtner H, Franck EU. Supercritical water as a solvent. Angew Chem Int Ed 2005;44:2672-92.

[62] Xu X, De Almeida C, Antal MJ. Mechanism and kinetics of the acid-catalyzed dehydration of ethanol in supercritical water. The Journal of Supercritical Fluids 1990;3:228-32.

[63] Sasaki M, Furukawa M, Minami K, Adschiri T, Arai K. Kinetics and mechanism of cellobiose hydrolysis and retro-aldol condensation in subcritical and supercritical water. Industrial & engineering chemistry research 2002;41:6642-9.

[64] Möller M, Nilges P, Harnisch F, Schröder U. Subcritical water as reaction environment: fundamentals of hydrothermal biomass transformation. ChemSusChem 2011;4:566-79.

[65] Broell D, Kaul C, Kraemer A, Krammer P, Richter T, Jung M, et al. Chemistry in supercritical water. Angew Chem Int Ed 1999;38:2998-3014.

[66] Marshall WL, Franck E. Ion product of water substance, 0–1000° C, 1–10,000 bars new international formulation and its background. J Phys Chem Ref Data 1981;10:295-304.

[67] Kritzer P. Corrosion in high-temperature and supercritical water and aqueous solutions: a review. The Journal of Supercritical Fluids 2004;29:1-29.

[68] Ding ZY, Frisch MA, Li L, Gloyna EF. Catalytic oxidation in supercritical water. Industrial & Engineering Chemistry Research 1996;35:3257-79.

[69] Henrikson JT, Chen Z, Savage PE. Inhibition and acceleration of phenol oxidation by supercritical water. Industrial & engineering chemistry research 2003;42:6303-9.

[70] Penninger J, Kersten R, Baur H. Reactions of diphenylether in supercritical water—mechanism and kinetics. The Journal of supercritical fluids 1999;16:119-32.

[71] Penninger J, Kersten R, Baur H. Hydrolysis of diphenylether in supercritical water: effects of dissolved NaCl. The Journal of Supercritical Fluids 2000;17:215-26.

[72] Ogunsola OM, Berkowitz N. Removal of heterocyclic S and N from oil precursors by supercritical water. Fuel 1995;74:1485-90.

[73] Onwudili J, Williams P. Hydrothermal gasification and oxidation as effective flameless conversion technologies for organic wastes. Journal of the Energy Institute 2008;81:102-9.

[74] Kruse A. Supercritical water gasification. Biofuels, Bioproducts and Biorefining 2008;2:415-37.

[75] Kayserilioğlu BŞ, Bakir U, Yilmaz L, Akkaş N. Use of xylan, an agricultural by-product, in wheat gluten based biodegradable films: mechanical, solubility and water vapor transfer rate properties. Bioresour Technol 2003;87:239-46.

[76] Vegas R, Kabel M, Schols HA, Alonso JL, Parajó JC. Hydrothermal processing of rice husks: effects of severity on product distribution. Journal of Chemical Technology & Biotechnology 2008;83:965-72.

[77] Nabarlatz D, Farriol X, Montane D. Kinetic modeling of the autohydrolysis of lignocellulosic biomass for the production of hemicellulose-derived oligosaccharides. Industrial & engineering chemistry research 2004;43:4124-31.

[78] Carvalheiro F, Esteves M, Parajó J, Pereira H, Gırio F. Production of oligosaccharides by autohydrolysis of brewery's spent grain. Bioresour Technol 2004;91:93-100.

[79] Kabel M, Carvalheiro F, Garrote G, Avgerinos E, Koukios E, Parajó J, et al. Hydrothermally treated xylan rich by-products yield different classes of xylo-oligosaccharides. Carbohydr Polym 2002;50:47-56.

[80] Gullón P, Pereiro G, Alonso JL, Parajó JC. Aqueous pretreatment of agricultural wastes: characterization of soluble reaction products. Bioresour Technol 2009;100:5840-5.

[81] Garrote G, Domínguez H, Parajó J. Manufacture of xylose-based fermentation media from corncobs by posthydrolysis of autohydrolysis liquors. Appl Biochem Biotechnol 2001;95:195-207.

[82] Rivas B, Domınguez J, Domınguez H, Parajó J. Bioconversion of posthydrolysed autohydrolysis liquors: an alternative for xylitol production from corn cobs. Enzyme Microb Technol 2002;31:431-8.

[83] Duarte LC, Carvalheiro F, Lopes S, Marques S, Parajo JC, Gírio FM. Comparison of two posthydrolysis processes of brewery's spent grain autohydrolysis liquor to produce a pentose-containing culture medium. Proceedings of the Twenty-Fifth Symposium on Biotechnology for Fuels and Chemicals Held May 4–7, 2003, in Breckenridge, CO: Springer; 2004. p. 1041-58.

[84] Vila C, Campos AR, Cristovão C, Cunha AM, Santos V, Parajó JC. Sustainable biocomposites based on autohydrolysis of lignocellulosic substrates. Compos Sci Technol 2008;68:944-52.

[85] Michelin M, Maria de Lourdes T, Ruzene DS, Silva DP, Ruiz HA, Vicente AA, et al. Production of xylanase and β-xylosidase from autohydrolysis liquor of corncob using two fungal strains. Bioprocess and biosystems engineering 2012;35:1185-92.

[86] Montané D, Nabarlatz D, Martorell A, Torné-Fernández V, Fierro V. Removal of lignin and associated impurities from xylo-oligosaccharides by activated carbon adsorption. Industrial & engineering chemistry research 2006;45:2294-302.

[87] Vegas R, Moure A, Domínguez H, Parajó JC, Álvarez JR, Luque S. Purification of oligosaccharides from rice husk autohydrolysis liquors by ultra-and nano-filtration. Desalination 2006;199:541-3.

[88] Garrote G, Parajó J. Non-isothermal autohydrolysis of Eucalyptus wood. Wood Science and Technology 2002;36:111-23.

[89] Liu C, Wyman CE. Impact of fluid velocity on hot water only pretreatment of corn stover in a flowthrough reactor. Proceedings of the Twenty-Fifth Symposium on Biotechnology for Fuels and Chemicals Held May 4–7, 2003, in Breckenridge, CO: Springer; 2004. p. 977-87.

[90] Makishima S, Mizuno M, Sato N, Shinji K, Suzuki M, Nozaki K, et al. Development of continuous flow type hydrothermal reactor for hemicellulose fraction recovery from corncob. Bioresour Technol 2009;100:2842-8.

[91] Buranov AU, Mazza G. Lignin in straw of herbaceous crops. Industrial crops and products 2008;28:237-59.

[92] Pandey MP, Kim CS. Lignin depolymerization and conversion: a review of thermochemical methods. Chemical Engineering & Technology 2011;34:29-41.

[93] Kristensen JB, Thygesen LG, Felby C, Jørgensen H, Elder T. Cell-wall structural changes in wheat straw pretreated for bioethanol production. Biotechnol Biofuels 2008;1:1-9.

[94] Zhang T, Wyman CE, Jakob K, Yang B. Rapid selection and identification of Miscanthus genotypes with enhanced glucan and xylan yields from hydrothermal pretreatment followed by enzymatic hydrolysis. Biotechnology for biofuels 2012;5:56.

[95] Cannella D, Hsieh C-W, Felby C, Jørgensen H. Production and effect of aldonic acids during enzymatic hydrolysis of lignocellulose at high dry matter content. Biotechnol Biofuels 2012;5:26.

[96] Garrote G, Dominguez H, Parajo J. Hydrothermal processing of lignocellulosic materials. European Journal of Wood and Wood Products 1999;57:191-202.

[97] Gullón P, Conde E, Moure A, Domínguez H, Parajó JC. Selected process alternatives for biomass refining: a review. Open Agriculture Journal 2010;4:135-44.

[98] Zhang B, Huang H-J, Ramaswamy S. Reaction kinetics of the hydrothermal treatment of lignin. Appl Biochem Biotechnol 2008;147:119-31.

[99] Chi C, Zhang Z, Chang H-m, Jameel H. Determination of furfural and hydroxymethylfurfural formed from biomass under acidic conditions. J Wood Chem Technol 2009;29:265-76.

[100] Schmidt JA. 3 Electronic Spectroscopy of Lignins. Lignin and lignans: advances in chemistry 2009:49.

[101] Conde E, Moure A, Domínguez H, Parajó JC. Production of antioxidants by non-isothermal autohydrolysis of lignocellulosic wastes. LWT-Food Science and Technology 2011;44:436-42.

[102] Garrote G, Cruz J, Moure A, Domınguez H, Parajó J. Antioxidant activity of byproducts from the hydrolytic processing of selected lignocellulosic materials. Trends in Food Science & Technology 2004;15:191-200.

[103] Tsubaki S, Sakamoto M, Azuma J-i. Microwave-assisted extraction of phenolic compounds from tea residues under autohydrolytic conditions. Food Chem 2010;123:1255-8.

[104] Ruiz HA, Rodríguez-Jasso RM, Fernandes BD, Vicente AA, Teixeira JA. Hydrothermal processing, as an alternative for upgrading agriculture residues and marine biomass according to the biorefinery concept: A review. Renew Sustain Energy Rev 2013;21:35-51.

[105] Savage PE LR, Huelsman CM. In: Crocker M, editor. Hydrothermal processing of biomass: thermochemical conversion of biomass to liquid: Cambridge: RSCPublishing

[106] Savage P, Levine R, Huelsman C. Thermochemical Conversion of Biomass to Liquid Fuels and Chemicals. 2010.

[107] Tekin K, Akalin MK, Karagöz S. The effects of water tolerant Lewis acids on the hydrothermal liquefaction of lignocellulosic biomass. Journal of the Energy Institute 2016;89:627-35.

[108] Kumar K, Ghosh S, Angelidaki I, Holdt SL, Karakashev DB, Morales MA, et al. Recent developments on biofuels production from microalgae and macroalgae. Renew Sustain Energy Rev 2016;65:235-49.

[109] Li C, Aston JE, Lacey JA, Thompson VS, Thompson DN. Impact of feedstock quality and variation on biochemical and thermochemical conversion. Renew Sustain Energy Rev 2016;65:525-36.

[110] Arvindnarayan S, Sivagnana Prabhu KK, Shobana S, Kumar G, Dharmaraja J. Upgrading of micro algal derived bio-fuels in thermochemical liquefaction path and its perspectives: A review. Int Biodeterior Biodegrad.

[111] Maurya R, Paliwal C, Ghosh T, Pancha I, Chokshi K, Mitra M, et al. Applications of de-oiled microalgal biomass towards development of sustainable biorefinery. Bioresour Technol 2016;214:787-96.

[112] López Barreiro D, Gómez BR, Ronsse F, Hornung U, Kruse A, Prins W. Heterogeneous catalytic upgrading of biocrude oil produced by hydrothermal liquefaction of microalgae: State of the art and own experiments. Fuel Process Technol 2016;148:117-27.

[113] Haarlemmer G, Guizani C, Anouti S, Déniel M, Roubaud A, Valin S. Analysis and comparison of bio-oils obtained by hydrothermal liquefaction and fast pyrolysis of beech wood. Fuel 2016;174:180-8.

[114] Patel B, Guo M, Shah N, Hellgardt K. Environmental profile of algal Hydrothermal Liquefaction — A country specific case study. Algal Research 2016;16:127-40.

[115] Saber M, Nakhshiniev B, Yoshikawa K. A review of production and upgrading of algal bio-oil. Renew Sustain Energy Rev 2016;58:918-30.

[116] Pearce M, Shemfe M, Sansom C. Techno-economic analysis of solar integrated hydrothermal liquefaction of microalgae. Applied Energy 2016;166:19-26.

[117] Albrecht KO, Zhu Y, Schmidt AJ, Billing JM, Hart TR, Jones SB, et al. Impact of heterotrophically stressed algae for biofuel production via hydrothermal liquefaction and catalytic hydrotreating in continuous-flow reactors. Algal Research 2016;14:17-27.

[118] Déniel M, Haarlemmer G, Roubaud A, Weiss-Hortala E, Fages J. Energy valorisation of food processing residues and model compounds by hydrothermal liquefaction. Renew Sustain Energy Rev 2016;54:1632-52.

[119] Patel B, Guo M, Izadpanah A, Shah N, Hellgardt K. A review on hydrothermal pre-treatment technologies and environmental profiles of algal biomass processing. Bioresour Technol 2016;199:288-99.

[120] Chaudry S, Bahri PA, Moheimani NR. Pathways of processing of wet microalgae for liquid fuel production: A critical review. Renew Sustain Energy Rev 2015;52:1240-50.

[121] Summers HM, Ledbetter RN, McCurdy AT, Morgan MR, Seefeldt LC, Jena U, et al. Techno-economic feasibility and life cycle assessment of dairy effluent to renewable diesel via hydrothermal liquefaction. Bioresour Technol 2015;196:431-40.

[122] Huang H-j, Yuan X-z. Recent progress in the direct liquefaction of typical biomass. Prog Energy Combust Sci 2015;49:59-80.

[123] Guo Y, Yeh T, Song W, Xu D, Wang S. A review of bio-oil production from hydrothermal liquefaction of algae. Renew Sustain Energy Rev 2015;48:776-90.

[124] Gerber Van Doren L, Posmanik R, Bicalho FA, Tester JW, Sills DL. Prospects for energy recovery during hydrothermal and biological processing of waste biomass. Bioresour Technol 2017;225:67-74.

[125] López Barreiro D, Prins W, Ronsse F, Brilman W. Hydrothermal liquefaction (HTL) of microalgae for biofuel production: State of the art review and future prospects. Biomass Bioenergy 2013;53:113-27.

[126] Chornet E, Overend RP. Biomass liquefaction: an overview. Fundamentals of thermochemical biomass conversion: Springer; 1985. p. 967-1002.

[127] Kumar S, Gupta RB. Biocrude production from switchgrass using subcritical water. Energy & Fuels 2009;23:5151-9.

[128] Patil V, Tran K-Q, Giselrød HR. Towards sustainable production of biofuels from microalgae. International journal of molecular sciences 2008;9:1188-95.

[129] Peterson AA, Vogel F, Lachance RP, Froling M, Antal JMJ, Tester JW. Thermochemical biofuel production in hydrothermal media: A review of sub- and supercritical water technologies. Energy & Environmental Science 2008;1:32-65.

[130] Savage PE. A perspective on catalysis in sub- and supercritical water. The Journal of Supercritical Fluids 2009;47:407-14.

[131] Wahyudiono, Sasaki M, Goto M. Recovery of phenolic compounds through the decomposition of lignin in near and supercritical water. Chemical Engineering and Processing: Process Intensification 2008;47:1609-19.

[132] He W, Li G, Kong L, Wang H, Huang J, Xu J. Application of hydrothermal reaction in resource recovery of organic wastes. Resources, Conservation and Recycling 2008;52:691-9.

[133] Molten P, Demmitt T, Donovan J, Miller R. Mechanism of conversion of cellulose wastes to liquid in alkaline solution. Energy from biomass and wastes III Chicago, IL: Institute of Gas Technology 1983;293.

[134] Yang W, Li X, Li Z, Tong C, Feng L. Understanding low-lipid algae hydrothermal liquefaction characteristics and pathways through hydrothermal liquefaction of algal major components: Crude polysaccharides, crude proteins and their binary mixtures. Bioresour Technol 2015;196:99-108.

[135] Oomori T, Khajavi SH, Kimura Y, Adachi S, Matsuno R. Hydrolysis of disaccharides containing glucose residue in subcritical water. Biochem Eng J 2004;18:143-7.

[136] Liu H-M, Li M-F, Yang S, Sun R-C. Understanding the mechanism of cypress liquefaction in hot-compressed water through characterization of solid residues. Energies 2013;6:1590-603.

[137] Yaylayan V, Kaminsky E. Isolation and structural analysis of Maillard polymers: caramel and melanoidin formation in glycine/glucose model system. Food Chem 1998;63:25-31.

[138] Peterson AA, Lachance RP, Tester JW. Kinetic evidence of the Maillard reaction in hydrothermal biomass processing: glucose- glycine interactions in high-temperature, high-pressure water. Industrial & Engineering Chemistry Research 2010;49:2107-17.

[139] Xu C, Etcheverry T. Hydro-liquefaction of woody biomass in sub-and super-critical ethanol with iron-based catalysts. Fuel 2008;87:335-45.

[140] Karagöz S, Bhaskar T, Muto A, Sakata Y. Hydrothermal upgrading of biomass: effect of K 2 CO 3 concentration and biomass/water ratio on products distribution. Bioresour Technol 2006;97:90-8.

[141] Xiu S, Shahbazi A, Shirley V, Cheng D. Hydrothermal pyrolysis of swine manure to bio-oil: effects of operating parameters on products yield and characterization of bio-oil. J Anal Appl Pyrolysis 2010;88:73-9.

[142] Muppaneni T, Reddy HK, Selvaratnam T, Dandamudi KPR, Dungan B, Nirmalakhandan N, et al. Hydrothermal liquefaction of Cyanidioschyzon merolae and the influence of catalysts on products. Bioresour Technol 2017;223:91-7.

[143] Sudasinghe N, Reddy H, Csakan N, Deng S, Lammers P, Schaub T. Temperature-Dependent Lipid Conversion and Nonlipid Composition of Microalgal Hydrothermal Liquefaction Oils Monitored by Fourier Transform Ion Cyclotron Resonance Mass Spectrometry. BioEnergy Research 2015;8:1962-72.

[144] Durak H, Aysu T. Effects of catalysts and solvents on liquefaction of Onopordum heteracanthum for production of bio-oils. Bioresour Technol 2014;166:309-17.

[145] Chan YH, Yusup S, Quitain AT, Uemura Y, Sasaki M. Bio-oil production from oil palm biomass via subcritical and supercritical hydrothermal liquefaction. The Journal of Supercritical Fluids 2014;95:407-12.

[146] Chen W-T, Zhang Y, Zhang J, Yu G, Schideman LC, Zhang P, et al. Hydrothermal liquefaction of mixed-culture algal biomass from wastewater treatment system into bio-crude oil. Bioresour Technol 2014;152:130-9.

[147] Vo TK, Lee OK, Lee EY, Kim CH, Seo J-W, Kim J, et al. Kinetics study of the hydrothermal liquefaction of the microalga Aurantiochytrium sp. KRS101. Chem Eng J 2016;306:763-71.

[148] Huang Y, Chen Y, Xie J, Liu H, Yin X, Wu C. Bio-oil production from hydrothermal liquefaction of high-protein high-ash microalgae including wild Cyanobacteria sp. and cultivated Bacillariophyta sp. Fuel 2016;183:9-19.

[149] Reddy HK, Muppaneni T, Ponnusamy S, Sudasinghe N, Pegallapati A, Selvaratnam T, et al. Temperature effect on hydrothermal liquefaction of Nannochloropsis gaditana and Chlorella sp. Applied Energy 2016;165:943-51.

[150] Pedersen TH, Jasiūnas L, Casamassima L, Singh S, Jensen T, Rosendahl LA. Synergetic hydrothermal co-liquefaction of crude glycerol and aspen wood. Energy Convers Manage 2015;106:886-91.

[151] López Barreiro D, Beck M, Hornung U, Ronsse F, Kruse A, Prins W. Suitability of hydrothermal liquefaction as a conversion route to produce biofuels from macroalgae. Algal Research 2015;11:234-41.

[152] Gao Y, Liu S, Du J, Wang Z, Wang H, Zhao T. Conversion and extracting bio-oils from rod-shaped cornstalk by sub-critical water. J Anal Appl Pyrolysis 2015;115:316-25.

[153] Singh R, Chaudhary K, Biswas B, Balagurumurthy B, Bhaskar T. Hydrothermal liquefaction of rice straw: Effect of reaction environment. The Journal of Supercritical Fluids 2015;104:70-5.

[154] Sangon S, Ratanavaraha S, Ngamprasertsith S, Prasassarakich P. Coal liquefaction using supercritical toluene–tetralin mixture in a semi-continuous reactor. Fuel Process Technol 2006;87:201-7.

[155] Kabyemela BM, Adschiri T, Malaluan RM, Arai K. Kinetics of glucose epimerization and decomposition in subcritical and supercritical water. Industrial & Engineering Chemistry Research 1997;36:1552-8.

[156] Kabyemela B, Takigawa M, Adschiri T, Malaluan R, Arai K. Mechanism and kinetics of cellobiose decomposition in sub-and supercritical water. Industrial & Engineering Chemistry Research 1998;37:357-61.

[157] Chan YH, Yusup S, Quitain AT, Tan RR, Sasaki M, Lam HL, et al. Effect of process parameters on hydrothermal liquefaction of oil palm biomass for bio-oil production and its life cycle assessment. Energy Convers Manage 2015;104:180-8.

[158] Zhang B, von Keitz M, Valentas K. Thermochemical liquefaction of high-diversity grassland perennials. J Anal Appl Pyrolysis 2009;84:18-24.

[159] Karagöz S, Bhaskar T, Muto A, Sakata Y, Uddin MA. Low-temperature hydrothermal treatment of biomass: effect of reaction parameters on products and boiling point distributions. Energy & fuels 2004;18:234-41.

[160] Boocock D, Sherman K. Further aspects of powdered poplar wood liquefaction by aqueous pyrolysis. The Canadian Journal of Chemical Engineering 1985;63:627-33.

[161] Yan Y, Xu J, Li T, Ren Z. Liquefaction of sawdust for liquid fuel. Fuel Process Technol 1999;60:135-43.

[162] Meryemoğlu B, Hasanoğlu A, Irmak S, Erbatur O. Biofuel production by liquefaction of kenaf (Hibiscus cannabinus L.) biomass. Bioresour Technol 2014;151:278-83.

[163] Grigoras IF, Stroe RE, Sintamarean IM, Rosendahl LA. Effect of biomass pretreatment on the product distribution and composition resulting from the hydrothermal liquefaction of short rotation coppice willow. Bioresour Technol.

[164] Li R, Xie Y, Yang T, Li B, Zhang Y, Kai X. Characteristics of the products of hydrothermal liquefaction combined with cellulosic bio-ethanol process. Energy 2016;114:862-7.

[165] Hietala DC, Faeth JL, Savage PE. A quantitative kinetic model for the fast and isothermal hydrothermal liquefaction of Nannochloropsis sp. Bioresour Technol 2016;214:102-11.

[166] Yang L, Nazari L, Yuan Z, Corscadden K, Xu C, He Q. Hydrothermal liquefaction of spent coffee grounds in water medium for bio-oil production. Biomass Bioenergy 2016;86:191-8.

[167] Xu D, Savage PE. Effect of reaction time and algae loading on water-soluble and insoluble biocrude fractions from hydrothermal liquefaction of algae. Algal Research 2015;12:60-7.

[168] Biller P, Sharma BK, Kunwar B, Ross AB. Hydroprocessing of bio-crude from continuous hydrothermal liquefaction of microalgae. Fuel 2015;159:197-205.

[169] Guo Y, Song W, Lu J, Ma Q, Xu D, Wang S. Hydrothermal liquefaction of Cyanophyta: Evaluation of potential bio-crude oil production and component analysis. Algal Research 2015;11:242-7.

[170] Zheng J-L, Zhu M-Q, Wu H-t. Alkaline hydrothermal liquefaction of swine carcasses to bio-oil. Waste Manage (Oxford) 2015;43:230-8.

[171] Gai C, Li Y, Peng N, Fan A, Liu Z. Co-liquefaction of microalgae and lignocellulosic biomass in subcritical water. Bioresour Technol 2015;185:240-5.

[172] Akhtar J, Amin NAS. A review on process conditions for optimum bio-oil yield in hydrothermal liquefaction of biomass. Renew Sustain Energy Rev 2011;15:1615-24.

[173] Abu El-Rub Z, Bramer E, Brem G. Review of catalysts for tar elimination in biomass gasification processes. Industrial & engineering chemistry research 2004;43:6911-9.

[174] Zhou D, Zhang L, Zhang S, Fu H, Chen J. Hydrothermal liquefaction of macroalgae Enteromorpha prolifera to bio-oil. Energy & Fuels 2010;24:4054-61.

[175] Yin S, Dolan R, Harris M, Tan Z. Subcritical hydrothermal liquefaction of cattle manure to bio-oil: Effects of conversion parameters on bio-oil yield and characterization of bio-oil. Bioresour Technol 2010;101:3657-64.

[176] Sugano M, Takagi H, Hirano K, Mashimo K. Hydrothermal liquefaction of plantation biomass with two kinds of wastewater from paper industry. Journal of Materials Science 2008;43:2476-86.

[177] Kersten SR, Potic B, Prins W, Van Swaaij WP. Gasification of model compounds and wood in hot compressed water. Industrial & engineering chemistry research 2006;45:4169-77.

[178] Xu C, Lancaster J. Conversion of secondary pulp/paper sludge powder to liquid oil products for energy recovery by direct liquefaction in hot-compressed water. Water Res 2008;42:1571-82.

[179] Sasaki M, Adschiri T, Arai K. Production of cellulose II from native cellulose by near-and supercritical water solubilization. J Agric Food Chem 2003;51:5376-81.

[180] ZHANG H-f, SU X-l, SUN D-k, ZHANG R, BI J-c. Investigation on degradation of polyethylene to oil in a continuous supercritical water reactor. Journal of Fuel Chemistry and Technology 2007;35:487-91.

[181] Zhong C, Wei X. A comparative experimental study on the liquefaction of wood. Energy 2004;29:1731-41.

[182] Mazaheri H, Lee KT, Mohamed AR. Influence of temperature on liquid products yield of oil palm shell via subcritical water liquefaction in the presence of alkali catalyst. Fuel Process Technol 2013;110:197-205.

[183] Minowa T, Zhen F, Ogi T. Cellulose decomposition in hot-compressed water with alkali or nickel catalyst. The Journal of supercritical fluids 1998;13:253-9.

[184] Mok WS, Antal Jr MJ, Varhegyi G. Productive and parasitic pathways in dilute acid-catalyzed hydrolysis of cellulose. Industrial & Engineering Chemistry Research 1992;31:94-100.

[185] Song C, Hu H, Zhu S, Wang G, Chen G. Nonisothermal catalytic liquefaction of corn stalk in subcritical and supercritical water. Energy & fuels 2004;18:90-6.

[186] Wang Y, Wang H, Lin H, Zheng Y, Zhao J, Pelletier A, et al. Effects of solvents and catalysts in liquefaction of pinewood sawdust for the production of bio-oils. Biomass Bioenergy 2013;59:158-67.

[187] Watanabe M, Aizawa Y, Iida T, Aida TM, Levy C, Sue K, et al. Glucose reactions with acid and base catalysts in hot compressed water at 473K. Carbohydr Res 2005;340:1925-30.

[188] Watanabe M, Iida T, Aizawa Y, Ura H, Inomata H, Arai K. Conversions of some small organic compounds with metal oxides in supercritical water at 673 K. Green Chem 2003;5:539-44.

[189] Yang BY, Montgomery R. Alkaline degradation of glucose: effect of initial concentration of reactants. Carbohydr Res 1996;280:27-45.

[190] Zhu Z, Toor SS, Rosendahl L, Chen G. Analysis of product distribution and characteristics in hydrothermal liquefaction of barley straw in subcritical and supercritical water. Environmental Progress & Sustainable Energy 2014;33:737-43.

[191] Zhu Z, Toor SS, Rosendahl L, Yu D, Chen G. Influence of alkali catalyst on product yield and properties via hydrothermal liquefaction of barley straw. Energy 2015;80:284-92.

[192] Arturi KR, Strandgaard M, Nielsen RP, Søgaard EG, Maschietti M. Hydrothermal liquefaction of lignin in near-critical water in a new batch reactor: Influence of phenol and temperature. The Journal of Supercritical Fluids 2017;123:28-39.

[193] Jindal M, Jha M. Catalytic hydrothermal liquefaction of waste furniture sawdust to bio-oil. Indian Chemical Engineer 2016;58:157-71.

[194] Bi Z, Zhang J, Peterson E, Zhu Z, Xia C, Liang Y, et al. Biocrude from pretreated sorghum bagasse through catalytic hydrothermal liquefaction. Fuel 2017;188:112-20.

[195] Wang Y, Wang H, Lin H, Zheng Y, Zhao J, Pelletier A, et al. Effects of solvents and catalysts in liquefaction of pinewood sawdust for the production of bio-oils. Biomass Bioenergy 2013;59:158-67.

[196] Jena U, Das KC, Kastner JR. Comparison of the effects of Na2CO3, Ca3(PO4)2, and NiO catalysts on the thermochemical liquefaction of microalga Spirulina platensis. Applied Energy 2012;98:368-75.

[197] Nazari L, Yuan Z, Souzanchi S, Ray MB, Xu C. Hydrothermal liquefaction of woody biomass in hot-compressed water: Catalyst screening and comprehensive characterization of bio-crude oils. Fuel 2015;162:74-83.

[198] Déniel M, Haarlemmer G, Roubaud A, Weiss-Hortala E, Fages J. Optimisation of bio-oil production by hydrothermal liquefaction of agro-industrial residues: Blackcurrant pomace (Ribes nigrum L.) as an example. Biomass Bioenergy 2016;95:273-85.

[199] Chang C-C, Chen C-P, Yang C-S, Chen Y-H, Huang M, Chang C-Y, et al. Conversion of waste bamboo chopsticks to bio-oil via catalytic hydrothermal liquefaction using K2CO3. Sustainable Environment Research 2016;26:262-7.

[200] Cao L, Zhang C, Hao S, Luo G, Zhang S, Chen J. Effect of glycerol as co-solvent on yields of bio-oil from rice straw through hydrothermal liquefaction. Bioresour Technol 2016;220:471-8.

[201] Biller P, Madsen RB, Klemmer M, Becker J, Iversen BB, Glasius M. Effect of hydrothermal liquefaction aqueous phase recycling on bio-crude yields and composition. Bioresour Technol 2016;220:190-9.

[202] Qian L, Wang S, Savage PE. Hydrothermal Liquefaction of Sewage Sludge under Isothermal and Fast Conditions. Bioresour Technol.

[203] Shakya R, Whelen J, Adhikari S, Mahadevan R, Neupane S. Effect of temperature and Na2CO3 catalyst on hydrothermal liquefaction of algae. Algal Research 2015;12:80-90.

[204] Demirbaş A. Mechanisms of liquefaction and pyrolysis reactions of biomass. Energy Convers Manage 2000;41:633-46.

[205] Karagöz S, Bhaskar T, Muto A, Sakata Y, Oshiki T, Kishimoto T. Low-temperature catalytic hydrothermal treatment of wood biomass: analysis of liquid products. Chem Eng J 2005;108:127-37.

[206] Miyazawa T, Funazukuri T. Polysaccharide Hydrolysis Accelerated by Adding Carbon Dioxide under Hydrothermal Conditions. Biotechnol Progr 2005;21:1782-5.

[207] Arturi KR, Kucheryavskiy S, Søgaard EG. Performance of hydrothermal liquefaction (HTL) of biomass by multivariate data analysis. Fuel Process Technol 2016;150:94-103.

[208] Durak H, Aysu T. Structural analysis of bio-oils from subcritical and supercritical hydrothermal liquefaction of Datura stramonium L. The Journal of Supercritical Fluids 2016;108:123-35.

[209] Christensen PR, Mørup AJ, Mamakhel A, Glasius M, Becker J, Iversen BB. Effects of heterogeneous catalyst in hydrothermal liquefaction of dried distillers grains with solubles. Fuel 2014;123:158-66.

[210] Hammerschmidt A, Boukis N, Hauer E, Galla U, Dinjus E, Hitzmann B, et al. Catalytic conversion of waste biomass by hydrothermal treatment. Fuel 2011;90:555-62.

[211] Watanabe M, Iida T, Inomata H. Decomposition of a long chain saturated fatty acid with some additives in hot compressed water. Energy Convers Manage 2006;47:3344-50.

[212] Yim SC, Quitain AT, Yusup S, Sasaki M, Uemura Y, Kida T. Metal oxide-catalyzed hydrothermal liquefaction of Malaysian oil palm biomass to bio-oil under supercritical condition. The Journal of Supercritical Fluids 2017;120, Part 2:384-94.

[213] Shi W, Li S, Jin H, Zhao Y, Yu W. The hydrothermal liquefaction of rice husk to bio-crude using metallic oxide catalysts. Energy Sources, Part A: Recovery, Utilization, and Environmental Effects 2013;35:2149-55.

[214] Long J, Li Y, Zhang X, Tang L, Song C, Wang F. Comparative investigation on hydrothermal and alkali catalytic liquefaction of bagasse: Process efficiency and product properties. Fuel 2016;186:685-93.

[215] Saber M, Golzary A, Hosseinpour M, Takahashi F, Yoshikawa K. Catalytic hydrothermal liquefaction of microalgae using nanocatalyst. Applied Energy 2016;183:566-76.

[216] Zhou C, Zhu X, Qian F, Shen W, Xu H, Zhang S, et al. Catalytic hydrothermal liquefaction of rice straw in water/ethanol mixtures for high yields of monomeric phenols using reductive CuZnAl catalyst. Fuel Process Technol 2016;154:1-6.

[217] Duan P, Savage PE. Hydrothermal liquefaction of a microalga with heterogeneous catalysts. Industrial & Engineering Chemistry Research 2010;50:52-61.

[218] Davari M, Karimi S, Tavasoli A, Karimi A. Enhancement of activity, selectivity and stability of CNTs-supported cobalt catalyst in Fischer–Tropsch via CNTs functionalization. Applied Catalysis A: General 2014;485:133-42.

[219] Xu T, Zhang Q, Cen J, Xiang Y, Li X. Selectivity tailoring of Pd/CNTs in phenol hydrogenation by surface modification: Role of C O oxygen species. Appl Surf Sci 2015;324:634-9.

[220] Chen Y, Mu R, Yang M, Fang L, Wu Y, Wu K, et al. Catalytic hydrothermal liquefaction for bio-oil production over CNTs supported metal catalysts. Chem Eng Sci 2017;161:299-307.

[221] Xu CC, Su H, Cang D. Liquefaction of corn distillers dried grains with solubles (DDGS) in hot-compressed phenol. BioResources 2008;3:363-82.

[222] Jakab E, Liu K, Meuzelaar HL. Thermal decomposition of wood and cellulose in the presence of solvent vapors. Industrial & engineering chemistry research 1997;36:2087-95.

[223] Liu Z, Zhang F-S. Effects of various solvents on the liquefaction of biomass to produce fuels and chemical feedstocks. Energy Convers Manage 2008;49:3498-504.

[224] Mun SP, El Barbary MH. Liquefaction of lignocellulosic biomass with dioxane/polar solvent mixtures in the presence of an acid catalyst. Journal of Industrial and Engineering Chemistry 2004;10:473-7.

[225] Kržan A, Kunaver M, Tišler V. Wood liquefaction using dibasic organic acids and glycols. Acta Chim Slov 2005;52:253-8.

[226] Lee JH, Hwang H, Moon J, Choi JW. Characterization of hydrothermal liquefaction products from coconut shell in the presence of selected transition metal chlorides. J Anal Appl Pyrolysis 2016;122:415-21.

[227] Cherad R, Onwudili JA, Biller P, Williams PT, Ross AB. Hydrogen production from the catalytic supercritical water gasification of process water generated from hydrothermal liquefaction of microalgae. Fuel 2016;166:24-8.

[228] Ortiz FG, Ollero P, Serrera A, Galera S. An energy and exergy analysis of the supercritical water reforming of glycerol for power production. Int J Hydrogen Energy 2012;37:209-26.

[229] De Vlieger D, Chakinala A, Lefferts L, Kersten S, Seshan K, Brilman D. Hydrogen from ethylene glycol by supercritical water reforming using noble and base metal catalysts. Applied catalysis B: environmental 2012;111:536-44.

[230] Ruppert AM, Weinberg K, Palkovits R. Hydrogenolysis goes bio: from carbohydrates and sugar alcohols to platform chemicals. Angew Chem Int Ed 2012;51:2564-601.

[231] Azadi P, Syed K, Farnood R. Catalytic gasification of biomass model compound in near-critical water. Applied Catalysis A: General 2009;358:65-72.

[232] Knezevic D. Hydrothermal conversion of biomass: University of Twente; 2009.

[233] Knezevic D, van Swaaij W, Kersten S. Hydrothermal conversion of biomass. II. Conversion of wood, pyrolysis oil, and glucose in hot compressed water. Industrial & Engineering Chemistry Research 2009;49:104-12.

[234] Vertes AA, Qureshi N, Yukawa H, Blaschek H. Biomass to biofuels: strategies for global industries: Wiley Online Library; 2010.

[235] Sealock LJ, Elliott DC. Method for the catalytic conversion of lignocellulosic materials. Google Patents; 1991.

[236] Elliott DC, Sealock JL. Nickel/ruthenium catalyst and method for aqueous phase reactions. Pacific Northwest National Laboratory (PNNL), Richland, WA; 1998.

[237] Elliott DC, Baker EG, Butner RS, Sealock LJ. Bench-scale reactor tests of low temperature, catalytic gasification of wet industrial wastes. Journal of solar energy engineering 1993;115:52-6.

[238] Yoshida Y, Dowaki K, Matsumura Y, Matsuhashi R, Li D, Ishitani H, et al. Comprehensive comparison of efficiency and CO 2 emissions between biomass energy conversion technologies—position of supercritical water gasification in biomass technologies. Biomass Bioenergy 2003;25:257-72.

[239] Kruse A. Hydrothermal biomass gasification. The Journal of Supercritical Fluids 2009;47:391-9.

[240] Cantero DA, Dolores Bermejo M, José Cocero M. Reaction engineering for process intensification of supercritical water biomass refining. The Journal of Supercritical Fluids 2015;96:21-35.

[241] Van Rossum G, Potic B, Kersten S, Van Swaaij W. Catalytic gasification of dry and wet biomass. Catal Today 2009;145:10-8.

[242] Williams PT, Onwudili J. Composition of products from the supercritical water gasification of glucose: a model biomass compound. Industrial & engineering chemistry research 2005;44:8739-49.

[243] Bagnoud-Velásquez M, Brandenberger M, Vogel F, Ludwig C. Continuous catalytic hydrothermal gasification of algal biomass and case study on toxicity of aluminum as a step toward effluents recycling. Catal Today 2014;223:35-43.

[244] Hasler P, Nussbaumer T. Gas cleaning for IC engine applications from fixed bed biomass gasification. Biomass Bioenergy 1999;16:385-95.

[245] Kirkels AF, Verbong GP. Biomass gasification: Still promising? A 30-year global overview. Renew Sustain Energy Rev 2011;15:471-81.

[246] Güngören Madenoğlu T, Sağlam M, Yüksel M, Ballice L. Hydrothermal gasification of biomass model compounds (cellulose and lignin alkali) and model mixtures. The Journal of Supercritical Fluids 2016;115:79-85.

[247] Klingler D, Vogel H. Influence of process parameters on the hydrothermal decomposition and oxidation of glucose in sub-and supercritical water. The Journal of Supercritical Fluids 2010;55:259-70.

[248] Watanabe M, Aizawa Y, Iida T, Levy C, Aida TM, Inomata H. Glucose reactions within the heating period and the effect of heating rate on the reactions in hot compressed water. Carbohydr Res 2005;340:1931-9.

[249] Lundquist K. Low-molecular weight lignin hydrolysis products. Applied Polymer Symposium1976. p. 1393-407.

[250] Saisu M, Sato T, Watanabe M, Adschiri T, Arai K. Conversion of lignin with supercritical water- phenol mixtures. Energy & Fuels 2003;17:922-8.

[251] Bühler W, Dinjus E, Ederer H, Kruse A, Mas C. Ionic reactions and pyrolysis of glycerol as competing reaction pathways in near-and supercritical water. The Journal of Supercritical Fluids 2002;22:37-53.

[252] Lee I-G, Kim M-S, Ihm S-K. Gasification of glucose in supercritical water. Industrial & Engineering Chemistry Research 2002;41:1182-8.

[253] Guo Y, Wang S, Gong Y, Xu D, Tang X, Ma H. Partial oxidation of municipal sludge with activited carbon catalyst in supercritical water. J Hazard Mater 2010;180:137-44.

[254] Sinag A, Kruse A, Rathert J. Influence of the heating rate and the type of catalyst on the formation of key intermediates and on the generation of gases during hydropyrolysis of glucose in supercritical water in a batch reactor. Industrial & Engineering Chemistry Research 2004;43:502-8.

[255] Guo L, Lu Y, Zhang X, Ji C, Guan Y, Pei A. Hydrogen production by biomass gasification in supercritical water: a systematic experimental and analytical study. Catal Today 2007;129:275-86.

[256] Lu Y, Guo L, Zhang X, Yan Q. Thermodynamic modeling and analysis of biomass gasification for hydrogen production in supercritical water. Chem Eng J 2007;131:233-44.

[257] Lu Y, Guo L, Ji C, Zhang X, Hao X, Yan Q. Hydrogen production by biomass gasification in supercritical water: a parametric study. Int J Hydrogen Energy 2006;31:822-31.

[258] Kabyemela BM, Adschiri T, Malaluan RM, Arai K. Glucose and Fructose Decomposition in Subcritical and Supercritical Water: Detailed Reaction Pathway, Mechanisms, and Kinetics. Industrial & Engineering Chemistry Research 1999;38:2888-95.

[259] Susanti RF, Dianningrum LW, Yum T, Kim Y, Lee BG, Kim J. High-yield hydrogen production from glucose by supercritical water gasification without added catalyst. Int J Hydrogen Energy 2012;37:11677-90.

[260] Matsumura Y, Yanachi S, Yoshida T. Glucose Decomposition Kinetics in Water at 25 MPa in the Temperature Range of 448−673 K. Industrial & Engineering Chemistry Research 2006;45:1875−9.

[261] Safari F, Salimi M, Tavasoli A, Ataei A. Non-catalytic conversion of wheat straw, walnut shell and almond shell into hydrogen rich gas in supercritical water media. Chin J Chem Eng 2016;24:1097-103.

[262] Nanda S, Isen J, Dalai AK, Kozinski JA. Gasification of fruit wastes and agro-food residues in supercritical water. Energy Convers Manage 2016;110:296-306.

[263] Üremek Cengiz N, Eren S, Sağlam M, Yüksel M, Ballice L. Influence of temperature and pressure on hydrogen and methane production in the hydrothermal gasification of wood residues. The Journal of Supercritical Fluids 2016;107:243-9.

[264] Graz Y, Bostyn S, Richard T, Bocanegra PE, de Bilbao E, Poirier J, et al. Hydrothermal conversion of Ulva macro algae in supercritical water. The Journal of Supercritical Fluids 2016;107:182-8.

[265] Alshammari YM, Hellgardt K. Sub and supercritical water reforming of n-hexadecane in a tubular flow reactor. The Journal of Supercritical Fluids 2016;107:723-32.

[266] Seif S, Tavakoli O, Fatemi S, Bahmanyar H. Subcritical water gasification of beet-based distillery wastewater for hydrogen production. The Journal of Supercritical Fluids 2015;104:212-20.

[267] Su Y, Zhu W, Gong M, Zhou H, Fan Y, Amuzu-Sefordzi B. Interaction between sewage sludge components lignin (phenol) and proteins (alanine) in supercritical water gasification. Int J Hydrogen Energy 2015;40:9125-36.

[268] Deniz I, Vardar-Sukan F, Yüksel M, Saglam M, Ballice L, Yesil-Celiktas O. Hydrogen production from marine biomass by hydrothermal gasification. Energy Convers Manage 2015;96:124-30.

[269] Yanik J, Ebale S, Kruse A, Saglam M, Yüksel M. Biomass gasification in supercritical water: II. Effect of catalyst. Int J Hydrogen Energy 2008;33:4520-6.

[270] Watanabe M, Osada M, Inomata H, Arai K, Kruse A. Acidity and basicity of metal oxide catalysts for formaldehyde reaction in supercritical water at 673 K. Applied Catalysis A: General 2003;245:333-41.

[271] Jarana MG, Sánchez-Oneto J, Portela JR, Sanz EN, de la Ossa EM. Supercritical water gasification of industrial organic wastes. The Journal of Supercritical Fluids 2008;46:329-34.

[272] Watanabe M, Inomata H, Osada M, Sato T, Adschiri T, Arai K. Catalytic effects of NaOH and ZrO 2 for partial oxidative gasification of n-hexadecane and lignin in supercritical water☆. Fuel 2003;82:545-52.

[273] Nanda S, Dalai AK, Kozinski JA. Supercritical water gasification of timothy grass as an energy crop in the presence of alkali carbonate and hydroxide catalysts. Biomass Bioenergy 2016;95:378-87.

[274] Gökkaya DS, Saglam M, Yuksel M, Ballice L. Hydrothermal gasification of xylose: Effects of reaction temperature, pressure, and K2CO3 as a catalyst on product distribution. Biomass Bioenergy 2016;91:26-36.

[275] Kang K, Azargohar R, Dalai AK, Wang H. Hydrogen production from lignin, cellulose and waste biomass via supercritical water gasification: Catalyst activity and process optimization study. Energy Convers Manage 2016;117:528-37.

[276] Nanda S, Dalai AK, Gökalp I, Kozinski JA. Valorization of horse manure through catalytic supercritical water gasification. Waste Manage (Oxford) 2016;52:147-58.

[277] Louw J, Schwarz CE, Burger AJ. Catalytic supercritical water gasification of primary paper sludge using a homogeneous and heterogeneous catalyst: Experimental vs thermodynamic equilibrium results. Bioresour Technol 2016;201:111-20.

[278] Güngören Madenoğlu T, Üremek Cengiz N, Sağlam M, Yüksel M, Ballice L. Catalytic gasification of mannose for hydrogen production in near- and super-critical water. The Journal of Supercritical Fluids 2016;107:153-62.

[279] Ferreira-Pinto L, Feirhrmann AC, Corazza ML, Fernandes-Machado NRC, dos Reis Coimbra JS, Saldaña MDA, et al. Hydrogen production and TOC reduction from gasification of lactose by supercritical water. Int J Hydrogen Energy 2015;40:12162-8.

[280] Selvi Gökkaya D, Saglam M, Yüksel M, Ballice L. Supercritical water gasification of phenol as a model for plant biomass. Int J Hydrogen Energy 2015;40:11133-9.

[281] Akgül G, Madenoğlu TG, Cengiz NÜ, Gökkaya D, Sağlam M, Yüksel M. Hydrothermal gasification of Rosa Damascena residues: Gaseous and aqueous yields. The Journal of Supercritical Fluids 2014;85:135-42.

[282] Güngören Madenoğlu T, Boukis N, Sağlam M, Yüksel M. Supercritical water gasification of real biomass feedstocks in continuous flow system. Int J Hydrogen Energy 2011;36:14408-15.

[283] Schmieder H, Abeln J, Boukis N, Dinjus E, Kruse A, Kluth M, et al. Hydrothermal gasification of biomass and organic wastes. The Journal of Supercritical Fluids 2000;17:145-53.

[284] Gong M, Nanda S, Romero MJ, Zhu W, Kozinski JA. Subcritical and supercritical water gasification of humic acid as a model compound of humic substances in sewage sludge. The Journal of Supercritical Fluids 2017;119:130-8.

[285] Louw J, Schwarz CE, Burger AJ. Supercritical water gasification of Eucalyptus grandis and related pyrolysis char: Effect of feedstock composition. Bioresour Technol 2016;216:1030-9.

[286] Sinag A, Kruse A, Schwarzkopf V. Key compounds of the hydropyrolysis of glucose in supercritical water in the presence of K2CO3. Industrial & Engineering Chemistry Research 2003;42:3516-21.

[287] Guo Y, Wang SZ, Xu DH, Gong YM, Ma HH, Tang XY. Review of catalytic supercritical water gasification for hydrogen production from biomass. Renew Sustain Energy Rev 2010;14:334-43.

[288] Ding N, Azargohar R, Dalai AK, Kozinski JA. Catalytic gasification of glucose to H2 in supercritical water. Fuel Process Technol 2014;127:33-40.

[289] Gong M, Zhu W, Zhang HW, Ma Q, Su Y, Fan YJ. Influence of NaOH and Ni catalysts on hydrogen production from the supercritical water gasification of dewatered sewage sludge. Int J Hydrogen Energy 2014;39:19947-54.

[290] Guo Y, Wang S, Wang Y, Zhang J, Xu D, Gong Y. Gasification of two and three-components mixture in supercritical water: Influence of NaOH and initial reactants of acetic acid and phenol. Int J Hydrogen Energy 2012;37:2278-86.

[291] Lin S-Y, Suzuki Y, Hatano H, Harada M. Hydrogen production from hydrocarbon by integration of water-carbon reaction and carbon dioxide removal (HyPr-RING method). Energy & Fuels 2001;15:339-43.

[292] Muangrat R, Onwudili JA, Williams PT. Alkali-promoted hydrothermal gasification of biomass food processing waste: A parametric study. Int J Hydrogen Energy 2010;35:7405-15.

[293] Onwudili JA, Williams PT. Role of sodium hydroxide in the production of hydrogen gas from the hydrothermal gasification of biomass. Int J Hydrogen Energy 2009;34:5645-56.

[294] Watanabe M, Inomata H, Osada M, Sato T, Adschiri T, Arai K. Catalytic effects of NaOH and ZrO2 for partial oxidative gasification of n-hexadecane and lignin in supercritical water. Fuel 2003;82:545-52.

[295] Sınağ A, Kruse A, Rathert J. Influence of the Heating Rate and the Type of Catalyst on the Formation of Key Intermediates and on the Generation of Gases During Hydropyrolysis of Glucose in Supercritical Water in a Batch Reactor. Industrial & Engineering Chemistry Research 2004;43:502-8.

[296] Lu YJ, Jin H, Guo LJ, Zhang XM, Cao CQ, Guo X. Hydrogen production by biomass gasification in supercritical water with a fluidized bed reactor. Int J Hydrogen Energy 2008;33:6066-75.

[297] Güngören Madenoğlu T, Yıldırır E, Sağlam M, Yüksel M, Ballice L. Improvement in hydrogen production from hard-shell nut residues by catalytic hydrothermal gasification. The Journal of Supercritical Fluids 2014;95:339-47.

[298] Antal MJ, Allen SG, Schulman D, Xu X, Divilio RJ. Biomass Gasification in Supercritical Water†. Industrial & Engineering Chemistry Research 2000;39:4040-53.

[299] Xu X, Antal MJ. Gasification of sewage sludge and other biomass for hydrogen production in supercritical water. Environ Prog 1998;17:215-20.

[300] Cao W, Cao C, Guo L, Jin H, Dargusch M, Bernhardt D, et al. Hydrogen production from supercritical water gasification of chicken manure. Int J Hydrogen Energy 2016;41:22722-31.

[301] Matsumura Y, Xu X, Antal M. Gasification characteristics of an activated carbon in supercritical water. Carbon 1997;35:819-24.

[302] Elliott DC, Phelps MR, Sealock LJ, Baker EG. Chemical Processing in High-Pressure Aqueous Environments. 4. Continuous-Flow Reactor Process Development Experiments for Organics Destruction. Industrial & Engineering Chemistry Research 1994;33:566-74.

[303] Minowa T, Ogi T. Hydrogen production from cellulose using a reduced nickel catalyst. Catal Today 1998;45:411-6.

[304] Resende FL, Savage PE. Effect of metals on supercritical water gasification of cellulose and lignin. Industrial & Engineering Chemistry Research 2010;49:2694-700.

[305] Yin J, Cheng Z, Guo L, Li S, Jin H. Products distribution and influence of nickel catalyst on glucose hydrothermal decomposition. Int J Hydrogen Energy.

[306] Nanda S, Reddy SN, Dalai AK, Kozinski JA. Subcritical and supercritical water gasification of lignocellulosic biomass impregnated with nickel nanocatalyst for hydrogen production. Int J Hydrogen Energy 2016;41:4907-21.

[307] Byrd AJ, Pant KK, Gupta RB. Hydrogen production from glycerol by reforming in supercritical water over Ru/Al2O3 catalyst. Fuel 2008;87:2956-60.

[308] Wang H-m, Miao R-r, Yang Y, Qiao Y-h, Zhang Q-f, Li C-s, et al. Study on the catalytic gasification of alkali lignin over Ru/C nanotubes in supercritical water. Journal of Fuel Chemistry and Technology 2015;43:1195-201.

[309] Huo Z-B, Liu J-K, Yao G-D, Zeng X, Luo J, Jin F-M. Efficient hydrothermal conversion of cellulose into methane over porous Ni catalyst. Applied Catalysis A: General 2015;490:36-41.

[310] Azadi P, Afif E, Azadi F, Farnood R. Screening of nickel catalysts for selective hydrogen production using supercritical water gasification of glucose. Green Chemistry 2012;14:1766-77.

[311] de Vlieger DJM, Mojet BL, Lefferts L, Seshan K. Aqueous Phase Reforming of ethylene glycol – Role of intermediates in catalyst performance. J Catal 2012;292:239-45.

[312] Pairojpiriyakul T, Croiset E, Kiatkittipong K, Kiatkittipong W, Arpornwichanop A, Assabumrungrat S. Catalytic reforming of glycerol in supercritical water with nickel-based catalysts. Int J Hydrogen Energy 2014;39:14739-50.

[313] Rashidi M, Tavasoli A. Hydrogen rich gas production via supercritical water gasification of sugarcane bagasse using unpromoted and copper promoted Ni/CNT nanocatalysts. The Journal of Supercritical Fluids 2015;98:111-8.

[314] Yan B, Wu J, Xie C, He F, Wei C. Supercritical water gasification with Ni/ZrO2 catalyst for hydrogen production from model wastewater of polyethylene glycol. The Journal of Supercritical Fluids 2009;50:155-61.

[315] Zhang L, Champagne P, Xu C. Supercritical water gasification of an aqueous by-product from biomass hydrothermal liquefaction with novel Ru modified Ni catalysts. Bioresour Technol 2011;102:8279-87.

[316] Huang J, Lian X, Wang L, Zhu C, Jin H, Wang R. Hydrogen production from glucose by supercritical water gasification with Ni/Zr(Ce,Y)O2-δ catalysts. Int J Hydrogen Energy.

[317] Elliott DC, Neuenschwander GG, Phelps MR, Hart TR, Zacher AH, Silva LJ. Chemical Processing in High-Pressure Aqueous Environments. 6. Demonstration of Catalytic Gasification for Chemical Manufacturing Wastewater Cleanup in Industrial Plants. Industrial & Engineering Chemistry Research 1999;38:879-83.

[318] Elliott DC. Catalytic hydrothermal gasification of biomass. Biofuels, Bioproducts and Biorefining 2008;2:254-65.

[319] Waldner MH, Vogel F. Renewable production of methane from woody biomass by catalytic hydrothermal gasification. Industrial & Engineering Chemistry Research 2005;44:4543-51.

[320] Elliott DC, Hart TR, Neuenschwander GG. Chemical processing in high-pressure aqueous environments. 8. Improved catalysts for hydrothermal gasification. Industrial & engineering chemistry research 2006;45:3776-81.

[321] Lu Y, Li S, Guo L. Hydrogen production by supercritical water gasification of glucose with Ni/CeO2/Al2O3: Effect of Ce loading. Fuel 2013;103:193-9.

[322] Furusawa T, Sato T, Saito M, Ishiyama Y, Sato M, Itoh N, et al. The evaluation of the stability of Ni/MgO catalysts for the gasification of lignin in supercritical water. Applied Catalysis A: General 2007;327:300-10.

[323] Furusawa T, Sato T, Sugito H, Miura Y, Ishiyama Y, Sato M, et al. Hydrogen production from the gasification of lignin with nickel catalysts in supercritical water. Int J Hydrogen Energy 2007;32:699-704.

[324] DiLeo GJ, Neff ME, Savage PE. Gasification of guaiacol and phenol in supercritical water. Energy & fuels 2007;21:2340-5.

[325] Osada M, Sato O, Arai K, Shirai M. Stability of supported ruthenium catalysts for lignin gasification in supercritical water. Energy & Fuels 2006;20:2337-43.

[326] Byrd AJ, Pant K, Gupta RB. Hydrogen production from glucose using Ru/Al2O3 catalyst in supercritical water. Industrial & engineering chemistry research 2007;46:3574-9.

[327] Sato T, Osada M, Watanabe M, Shirai M, Arai K. Gasification of alkylphenols with supported noble metal catalysts in supercritical water. Industrial & engineering chemistry research 2003;42:4277-82.

[328] Osada M, Sato T, Watanabe M, Adschiri T, Arai K. Low-temperature catalytic gasification of lignin and cellulose with a ruthenium catalyst in supercritical water. Energy & Fuels 2004;18:327-33.

[329] Elliott DC, Neuenschwander GG, Hart TR, Butner RS, Zacher AH, Engelhard MH, et al. Chemical Processing in High-Pressure Aqueous Environments. 7. Process Development for Catalytic Gasification of Wet Biomass Feedstocks. Industrial & Engineering Chemistry Research 2004;43:1999-2004.

[330] Onwudili JA. Supercritical water gasification of RDF and its components over RuO2/γ-Al2O3 catalyst: New insights into RuO2 catalytic reaction mechanisms. Fuel 2016;181:157-69.

[331] Onwudili JA, Williams PT. Catalytic supercritical water gasification of plastics with supported RuO2: A potential solution to hydrocarbons–water pollution problem. Process Saf Environ Prot 2016;102:140-9.

[332] Byrd AJ, Pant K, Gupta RB. Hydrogen production from glycerol by reforming in supercritical water over Ru/Al 2 O 3 catalyst. Fuel 2008;87:2956-60.

[333] Hao X, Guo L, Zhang X, Guan Y. Hydrogen production from catalytic gasification of cellulose in supercritical water. Chem Eng J 2005;110:57-65.

[334] Onwudili JA, Williams PT. Hydrogen and methane selectivity during alkaline supercritical water gasification of biomass with ruthenium-alumina catalyst. Applied Catalysis B: Environmental 2013;132–133:70-9.

[335] Zhang L, Champagne P, Xu C. Screening of supported transition metal catalysts for hydrogen production from glucose via catalytic supercritical water gasification. Int J Hydrogen Energy 2011;36:9591-601.

[336] Zöhrer H, Vogel F. Hydrothermal catalytic gasification of fermentation residues from a biogas plant. Biomass Bioenergy 2013;53:138-48.

[337] Lee I-G. Effect of metal addition to Ni/activated charcoal catalyst on gasification of glucose in supercritical water. Int J Hydrogen Energy 2011;36:8869-77.

[338] Elif D, Nezihe A. Hydrogen production by supercritical water gasification of fruit pulp in the presence of Ru/C. Int J Hydrogen Energy 2016;41:8073-83.

[339] Norouzi O, Safari F, Jafarian S, Tavasoli A, Karimi A. Hydrothermal gasification performance of Enteromorpha intestinalis as an algal biomass for hydrogen-rich gas production using Ru promoted Fe–Ni/γ-Al2O3 nanocatalysts. Energy Convers Manage.

[340] Zhu C, Guo L, Jin H, Huang J, Li S, Lian X. Effects of reaction time and catalyst on gasification of glucose in supercritical water: Detailed reaction pathway and mechanisms. Int J Hydrogen Energy 2016;41:6630-9.

[341] Behnia I, Yuan Z, Charpentier P, Xu C. Production of methane and hydrogen via supercritical water gasification of renewable glucose at a relatively low temperature: Effects of metal catalysts and supports. Fuel Process Technol 2016;143:27-34.

[342] Tiong L, Komiyama M, Uemura Y, Nguyen TT. Catalytic supercritical water gasification of microalgae: Comparison of Chlorella vulgaris and Scenedesmus quadricauda. The Journal of Supercritical Fluids 2016;107:408-13.

[343] Lee I-G, Nowacka A, Yuan C-H, Park S-J, Yang J-B. Hydrogen production by supercritical water gasification of valine over Ni/activated charcoal catalyst modified with Y, Pt, and Pd. Int J Hydrogen Energy 2015;40:12078-87.

[344] Ishihara A, Imai T, Hashimoto T, Nasu H. Hydrothermal gasification of phenol water on novel carbon-supported Ni catalysts prepared by the sol–gel method using tartaric acid and alminum tri-sec-butoxide. Fuel Process Technol 2015;136:34-40.

[345] Osada M, Hiyoshi N, Sato O, Arai K, Shirai M. Effect of sulfur on catalytic gasification of lignin in supercritical water. Energy & fuels 2007;21:1400-5.

[346] Osada M, Hiyoshi N, Sato O, Arai K, Shirai M. Reaction pathway for catalytic gasification of lignin in presence of sulfur in supercritical water. Energy & fuels 2007;21:1854-8.

[347] Peng G, Ludwig C, Vogel F. Catalytic supercritical water gasification: Interaction of sulfur with ZnO and the ruthenium catalyst. Applied Catalysis B: Environmental 2017;202:262-8.

[348] Cortright R, Davda R, Dumesic JA. Hydrogen from catalytic reforming of biomass-derived hydrocarbons in liquid water. Nature 2002;418:964-7.

[349] Watanabe M, Inomata H, Arai K. Catalytic hydrogen generation from biomass (glucose and cellulose) with ZrO 2 in supercritical water. Biomass Bioenergy 2002;22:405-10.

[350] Yamamura T, Mori T, Park KC, Fujii Y, Tomiyasu H. Ruthenium(IV) dioxide-catalyzed reductive gasification of intractable biomass including cellulose, heterocyclic compounds, and sludge in supercritical water. The Journal of Supercritical Fluids 2009;51:43-9.

[351] Seif S, Fatemi S, Tavakoli O, Bahmanyar H. Hydrogen production through hydrothermal gasification of industrial wastewaters using transition metal oxide catalysts. The Journal of Supercritical Fluids 2016;114:32-45.

[352] Tavasoli A, Barati M, Karimi A. Sugarcane bagasse supercritical water gasification in presence of potassium promoted copper nano-catalysts supported on γ-Al2O3. Int J Hydrogen Energy 2016;41:174-80.

[353] Boucard H, Watanabe M, Takami S, Weiss-Hortala E, Barna R, Adschiri T. Beneficial use of CeO2 nanocatalyst for black liquor conversion under sub and supercritical conditions. The Journal of Supercritical Fluids 2015;105:66-76.

[354] Tavasoli A, Barati M, Karimi A. Conversion of sugarcane bagasse to gaseous and liquid fuels in near-critical water media using K2O promoted Cu/γ-Al2O3–MgO nanocatalysts. Biomass Bioenergy 2015;80:63-72.

[355] Gadhe JB, Gupta RB. Hydrogen production by methanol reforming in supercritical water: suppression of methane formation. Industrial & engineering chemistry research 2005;44:4577-85.

[356] Boukis N, Diem V, Habicht W, Dinjus E. Methanol reforming in supercritical water. Industrial & Engineering Chemistry Research 2003;42:728-35.

[357] Yu D, Aihara M, Antal MJ. Hydrogen production by steam reforming glucose in supercritical water. Energy & Fuels 1993;7:574-7.

[358] Jin H, Zhao X, Su X, Zhu C, Cao C, Guo L. Supercritical water synthesis of bimetallic catalyst and its application in hydrogen production by furfural gasification in supercritical water. Int J Hydrogen Energy.

[359] Tushar MSHK, Dutta A, Xu C. Catalytic supercritical gasification of biocrude from hydrothermal liquefaction of cattle manure. Applied Catalysis B: Environmental 2016;189:119-32.

[360] Falco C, Baccile N, Titirici M-M. Morphological and structural differences between glucose, cellulose and lignocellulosic biomass derived hydrothermal carbons. Green Chemistry 2011;13:3273-81.

[361] Funke A, Ziegler F. Hydrothermal carbonization of biomass: a summary and discussion of chemical mechanisms for process engineering. Biofuels, Bioproducts and Biorefining 2010;4:160-77.

[362] Mumme J, Eckervogt L, Pielert J, Diakité M, Rupp F, Kern J. Hydrothermal carbonization of anaerobically digested maize silage. Bioresour Technol 2011;102:9255-60.

[363] Jain A, Balasubramanian R, Srinivasan MP. Hydrothermal conversion of biomass waste to activated carbon with high porosity: A review. Chem Eng J 2016;283:789-805.

[364] Dinjus E, Kruse A, Troeger N. Hydrothermal carbonization–1. Influence of lignin in lignocelluloses. Chemical engineering & technology 2011;34:2037-43.

[365] Chen W-H, Ye S-C, Sheen H-K. Hydrothermal carbonization of sugarcane bagasse via wet torrefaction in association with microwave heating. Bioresour Technol 2012;118:195-203.

[366] Heilmann SM, Jader LR, Sadowsky MJ, Schendel FJ, von Keitz MG, Valentas KJ. Hydrothermal carbonization of distiller's grains. Biomass Bioenergy 2011;35:2526-33.

[367] Hoekman SK, Broch A, Robbins C. Hydrothermal carbonization (HTC) of lignocellulosic biomass. Energy & Fuels 2011;25:1802-10.

[368] Xiao L-P, Shi Z-J, Xu F, Sun R-C. Hydrothermal carbonization of lignocellulosic biomass. Bioresour Technol 2012;118:619-23.

[369] Berge ND, Ro KS, Mao J, Flora JR, Chappell MA, Bae S. Hydrothermal carbonization of municipal waste streams. Environmental science & technology 2011;45:5696-703.

[370] Ramke H, Blöhse D, Lehmann H. Hydrothermal carbonization of organic municipal solid waste—scientific and technical principles. Müll und Abfall 2012;9:476-83.

[371] Stemann J, Ziegler F. Hydrothermal carbonisation (HTC): recycling of process water. Proceedings of 19th European Biomass Conference, Berlin2011.

[372] Erlach B, Tsatsaronis G. Upgrading of biomass by hydrothermal carbonisation: analysis of an industrial-scale plant design. 23rd International Conference on Efficiency, Cost, Optimization, Simulation and Environmental Impact of Energy Systems Lausanne, Switzerland2010. p. 14-7.

[373] Erlach B, Harder B, Tsatsaronis G. Combined hydrothermal carbonization and gasification of biomass with carbon capture. Energy 2012;45:329-38.

[374] Stemann J, Ziegler F. Assessment of the energetic efficiency of a continuously operating plant for hydrothermal carbonisation of biomass. World Renewable Energy Congress2011.

[375] Funke A, Ziegler F. Heat of reaction measurements for hydrothermal carbonization of biomass. Bioresour Technol 2011;102:7595-8.

[376] Wei L, Sevilla M, Fuertes AB, Mokaya R, Yushin G. Hydrothermal Carbonization of Abundant Renewable Natural Organic Chemicals for High-Performance Supercapacitor Electrodes. Advanced Energy Materials 2011;1:356-61.

[377] Tang K, Fu L, White RJ, Yu L, Titirici MM, Antonietti M, et al. Hollow Carbon Nanospheres with Superior Rate Capability for Sodium-Based Batteries. Advanced Energy Materials 2012;2:873-7.

[378] Tang K, White RJ, Mu X, Titirici MM, van Aken PA, Maier J. Hollow Carbon Nanospheres with a High Rate Capability for Lithium-Based Batteries. ChemSusChem 2012;5:400-3.

[379] Tusi MM, Brandalise M, Polanco NSdO, Correa OV, da Silva AC, Villalba JC, et al. Ni/Carbon Hybrid Prepared by Hydrothermal Carbonization and Thermal Treatment as Support for PtRu Nanoparticles for Direct Methanol Fuel Cell. Journal of Materials Science & Technology 2013;29:747-51.

[380] Wang Z-B, Li C-Z, Gu D-M, Yin G-P. Carbon riveted PtRu/C catalyst from glucose in-situ carbonization through hydrothermal method for direct methanol fuel cell. J Power Sources 2013;238:283-9.

[381] Kim D, Lee K, Park KY. Hydrothermal carbonization of anaerobically digested sludge for solid fuel production and energy recovery. Fuel 2014;130:120-5.

[382] He C, Giannis A, Wang J-Y. Conversion of sewage sludge to clean solid fuel using hydrothermal carbonization: Hydrochar fuel characteristics and combustion behavior. Applied Energy 2013;111:257-66.

[383] Kang S, Li X, Fan J, Chang J. Solid fuel production by hydrothermal carbonization of black liquor. Bioresour Technol 2012;110:715-8.

[384] Fang G, Kaneko S, Liu W, Xia B, Sun H, Zhang R, et al. Facile synthesis of nitrogen-doped carbon coated CoSnO3 via hydrothermal carbonization of carboxylated chitosan as anode materials for lithium-ion batteries. Appl Surf Sci 2013;283:963-7.

[385] Sevilla M, Gu W, Falco C, Titirici MM, Fuertes AB, Yushin G. Hydrothermal synthesis of microalgae-derived microporous carbons for electrochemical capacitors. J Power Sources 2014;267:26-32.

[386] Kurniawan A, Effendi C, Ong LK, Kurniawan F, Lin CX, Angkawijaya AE, et al. Preparation of nanoporous carbon microspheres by subcritical water carbonization and electrocapacitive study. Electrochim Acta 2013;111:99-107.

[387] Jiang W, Jia X, Luo Z, Wu X. Supercapacitor performance of spherical nanoporous carbon obtained by a CaCO3-assisted template carbonization method from polytetrafluoroethene waste and the electrochemical enhancement by the nitridation of CO(NH2)2. Electrochim Acta 2014;147:183-91.

[388] Tooming T, Thomberg T, Kurig H, Jänes A, Lust E. High power density supercapacitors based on the carbon dioxide activated d-glucose derived carbon electrodes and 1-ethyl-3-methylimidazolium tetrafluoroborate ionic liquid. J Power Sources 2015;280:667-77.

[389] Zheng C, Zhou X, Cao H, Wang G, Liu Z. Synthesis of porous graphene/activated carbon composite with high packing density and large specific surface area for supercapacitor electrode material. J Power Sources 2014;258:290-6.

[390] Unur E, Brutti S, Panero S, Scrosati B. Nanoporous carbons from hydrothermally treated biomass as anode materials for lithium ion batteries. Microporous Mesoporous Mater 2013;174:25-33.

[391] Álvarez-Murillo A, Sabio E, Ledesma B, Román S, González-García CM. Generation of biofuel from hydrothermal carbonization of cellulose. Kinetics modelling. Energy 2016;94:600-8.

[392] Patil SK, Lund CR. Formation and growth of humins via aldol addition and condensation during acid-catalyzed conversion of 5-hydroxymethylfurfural. Energy & Fuels 2011;25:4745-55.

[393] Rosatella AA, Simeonov SP, Frade RF, Afonso CA. 5-Hydroxymethylfurfural (HMF) as a building block platform: Biological properties, synthesis and synthetic applications. Green Chemistry 2011;13:754-93.

[394] Titirici M-M, White RJ, Falco C, Sevilla M. Black perspectives for a green future: hydrothermal carbons for environment protection and energy storage. Energy & Environmental Science 2012;5:6796-822.

[395] Falco C, Perez Caballero F, Babonneau F, Gervais C, Laurent G, Titirici M-M, et al. Hydrothermal carbon from biomass: structural differences between hydrothermal and pyrolyzed carbons via 13C solid state NMR. Langmuir 2011;27:14460-71.

[396] Kambo HS, Dutta A. Comparative evaluation of torrefaction and hydrothermal carbonization of lignocellulosic biomass for the production of solid biofuel. Energy Convers Manage 2015;105:746-55.

[397] Sevilla M, Fuertes AB. Chemical and structural properties of carbonaceous products obtained by hydrothermal carbonization of saccharides. Chemistry–A European Journal 2009;15:4195-203.

[398] Antal MJ, Mok WSL, Richards GN. Mechanism of formation of 5-(hydroxymethyl)-2-furaldehyde from d-fructose and sucrose. Carbohydr Res 1990;199:91-109.

[399] Sinag A, Kruse A, Schwarzkopf V. Formation and Degradation Pathways of Intermediate Products Formed during the Hydropyrolysis of Glucose as a Model Substance for Wet Biomass in a Tubular Reactor. Eng Life Sci 2003;3:469-73.

[400] Salak Asghari F, Yoshida H. Acid-catalyzed production of 5-hydroxymethyl furfural from D-fructose in subcritical water. Industrial & Engineering Chemistry Research 2006;45:2163-73.

[401] Sun X, Li Y. Colloidal Carbon Spheres and Their Core/Shell Structures with Noble-Metal Nanoparticles. Angew Chem 2004;116:607-11.

[402] Kambo HS, Dutta A. Strength, storage, and combustion characteristics of densified lignocellulosic biomass produced via torrefaction and hydrothermal carbonization. Applied Energy 2014;135:182-91.

[403] Hoekman SK, Broch A, Warren A, Felix L, Irvin J. Laboratory pelletization of hydrochar from woody biomass. Biofuels 2014;5:651-66.

[404] Gil MV, Oulego P, Casal MD, Pevida C, Pis JJ, Rubiera F. Mechanical durability and combustion characteristics of pellets from biomass blends. Bioresour Technol 2010;101:8859-67.

[405] Reza MT, Lynam JG, Vasquez VR, Coronella CJ. Pelletization of biochar from hydrothermally carbonized wood. Environmental Progress & Sustainable Energy 2012;31:225-34.

[406] Liu Z, Guo Y, Balasubramanian R, Hoekman SK. Mechanical stability and combustion characteristics of hydrochar/lignite blend pellets. Fuel 2016;164:59-65.

[407] José-Vicente O-V, Enrique G-A, Patricia G-G. ANALYSIS OF DURABILITY AND DIMENSIONAL STABILITY OF HYDROTHERMAL CARBONIZED WOODEN PELLETS. WOOD RESEARCH 2016;61:321-30.

[408] Wirth B, Mumme J. Anaerobic digestion of waste water from hydrothermal carbonization of corn silage. Applied Bioenergy 2014;1.

[409] Erdogan E, Atila B, Mumme J, Reza MT, Toptas A, Elibol M, et al. Characterization of products from hydrothermal carbonization of orange pomace including anaerobic digestibility of process liquor. Bioresour Technol 2015;196:35-42.

[410] Wirth B, Reza T, Mumme J. Influence of digestion temperature and organic loading rate on the continuous anaerobic treatment of process liquor from hydrothermal carbonization of sewage sludge. Bioresour Technol 2015;198:215-22.

[411] Wirth B, Reza MT. Continuous anaerobic degradation of liquid condensate from steam-derived hydrothermal carbonization of sewage sludge. ACS Sustainable Chemistry & Engineering 2016;4:1673-8.

[412] Poerschmann J, Weiner B, Wedwitschka H, Baskyr I, Koehler R, Kopinke F-D. Characterization of biocoals and dissolved organic matter phases obtained upon hydrothermal carbonization of brewer's spent grain. Bioresour Technol 2014;164:162-9.

[413] Oliveira I, Blöhse D, Ramke H-G. Hydrothermal carbonization of agricultural residues. Bioresour Technol 2013;142:138-46.

[414] Uddin MH, Reza MT, Lynam JG, Coronella CJ. Effects of water recycling in hydrothermal carbonization of loblolly pine. Environmental Progress & Sustainable Energy 2014;33:1309-15.

[415] Stemann J, Putschew A, Ziegler F. Hydrothermal carbonization: process water characterization and effects of water recirculation. Bioresour Technol 2013;143:139-46.

[416] Weiner B, Poerschmann J, Wedwitschka H, Koehler R, Kopinke F-D. Influence of process water reuse on the hydrothermal carbonization of paper. ACS Sustainable Chemistry & Engineering 2014;2:2165-71.

[417] Kabadayi Catalkopru A, Kantarli IC, Yanik J. Effects of spent liquor recirculation in hydrothermal carbonization. Bioresour Technol 2017;226:89-93.

[418] Shen Y, Yu S, Ge S, Chen X, Ge X, Chen M. Hydrothermal carbonization of medical wastes and lignocellulosic biomass for solid fuel production from lab-scale to pilot-scale. Energy 2017;118:312-23.

[419] Tremel A, Stemann J, Herrmann M, Erlach B, Spliethoff H. Entrained flow gasification of biocoal from hydrothermal carbonization. Fuel 2012;102:396-403.

[420] Gao P, Zhou Y, Meng F, Zhang Y, Liu Z, Zhang W, et al. Preparation and characterization of hydrochar from waste eucalyptus bark by hydrothermal carbonization. Energy 2016;97:238-45.

[421] Álvarez-Murillo A, Sabio E, Ledesma B, Román S, González-García C. Generation of biofuel from hydrothermal carbonization of cellulose. Kinetics modelling. Energy 2016;94:600-8.

[422] Nakason K, Panyapinyopol B, Kanokkantapong V, Viriya-empikul N, Kraithong W, Pavasant P. Characteristics of hydrochar and liquid fraction from hydrothermal carbonization of cassava rhizome. Journal of the Energy Institute.

[423] Tekin K, Karagöz S, Bektaş S. A review of hydrothermal biomass processing. Renew Sustain Energy Rev 2014;40:673-87.

[424] Hoekman SK, Broch A, Felix L, Farthing W. Hydrothermal carbonization (HTC) of loblolly pine using a continuous, reactive twin-screw extruder. Energy Convers Manage 2017;134:247-59.

[425] Reza MT, Yang X, Coronella CJ, Lin H, Hathwaik U, Shintani D, et al. Hydrothermal carbonization (HTC) and pelletization of two arid land plants bagasse for energy densification. ACS Sustainable Chemistry & Engineering 2015;4:1106-14.

[426] Liu Z, Quek A, Balasubramanian R. Preparation and characterization of fuel pellets from woody biomass, agro-residues and their corresponding hydrochars. Applied Energy 2014;113:1315-22.

[427] Yang W, Wang H, Zhang M, Zhu J, Zhou J, Wu S. Fuel properties and combustion kinetics of hydrochar prepared by hydrothermal carbonization of bamboo. Bioresour Technol 2016;205:199-204.

[428] Elaigwu SE, Greenway GM. Microwave-assisted hydrothermal carbonization of rapeseed husk: A strategy for improving its solid fuel properties. Fuel Process Technol 2016;149:305-12.

[429] Fu Y, Ye J, Chang J, Lou H, Zheng X. Solid fuel production by hydrothermal carbonization of water-like phase of bio-oil. Fuel 2016;180:591-6.

[430] Koottatep T, Fakkaew K, Tajai N, Pradeep SV, Polprasert C. Sludge stabilization and energy recovery by hydrothermal carbonization process. Renewable Energy 2016;99:978-85.

[431] Guo S, Dong X, Wu T, Shi F, Zhu C. Characteristic evolution of hydrochar from hydrothermal carbonization of corn stalk. J Anal Appl Pyrolysis 2015;116:1-9.

[432] Mäkelä M, Benavente V, Fullana A. Hydrothermal carbonization of lignocellulosic biomass: Effect of process conditions on hydrochar properties. Applied Energy 2015;155:576-84.

[433] Kim D, Lee K, Park KY. Upgrading the characteristics of biochar from cellulose, lignin, and xylan for solid biofuel production from biomass by hydrothermal carbonization. Journal of Industrial and Engineering Chemistry 2016;42:95-100.

[434] Hamelinck CN, Faaij AP. Future prospects for production of methanol and hydrogen from biomass. J Power Sources 2002;111:1-22.

[435] Tijmensen MJ, Faaij AP, Hamelinck CN, van Hardeveld MR. Exploration of the possibilities for production of Fischer Tropsch liquids and power via biomass gasification. Biomass Bioenergy 2002;23:129-52.

[436] Phillips S. Technoeconomic analysis of a lignocellulosic biomass indirect gasification process to make ethanol via mixed alcohols synthesis. Industrial & Engineering Chemistry Research 2007;46:8887-97.

[437] Sarkar S, Kumar A. Biohydrogen production from forest and agricultural residues for upgrading of bitumen from oil sands. Energy 2010;35:582-91.

[438] Patel M, Zhang X, Kumar A. Techno-economic and life cycle assessment on lignocellulosic biomass thermochemical conversion technologies: A review. Renew Sustain Energy Rev 2016;53:1486-99.

[439] Dutta A, Talmadge M, Hensley J, Worley M, Dudgeon D, Barton D, et al. Process design and economics for conversion of lignocellulosic biomass to ethanol: Thermochemical pathway by indirect gasification and mixed alcohol synthesis. National Renewable Energy Laboratory (NREL), Golden, CO.; 2011.

[440] Mirkouei A, Haapala KR, Sessions J, Murthy GS. A review and future directions in techno-economic modeling and optimization of upstream forest biomass to bio-oil supply chains. Renew Sustain Energy Rev 2017;67:15-35.

[441] Zhao X, Brown TR, Tyner WE. Stochastic techno-economic evaluation of cellulosic biofuel pathways. Bioresour Technol 2015;198:755-63.

[442] Thilakaratne R, Wright MM, Brown RC. A techno-economic analysis of microalgae remnant catalytic pyrolysis and upgrading to fuels. Fuel 2014;128:104-12.

[443] Do TX, Lim Y-i, Yeo H. Techno-economic analysis of biooil production process from palm empty fruit bunches. Energy Convers Manage 2014;80:525-34.

[444] Brown D, Rowe A, Wild P. A techno-economic analysis of using mobile distributed pyrolysis facilities to deliver a forest residue resource. Bioresour Technol 2013;150:367-76.

[445] Rogers J, Brammer J. Estimation of the production cost of fast pyrolysis bio-oil. Biomass Bioenergy 2012;36:208-17.

[446] Ghezzaz H, Stuart P. Biomass availability and process selection for an integrated forest biorefinery. Pulp & Paper Canada 2011;112:19-26.

[447] Trippe F, Fröhling M, Schultmann F, Stahl R, Henrich E. Techno-economic analysis of fast pyrolysis as a process step within biomass-to-liquid fuel production. Waste and Biomass Valorization 2010;1:415-30.

[448] Anex RP, Aden A, Kazi FK, Fortman J, Swanson RM, Wright MM, et al. Techno-economic comparison of biomass-to-transportation fuels via pyrolysis, gasification, and biochemical pathways. Fuel 2010;89:S29-S35.

[449] Wright MM, Daugaard DE, Satrio JA, Brown RC. Techno-economic analysis of biomass fast pyrolysis to transportation fuels. Fuel 2010;89:S2-S10.

[450] Oasmaa A, Solantausta Y, Arpiainen V, Kuoppala E, Sipilä K. Fast pyrolysis bio-oils from wood and agricultural residues. Energy & Fuels 2009;24:1380-8.

[451] Magalhães AI, Rodriguez AL, Putra ZA, Thielemans G. Techno-economic assessment of biomass pre-conversion processes as a part of biomass-to-liquids line-up. Biofuels, Bioproducts and Biorefining 2009;3:584-600.

[452] Beckman D, Elliott D, Gevert B, Hörnell C, Kjellström B. Techno-economic assessment of selected biomass liquefaction processes. 1990.

[453] Kerssen M, Berends R. Life cycle analysis of the HTU process. Apeldoom, The Netherlands, Dutch Research Organization for Environment, Energy and Process Innovation, www. novem. nl/default. asp; 2005.

[454] Zhu Y, Biddy MJ, Jones SB, Elliott DC, Schmidt AJ. Techno-economic analysis of liquid fuel production from woody biomass via hydrothermal liquefaction (HTL) and upgrading. Applied Energy 2014;129:384-94.

[455] Kumar M, Oyedun AO, Kumar A. Hydrothermal liquefaction of biomass for production of diluents for bitumen transport (Submitted).

[456] Matsumura Y. Evaluation of supercritical water gasification and biomethanation for wet biomass utilization in Japan. Energy Convers Manage 2002;43:1301-10.

[457] Gasafi E, Reinecke M-Y, Kruse A, Schebek L. Economic analysis of sewage sludge gasification in supercritical water for hydrogen production. Biomass Bioenergy 2008;32:1085-96.

[458] Al-Mosuli D, Barghi S, Fang Z, Xu CC. Techno-economic Analysis of Renewable Hydrogen Production via SCWG of Biomass Using Glucose as a Model Compound. Near-critical and Supercritical Water and Their Applications for Biorefineries: Springer; 2014. p. 445-71.

[459] Zhu Y, Albrecht KO, Elliott DC, Hallen RT, Jones SB. Development of hydrothermal liquefaction and upgrading technologies for lipid-extracted algae conversion to liquid fuels. Algal Research 2013;2:455-64.

[460] Faeth JL, Valdez PJ, Savage PE. Fast hydrothermal liquefaction of Nannochloropsis sp. to produce biocrude. Energy & Fuels 2013;27:1391-8.

[461] Elliott DC, Neuenschwander GG, Hart TR. Combined hydrothermal liquefaction and catalytic hydrothermal gasification system and process for conversion of biomass feedstocks. Google Patents; 2013.

[462] Jones S, Zhu Y, Anderson D, Hallen R, Elliott DC, Schmidt AJ, et al. Process design and economics for the conversion of algal biomass to hydrocarbons: whole algae hydrothermal liquefaction and upgrading. US Department of Energy Bioenergy Technologies Office 2014.

[463] Spath PL, Mann M, Amos W. Update of hydrogen from biomass-determination of the delivered cost of hydrogen. Department of Energy and National Renewable Energy Laboratory, NREL/MP-510-33112 2003.

[464] Balat H, Kırtay E. Hydrogen from biomass – Present scenario and future prospects. Int J Hydrogen Energy 2010;35:7416-26.

[465] Kruse A, Abeln J, Dinjus E, Kluth M, Petrich G, Schacht M, et al. Gasification of biomass and model compounds in hot compressed water. International Meeting of the GVC-Fachausschuβ" Hochdruckverfahrenstechnik", Karlsruhe, Germany1999.

[466] Amos W. Assessment of supercritical water gasification: alternative designs. Golden, USA: National Renewable Energy Laboratory 1999.

[467] Brandenberger M, Matzenberger J, Vogel F, Ludwig C. Producing synthetic natural gas from microalgae via supercritical water gasification: A techno-economic sensitivity analysis. Biomass Bioenergy 2013;51:26-34.

[468] Knorr D, Lukas, J., Schoen, P. 2013. Production of Advanced Biofuels via Liquefaction – Hydrothermal Liquefaction Reactor Design: April 5, 2013. NREL/SR-5100-60462, National Renewable Energy Laboratory, Golden, Colorado, USA.

Figures

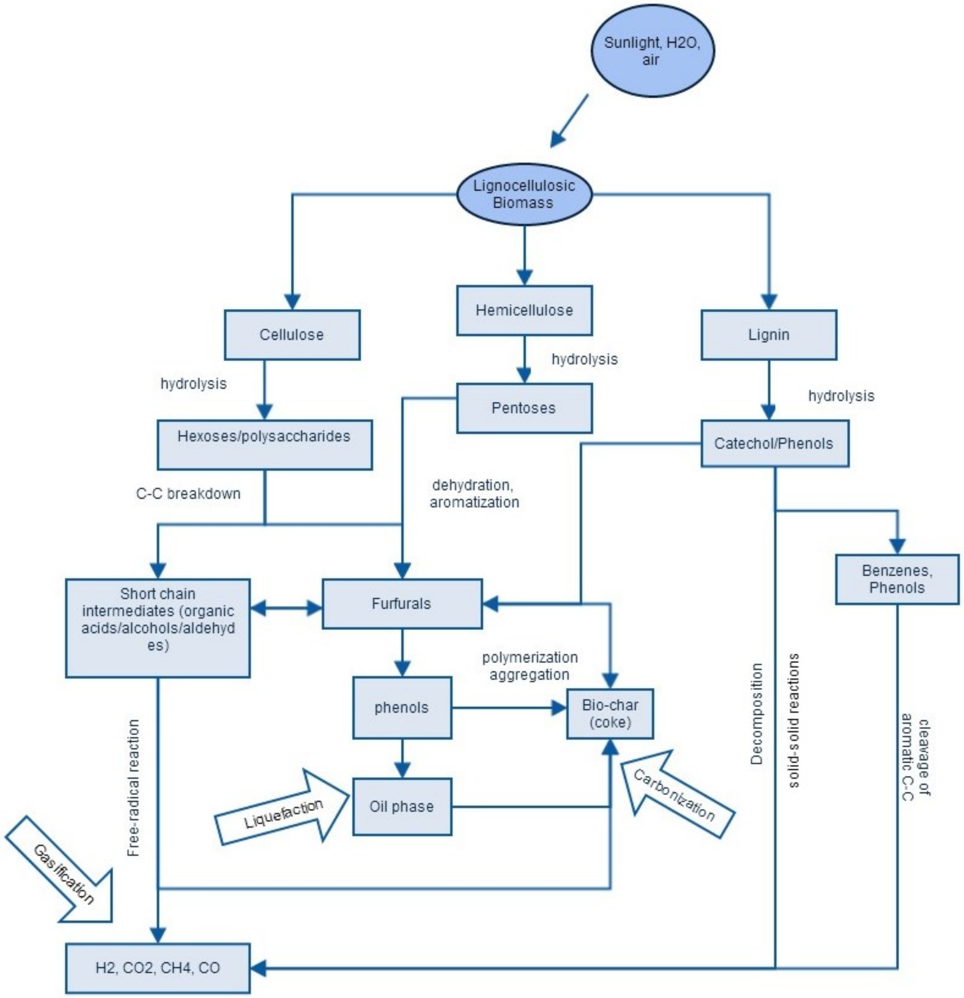

Figure 1: Schematic of a hydrothermal processing technology

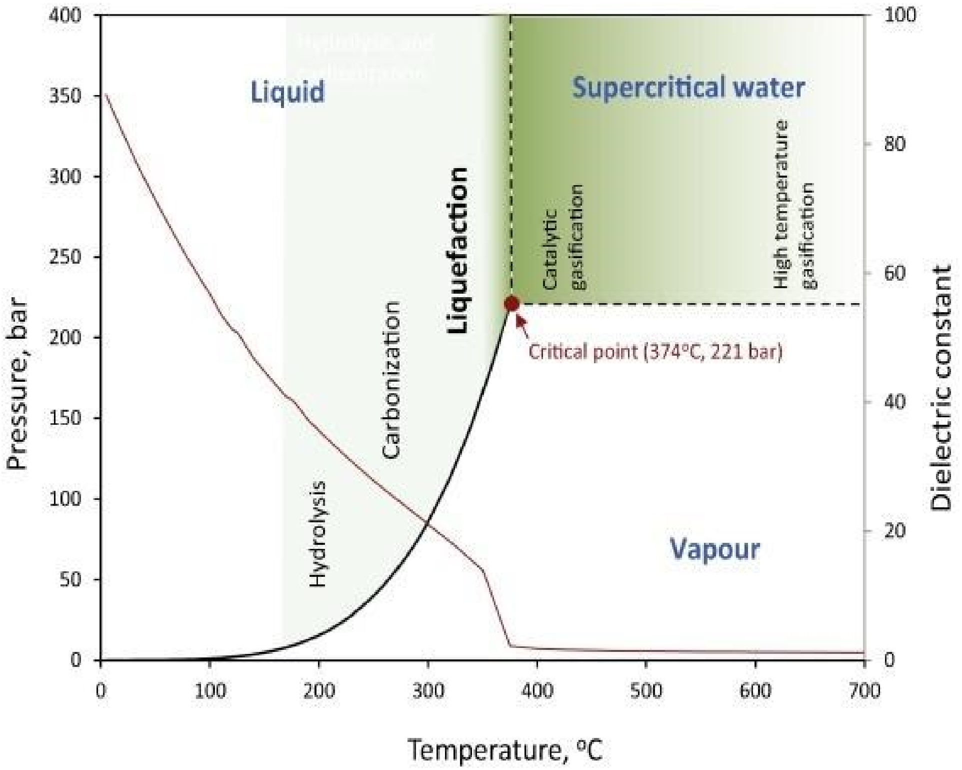

Figure 2: Phase diagram of water (pressure-temperature) and static dielectric constant at 200 bar (Adapted from: Tran et al. [36])

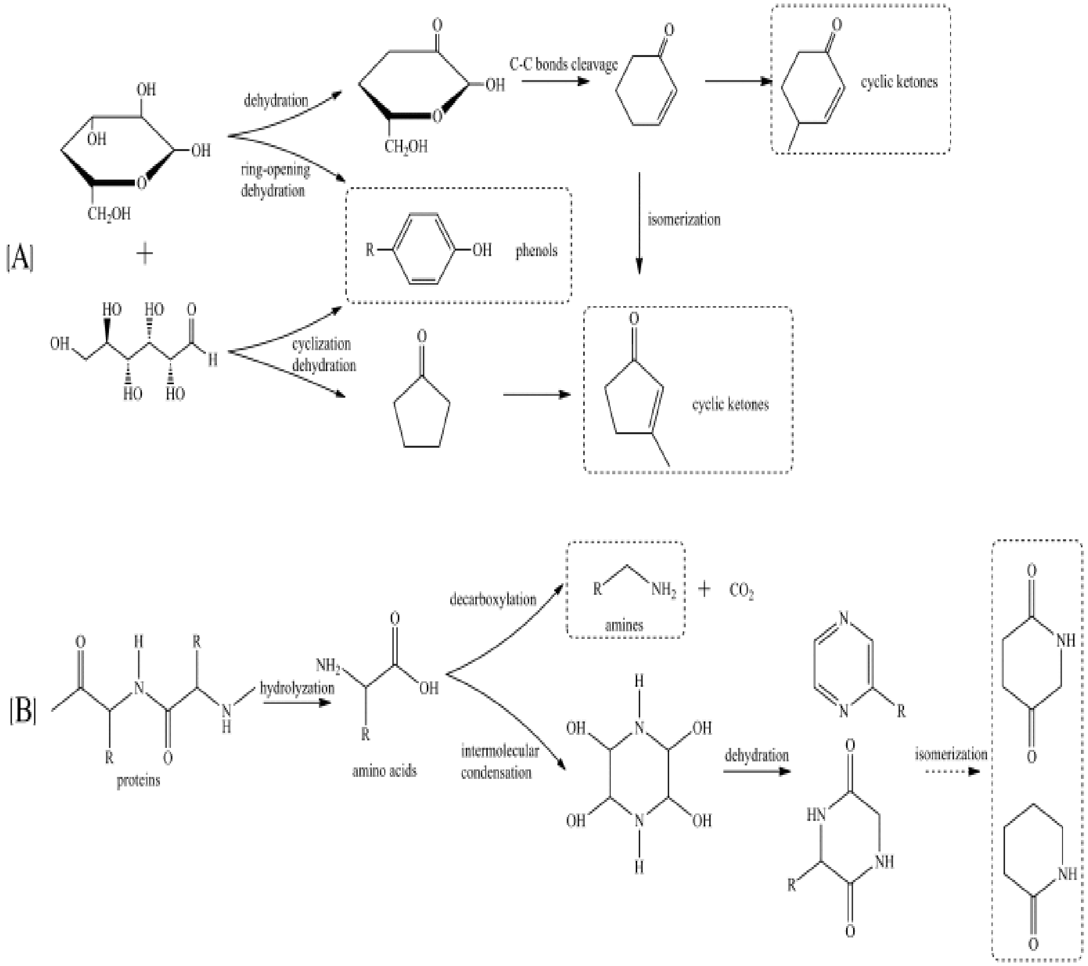

Figure 3: Plausible pathways of formation of bio-oils via hydrothermal liquefaction of biomass (Adapted from: Yang et al. [134])

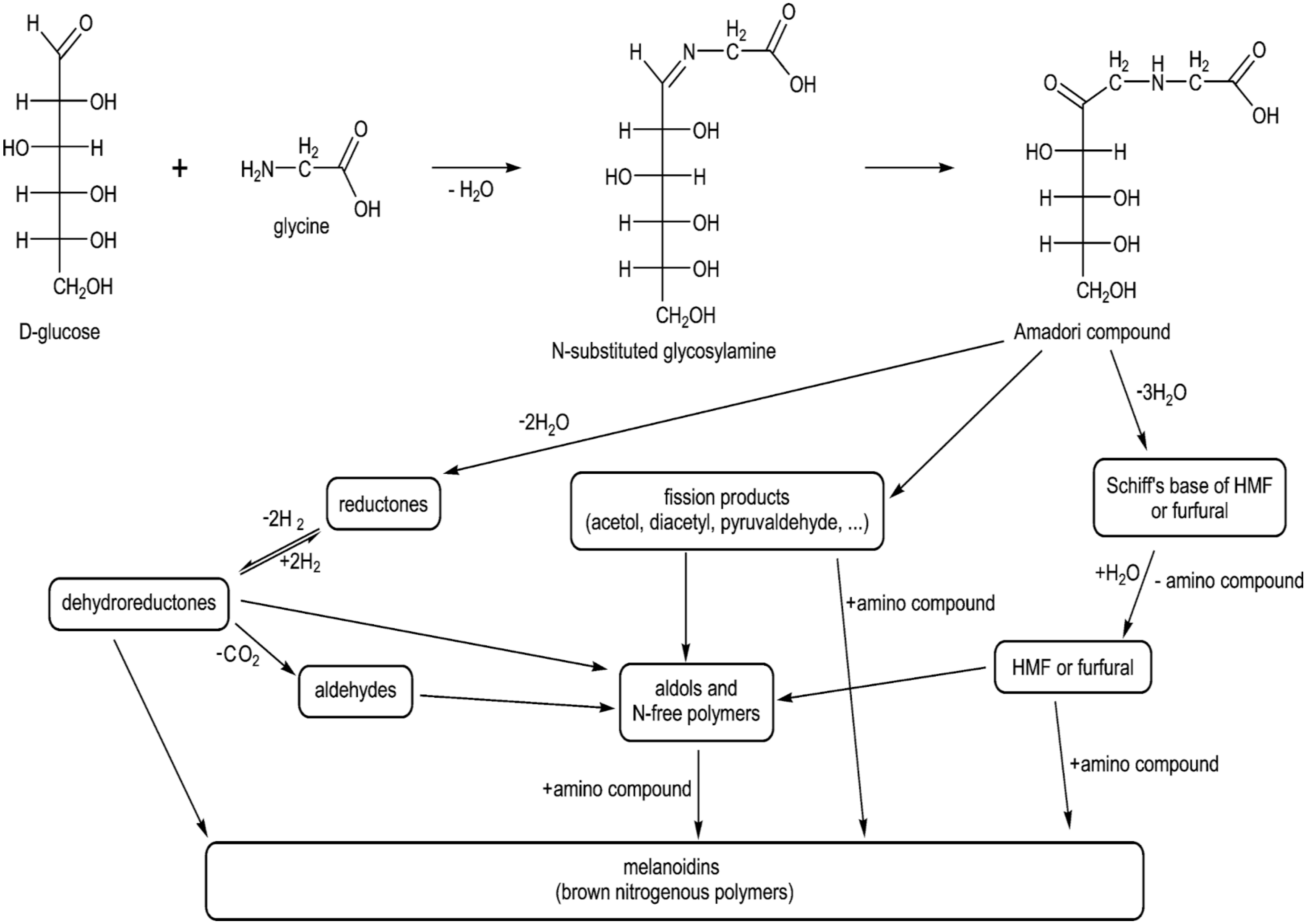

Figure 4: Schematic of Maillard reaction network (Adapted from Peterson et al. [138])

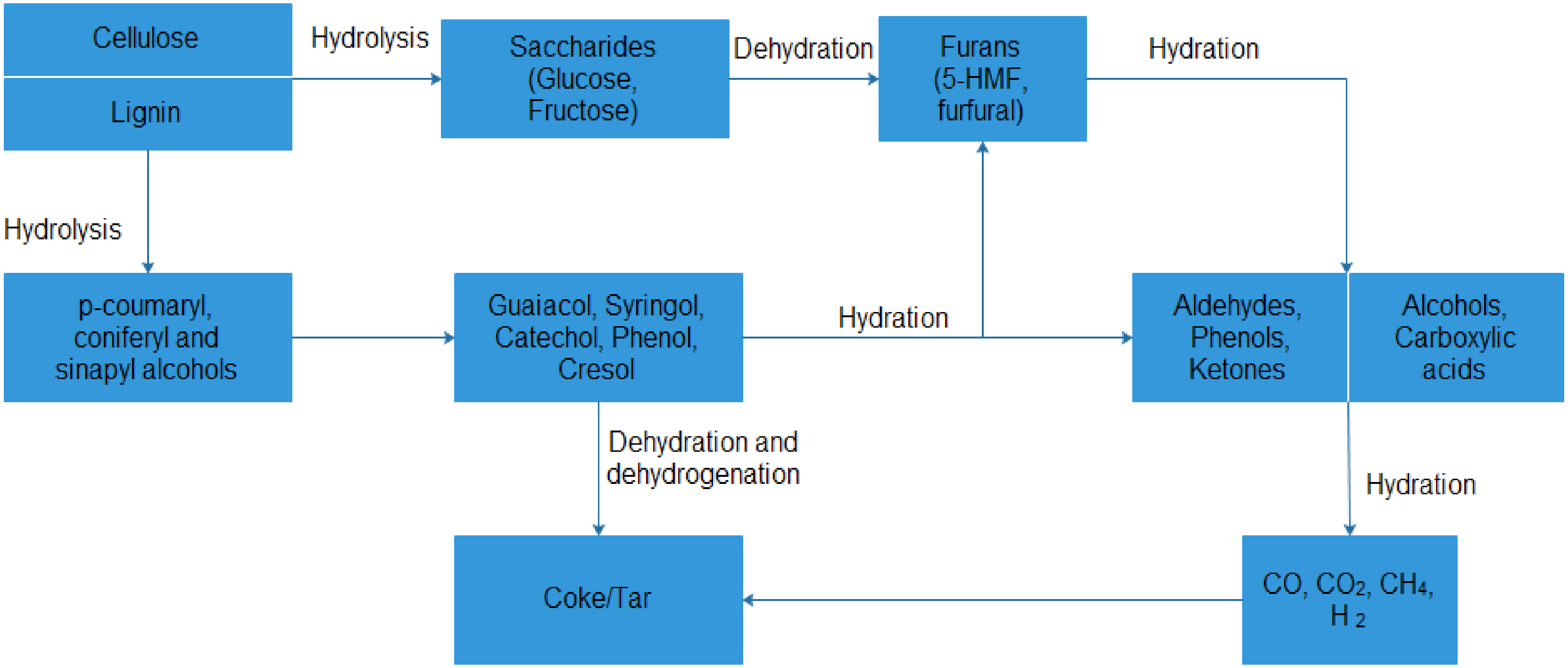

Figure 5: Hydrothermal gasification of biomass to gaseous products via aqueous intermediates (Adapted from: Madenoğlu et al. [246])

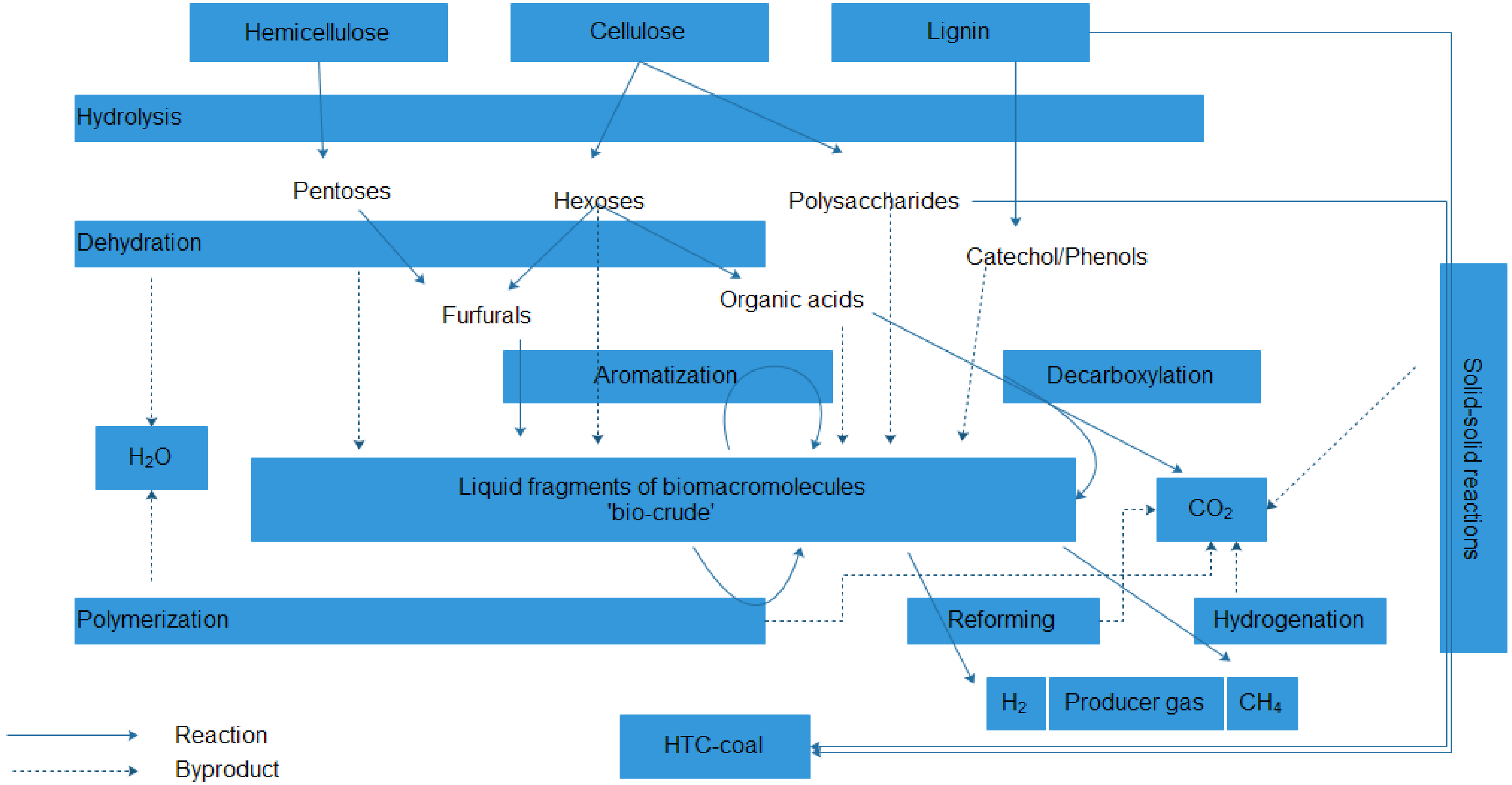

Figure 6: Reaction pathways involved in hydrothermal carbonization (Adapted from: Kruse et al. [13])

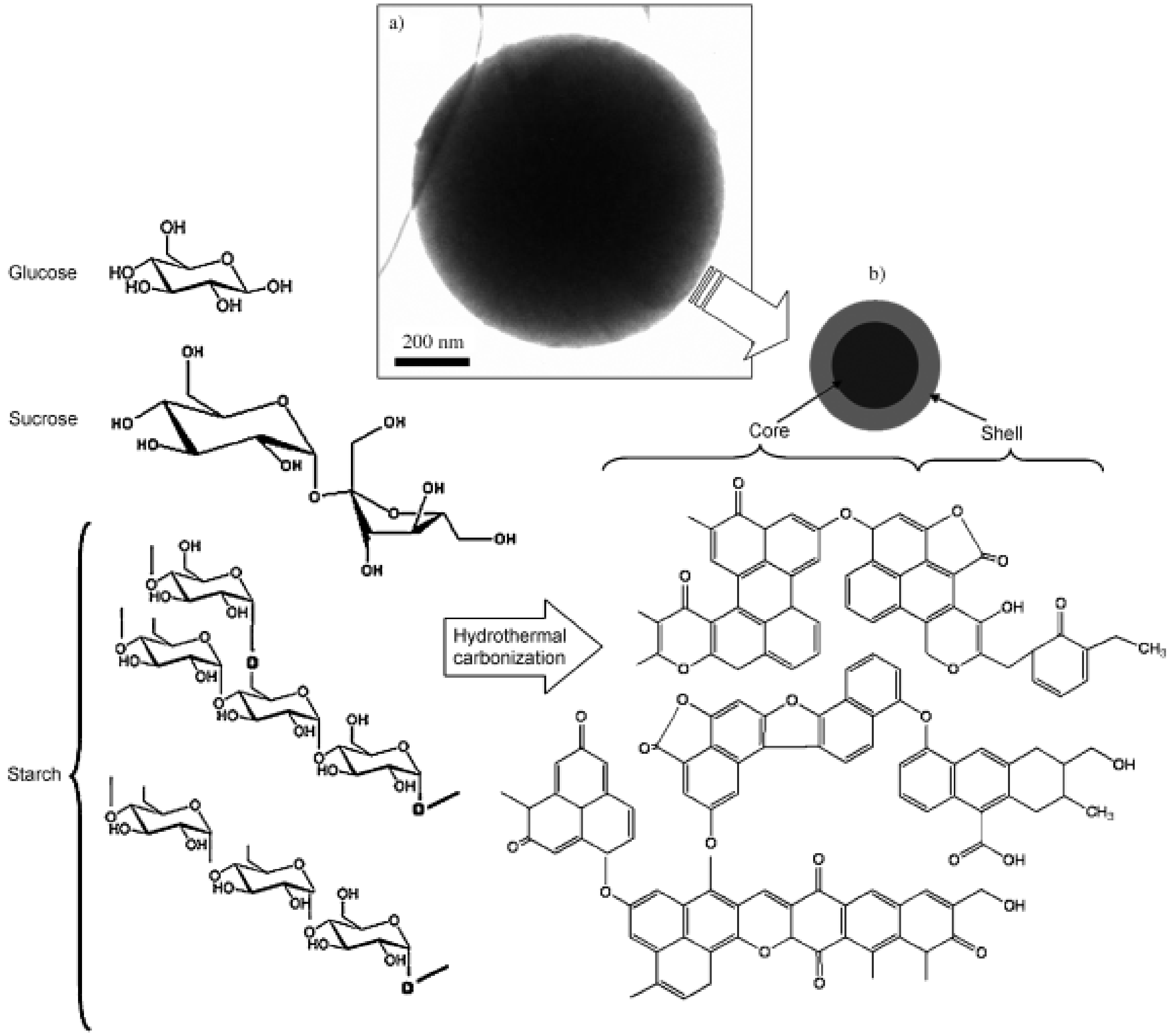

Figure 7: Diagram showing hydrophilic/hydrophobic core–shell structure of the hydrochar microspheres via hydrothermal carbonization (Adapted from Sevilla et al. [397]).

Table 1: Properties of water under different temperature regimes

Parameters	Normal water	Sub-critical water	Super-critical water
Temperature (°C)	25	250	400
Pressure (MPa)	0.1	5	25
Density (g/cm^3)	0.997	0.80	0.17
Viscosity (m Pa s)	0.89	0.11	0.03
Dielectric constant	78.5	27.1	5.9
Heat capacity (KJ kg^{-1} K^{-1})	4.22	4.86	13
pK$_{su}$	14.0	11.2	19.4
Thermal conductivity (mW m^{-1} K^{-1})	608	620	160

Table 2: Summary of factors influencing the hydrothermal liquefaction of biomass

Factors	Biomass type	Reaction conditions	Remarks	Ref.
Temperature	Jack pine powder	200 - 350 °C	25% increase in oil yield with 150 °C increase in temperature	[139]
	Microalgae	180-300 ˚C	Temperatures lower than 275 ˚C promote lipid extraction. Temperatures above 275 ˚C facilitate the degradation of protein and carbohydrates in biomass, which increases the oil yield.	[143]
	Palm biomass	330-390 ˚C	A temperature of 390 ˚C yields maximum bio-oil due to the increase in the rate of decomposition via the radical mechanism.	[145]
	Algal cultures	260-320 ˚C	The highest bio-crude yield	[146]

		was obtained at 300 ˚C. An increase in temperature caused the bio-crude to decompose into char/gas.	
Microalgae	250-400 ˚C	The maximum bio-oil yield of 51.22 wt% was obtained at 400 ˚C, the temperature considered to be optimum for bio-oil production.	[147]
Algae	330-370 ˚C	The maximum bio-oil yield was obtained at 360 ˚C. Increasing the temperature had positive influence on higher heating value.	[151]
Cornstalks	240-350 ˚C	Temperatures from 260 ˚C - 320 ˚C had no significant effect on bio-oil yield; however, the solid yield fell with an increase in temperature.	[152]
Rice straw	280-320 ˚C	Up to 300 ˚C, there was not significant change in the bio-oil product distribution. However, beyond 320 ˚C, bio-oil yield fell.	[153]
Sawdust	180- 280 °C	Oil yield increased with temperature.	[140]
Swine manure	260-340 °C	Increasing temperature from 260 to 340 °C increased the amount of bio-oil by 9.3 %.	[141]
Wood stalks	250 -290 ˚C	The bio-oil yield increased from 44.5% to 50.4% with an increase in temperature in	[144]

		ethanol solvent.	
Microalgae	250-350 ˚C	Conversion efficiency increased with temperature in this order: lipids > proteins > carbohydrates.	[148]
Oilmill wastewater	240-300 ˚C	Bio-oil yield improved from 28.25 wt% to 58.09 wt% with an increase in temperature while the solid yield fell from 43.87 wt% to 17.18 wt%. The optimal temperature was 280 ˚C.	[21]
Algae	180-330 ˚C	Nannochloropsis sp. attained the highest bio-oil yield of 47.5%. Increasing the temperature improved bio-crude yield.	[149]
Crude glycerol and aspen wood	380-420 ˚C	Biocrude and char yields, as well as biocrude composition, were not affected by temperature changes.	[150]
Algae	180-300 ˚C	Increasing the temperature improved the bio-crude oil yield. Biocrude yield increased from 11% at 250 ˚C to 16.98% at 300 ˚C, suggesting that the increase in bio-crude yield occurred not only from lipids, but also from other non-lipid components such as proteins	[142]

			and carbohydrates. The improvement in biocrude oil is attributed to hydrolysis and repolymerization.	
Particle size	Grass perennials	350 °C	Particle size has no effect on liquid oil yield.	[158]
Pressure	Coal	370 - 490 °C; up to 12.2 MPa	An increase in pressure resulted in high liquid yield due to improved solvent power and diffusivity.	[154]
	Glucose	300 - 400 °C, 25-40 MPa	Rate constant for glucose degradation was lowered by a rise in pressure, which could likely be due to the reduction in the epimerization rate to fructose.	[155]
	Cellobiose	300 - 400 °C, 25 - 40 MPa	Hydrolysis selectivity rose by 10 % with an increase in pressure from 30 to 40 MPa.	[156]
	Fruit bunch, palm, kernel shell	330-390 ˚C, 25-35 MPa	The increase in pressure caused an increase in solvent density and solubility. However, the increase in pressure also caused a caging effect. At 390 ˚C, the increase of pressure from 25 to 35 MPa reduced bio-oil yields.	[157]
Residence time	Sawdust	180 - 280 °C	In temperatures from 250 to 280 °C, longer reaction	[159]

		times reduced oil yield due to secondary reactions; however, oil yield increased at a low temperature (180 °C).	
Poplar wood	350 °C	Poplar suppressed the bio-oil yield except for very high biomass-to-water ratios	[160]
Sawdust	150–450 °C	The conversion and yield of gaseous products are the same but the yield of *bio-oil* increases with an increase in reaction time.	[161]
Kenaf	300 ˚C	The liquefaction time of 60 min resulted in an oil yield of 77.2%.	[162]
Willow	400 ˚C, 32 MPa, 0-20 min	A longer reaction time negatively influenced the bio-crude yield while solid residues and gas yield increased, signifying that re-polymerization and gasification are favored at longer residence times.	[163]
Oilmill wastewater	240-300 ˚C, 15-45 min	Increasing residence time promoted bio-oil yield, in this case, an increase from 55.76 wt% at 15 min to 58.09 wt% after 30 min. With a further increase in time, gas and solid residue yield increased. This could be attributed to competing	[21]

		depolymerization and hydrolysis reactions.	
Fermented corn stalks	250-400 ˚C 15-105 min	Bio-oil yield increased until 30 min, after which it fell, indicating that a longer residence time caused depolymerization and cracking of bio-oil.	[164]
Microalgae	100-400 ˚C, 10 s – 60 min	Solid product yields fell with longer reaction times. However, longer residence times (t > 40 min) at higher temperatures (300 ˚C) reduced bio-crude yield.	[165]
Spent coffee grounds	5-30 min	The highest bio-crude yield (31.63%) was reached after 10 min, after which yield fell. The bio-oil decomposed with time.	[166]
Algae	350 ˚C, 10-60 min	A longer reaction time reduced the yield of water-soluble biocrude and increased the yield of water-insoluble biocrude. However, total bio-crude yield was not affected by residence time.	[167]
Microalgae	350 ˚C; 1.4-5.8 min	Higher bio-crude yields were obtained at lower residence times, and greater energy recovery was possible at a residence time of 5.8 min.	[168]

	Algae	220-400 ˚C, 10-60 min	Initially, biocrude yield increased (39.54% at 50 min), but after 50 min. it decreased.	[169]
	Swine carcasses	150-250 ˚C; 20-120 min	The yield of bio-oil improved from 45.5 wt% (20 min) to 58.2 wt% (60 min). The longer reaction time (60-120 min) lowered the yield due to prevailing reactions involving secondary cracking.	[170]
	Microalgae and lignocellulosics	300 ˚C, 20-90 min	Bio-crude yield increased with an increase in reaction time up to 60 min, after which it decreased. The decrease is attributed to the repolymerization and recondensation of bio-crude.	[171]

Table 3: Homogeneous catalysts used for the hydrothermal liquefaction of model compounds and biomass

Model compounds/ Real biomass	Operating parameters	Reactor/ device/ tubing	Catalysts (with/ without support)	Key findings/remarks/observations	Ref.
Algae	300 ˚C	Bench-scale micro-reactor	KOH	Bio-crude yield increased from 16.98% (without catalyst) to 22.67% with KOH after 30 min at 10% solid loading. The incorporation of the catalyst improved the extraction of carbohydrates.	[142]
Kraft lignin	280-350 ˚C	Batch	K_2CO_3	The catalyst increased the yield of liquid products and reduced char formation. The catalyst improved the yield of monomeric aromatics.	[192]
Wood	280 ˚C	Batch	K_2CO_3, KOH, Na_2CO_3, NaOH	With K_2CO_3, the highest bio-oil yield of 34.9 wt% with the lowest solid residue yield of 6.8 wt% was obtained. The order of reactivity	[193]

				based on liquid yield was: K_2CO_3 > KOH > Na_2CO_3 > NaOH	
Sorghum	300 ˚C	Tubular	KOH, K_2CO_3	With K_2CO_3, biocrude had a HHV of 33.1 MJ kg^{-1}, and the highest biocrude yield was 61.8%.	[194]
Pinewood sawdust	300 ˚C	Autoclave	K_2CO_3	The use of K_2CO_3 doubled the bio-oil yield. The maximum bio-oil yield (30.8 wt%) and the minimum solid yield (28.9 wt%) were obtained with ethanol solvent. The use of water as solvent reduced the bio-oil yield as a fraction of bio-oil was found in the aqueous phase.	[195]
Microalga		Batch	Na_2CO_3	Na_2CO_3 increased bio-crude yield to 51.6% from around 29.2% without a catalyst. The catalyst also led to the lowest energy consumption ratio during the hydrothermal run.	[196]
Birchwood sawdust	300 ˚C	Bench top	KOH, K_2CO_3	Bio-crude oil yield with KOH more than doubled (~ 40 wt%) that under non-catalytic reaction. Also, solid residue decreased from ~ 33 to 12 wt%.	[197]
Blackcurrant pomace	290-335 ˚C	Batch	NaOH	The catalyst increased bio-oil yield and reduced char formation.	[198]
Bamboo chopsticks	290-380 ˚C	Autoclave	K_2CO_3	At 290 ˚C, yield reached 21.2 wt% compared to 3.8 wt% in a non-catalytic run. In addition, the heating value increased to 31.6 MJ kg^{-1}, showing the effectiveness of the catalyst.	[199]
Rice straw	220-300 ˚C	Autoclave	Na_2CO_3	The catalyst improved hydrolysis	[200]

				of cellulose and hemicellulose in the presence of glycerol. Na_2CO_3 promoted alcohol formation. Bio-oil yield was 50.31 wt% under optimum conditions of 260 ˚C.	
Dried distiller grain with solubles	350 ˚C	Bomb type	K_2CO_3	The catalyst, together with the recycled HTL aqueous phase, increased the yield compared to non-catalytic HTL; however, the water content in the bio-crude also increased.	[201]
Sewage sludge	400-500 ˚C	Batch	K_2CO_3, Na_2CO_3	Catalysts decreased the yield of bio-crude at 50 wt% of dried sludge.	[202]
Algae	250-350 ˚C		Na_2CO_3	The catalyst improved the bio-crude yield for high-carbohydrate biomass at higher temperatures (300-350 ˚C), while high-protein biomass yielded more bio-oil at a lower temperature (250 ˚C).	[203]
Wood	280 °C	autoclave	K_2CO_3	The absence of water yielded liquid products equivalent to a biomass/water ratio of 6. 1 M. K_2CO_3 showed the maximum biomass conversion along with considerable drop in solid residue (by 4%).	[140]
Corn stalk	410 °C, 25 MPa	fixed-bed	Na_2CO_3	The catalyst had a positive effect at relatively higher temperatures. Yield conversions increased to 95 wt % (dry basis); 77% liquid product yield was reported at 25 MPa.	[185]

Pinewood sawdust	300 °C, ~ 7.93 MPa	autoclave	K_2CO_3	K_2CO_3 doubled bio-oil yield. Maximum bio-oil was attained (30.8 wt%) and the minimum solid residue yield (28.9 wt%) when ethanol was used as a solvent.	[186]
Oil palm shell	210 - 330 °C	autoclave	K_2CO_3, Na_2CO_3, NaOH	Similar results were obtained with 10% K_2CO_3 and 10% Na_2CO_3 while 10% NaOH had maximum solid conversion (84 %) and liquid product (53.4%). 10 % NaOH also reduced the gaseous product yield.	[182]
Barley straw	300 °C	autoclave	K_2CO_3	K_2CO_3 produced more phenolic compounds and less carboxylic acid. Further analysis of solid residue confirmed improved decarboxylation of barley straw liquefaction with K_2CO_3. Carbon and energy recovery doubled with the catalyst. High bio-crude yield (34.85 wt%) was achieved with K_2CO_3.	[191]
Barley straw	280 - 400 °C	Batch	K_2CO_3	A lower temperature favored the formation of biocrude. High biomass conversion (> 87 wt %) was observed. The bio-crude yields were in the range of 20.35-35.24 wt%. Optimal HTL conditions were 300 °C. HHVs of bio-crude increased with temperature, ranging from 26.75 to 35.48 MJ/kg. Bio-crude consisted of carboxylic acid, phenolics, ketones,	[190]

				and aldehydes.	
Cellulose	200 – 350 °C, 3 MPa	Autoclave	Na_2CO_3	Alkali catalyst inhibited the formation of char from oil and caused stabilization of oil.	[183]
Polysaccharides	200 °C	Bomb-type batch	CO_2	The yield of glucose increased by 49.3 %. The production of 5-HMF, a secondary decomposition product of hexoses, dropped more in CO_2-enriched water than in aqueous HCl.	[206]

Table 4: Heterogeneous catalysts used for the hydrothermal liquefaction of model compounds or biomass

Model compounds/ Real biomass	**Operating conditions**	**Reactor/device/ tubing**	**Catalysts (with/without support)**	**Key findings/remarks/ observations**	**Ref.**
Dunaliella tertiolecta	320 ˚C	Autoclave	Co/CNTs	95.78% conversion was achieved along with a bio-oil yield of 40.25 wt % . The catalyst produced bio-oil with low O/C ratios.	[220]
Sorghum	300-350 ˚C	Tubular	Ni_2P, Ni/Si-Al, zeolite	Ni/Si-Al performed better than all catalysts tested. The resulting bio-crude yield was 45% at 300 ˚C.	[194]
Fruit bunch	390 ˚C	Inconel batch	CaO, MgO, MnO, ZnO, NiO, SnO, CeO_2, Al_2O_3	Catalysts, namely CaO, La_2O_3, MnO, and CeO_2, yielded highest bio-oil yield (about 1.40 times without catalyst).	[212]
Rice husk	300 ˚C	Micro-reactor	La_2O_3, Dy_2O_3	La_2O_3 produced the highest bio-crude yield of 32.5 wt% at a water/rice husk mass ratio of 5. The highest HHV (31.78 MJ kg^{-1}) of bio-crude was also obtained. The catalyst reduced the amount of phenols and acids and promoted hydrocarbon formation.	[213]

Bagasse	200-330 ˚C	Autoclave	$MgMnO_2$	At optimized conditions (250 ˚C for 15 min), the catalyst liquefied 93.7% biomass. The catalyst showed good recyclability. The increased OH concentration due to thermal hydrolysis of the catalyst improved biomass liquefaction.	[214]
Coconut shell	240-330 ˚C	Batch	$ZnCl_2$, $CuCl_2$, and $NiCl_2$	The highest yield of 13.9 wt% of bio-oil was reported. The catalytic effect of the transition metal on cellulose decomposition was observed.	[226]
Microalgae	210-250 ˚C; 20 MPa	Batch	Ni/SiO_2	The catalyst improved the yield of bio-oil. The highest bio-oil yield of 30 wt% was reached at 250 ˚C.	[215]
Grassland perennials	300 - 450 °C	Parr high-pressure vessel	SO_4^{2-}/ZrO_2–Al_2O_3, solid alkali CaO–ZrO_2	At a heating rate of 140 °C/min, a liquid yield of 82.1% was reported for 1 min at 374 °C. Particle size and catalysts had little influence on liquid yield. The liquefaction process	[158]

				with a fast heating rate shored more potential.	
Stearic acid	400 °C, 25 MPa	bomb type	ZrO_2, CeO_2, Y_2O_3	Catalysts enhanced decarboxylation of C_{17}-acid into CO_2 and C_{16} alkene.	[211]
Distillers grains	350 °C, 25 MPa	Stop-flow	ZrO_2	No major effect of either catalyst or reactor wall was observed on bio-oil yield or quality. ZrO_2 acted as a poor catalyst for HTL.	[209]
Waste	330 °C, 25 MPa	Continuous (loop)	ZrO_2, K_2CO_3	A high calorific value bio-oil was obtained. A BET surface area (32.7 m^2/g) of ZrO_2 was used	[210]

Table 5: Experiments in the hydrothermal gasification of model compounds or biomass without catalysts

Model compounds/ Real biomass	**Operating conditions**	**Reactor/device/ tubing**	**Key findings/remarks/ observations**	**Ref.**
Glucose, fructose	300 - 400 °C, 25 - 40 MPa	Continuous	The decomposition of glucose produced fructose (isomerization), 1,6-anhydroglucose (dehydration), and erythrose and glyceraldehyde (C-C bond splitting). Fructose didn't form 1,6-anhydroglucose and showed no isomerization into glucose. The proposed mechanism for products involved C-C bond cleavage by reverse aldol condensation and Lobry de Bruyn Alberda van Ekenstein transformation.	[258]
Glucose	600 - 767 °C, 25 MPa	Continuous tubular	At 1.8 wt % glucose, a H_2 yield of 11.5 mol/mol glucose was reported. High CE (91 %) and low TOC (23 ppm) indicated complete conversion of glucose into gaseous products, which was attributed to the enhanced water-gas shift reaction and flow stability.	[259]
Glucose	175 - 400 °C, 25 MPa	Continuous	Decomposition kinetics studies showed that the reaction order fell from 1.0 at 448 K to around 0.7 at 673 K. This was attributed to a shift of reaction from an ionic mechanism to a radicalic one.	[260]

Wheat straw, walnut shell and almond shell	420-440 ˚C, 25 MPa	Batch	Wheat straw showed the highest hydrogen gasification (23%) and carbon gasification (44.92%) efficiencies. With an increase in reaction time, the gasification efficiencies increased. Total gas yield increased up to 30 min and remained constant thereafter.	[261]
Fruit wastes, Agro wastes	400-600 ˚C, 15-45 min	Tubular batch	Temperature was the dominant factor in the gasification of biomass. A longer reaction time improved thermal cracking reactions. At 45 min, H_2 yield was 0.91 mmol g^{-1} compared to 0.69 mmol g^{-1} at 15 min.	[262]
Wood residues	500-600 ˚C, 20-42.5 MPa	Autoclave	Biomass with lower lignin and higher extractives produced more gaseous products. With increased pressure, carbon gasification efficiency reduced.	[263]
Ulva macroalgae	400-550 ˚C; 25 MPa	Batch	A short residence time (7 min) was sufficient for a suitable conversion rate. At 550 ˚C, H_2, and CH_4 exceeded 15 mol%.	[264]
N-hexadecane	525-605 ˚C; 15-22 MPa	Tubular	With an increase in temperature, yields of H_2 and CO_2 improved, suggesting an improved water gas shift reaction. A reduction in pressure improved the yields of gaseous products.	[265]

Beet-based distillery wastewater	300-375 ˚C	Batch	After 45 min of reaction time, the H_2 mole fraction reached 48.8% at 375 ˚C. At a longer reaction time, the water-gas shift reaction reaches equilibrium, indicating a gradual increase in H_2 along with a moderate reduction in CO and CO_2 fractions.	[266]
Phenol and alanine	400 ˚C; 22-26 MPa	Batch	With 60 wt% alanine, the highest H_2 yield was reported. The reaction mechanism involved the decomposition of alanine to aldehyde, acids, and gases. The aldehyde and phenol condensed to form phenolic resin tar.	[267]
Marine biomass	300-600 ˚C	Batch	With biomass loading of 0.08 g ml^{-1}, corresponding H_2 and CH_4 yields were 10.37 mol kg^{-1} and 6.34 mol kg^{-1} at 600 ˚C. An increase in temperature and decrease in biomass loading improved gasification yield.	[268]

Table 6: Homogeneous catalyst use for the hydrothermal gasification of model compounds or biomass

Model compounds / biomass	**Operating conditions**	**Reactor/device /tubing**	**Catalysts (with/without support)**	**Key findings/remarks/observations**	**Ref.**
Humic acid	375- 600 ˚C, ~24 MPa	Fixed-bed batch	K_2CO_3	The catalyst increased the gas yield to 1.64 mol kg^{-1}. However, the H_2 yield decreased more than it did without	[284]

				catalytic SCWG.	
Timothy grass	450-650 ˚C; 23-25 MPa	Tubular	KOH, K_2CO_3, NaOH	KOH acted as the best catalyst in increasing H_2 and CO yield via the water-gas shift reaction. The yield of 8.91 mol kg^{-1} was obtained.	[273]
Wood and char products from pyrolysis	450 ˚C, 27 MPa	Batch	K_2CO_3	K_2CO_3 increased the yield of H_2 through the water-gas shift reaction.	[285]
Cellulose, Lignin alkali	300-600 ˚C	Batch	K_2CO_3	At 600 ˚C, maximum yields of H_2 and CH_4 were obtained in the presence of a catalyst. The catalyst promoted gasification and prevented char formation.	[246]
Xylose	600 ˚C, 42.5 MPa	Batch	K_2CO_3	The catalyst improved the carbon gasification efficiency (86%) at 600 ˚C and 20 MPa. Maximum H_2 and CO_2 yields were obtained using a catalyst.	[274]
Lignin, Cellulose, Waste biomass	650 ˚C, 26 MPa	Batch	K_2CO_3	A high temperature (~650 ˚C) and catalyst loading (~100%) resulted in a high H_2 yield.	[275]
Horse manure	400-600 ˚C, 23-25 MPa	Tubular batch	Na_2CO_3, K_2CO_3, NaOH	A high H_2 yield was observed at 600 ˚C after 45 min. A H_2 yield with a 2 wt% catalyst followed the order: $Na_2CO_3>K_2CO_3>NaOH$.	[276]
Paper waste sludge	450 ˚C	Batch	K_2CO_3	The catalyst resulted in a H_2 yield of 7.5 mol kg^{-1} through the water-gas shift reaction. It also enhanced H_2 and CO_2 production, while not affecting CH_4 much.	[277]

Mannose	700 ˚C, 20 MPa	Batch	K_2CO_3	The catalyst improved the H_2 yield to 10.34 mol mol^{-1} from mannose. Acetic acid was the main component in the aqueous phase during gasification.	[278]
Lactose	550-700 ˚C; 22.5 MPa	Continuous	NaOH, KOH, Na_2CO_3	Catalysts inhibited char formation and promoted H_2 at low temperatures. The main gases produced were H_2 and CO_2.	[279]
Phenol	400-600 ˚C, 20-42.5 MPa	Batch	K_2CO_3	The catalyst, at high temperature s, enhanced gasification. The reaction produced a CH_4-rich gas along with CO_2, H_2, and CO.	[280]
Pyrocatechol	500 °C, 25 MPa	Tumbling and tubular	KOH	At 600 °C (2 min) or 700 °C (1 min), 99 % of the feedstock was gasified.	[43]
cotton stalk; corncob; tannery waste	500 °C, 3 °C/min	autoclave	K_2CO_3, Trona, red mud	The catalyst improved in the H_2 yield through an accelerated water-gas shift reaction and the methane reformation. Fe-based catalysts show potential for gasification.	[269]
Para-formaldehyde	400 °C	bomb	NaOH	The primary reactions were the Cannizzaro reaction and the self-decomposition of HCHO. The Cannizzaro reaction dominated with increased OH^- in the homogeneous phase.	[270]
Wastewater (organics)	450 - 550 °C, 25 MPa	Continuous	KOH	Maximum H_2 generation was achieved by accelerating the water-gas shift reaction rate. The H_2 amount in the gas phase increased with oxidants in a limited range due to the competing oxidation and gasification reactions.	[271]

n-hexadecane (*n*-C_{16}) and organosolv-lignin	273 °C, 30 - 40 MPa	bomb	NaOH	The catalyst showed no effect on the conversion of *n*-C_{16} and promoted the formation of 1-alkenes and H_2. The H_2 yield with NaOH was almost four times higher than that without a catalyst (with and without O_2).	[272]
Rosa Damascena residues	500 - 600 °C, 35 - 45 MPa	batch	K_2CO_3, Trona	The gaseous products consisted mostly of H_2, CO_2, and CH_4. Total yields of combustible gases were more than the CO_2 yield. Aqueous gasification products had carboxylic acids as the main component. High temperatures increased total gaseous yields but decreased aqueous products. Conversions amounting to 90% gaseous and 8% aqueous at 600 °C were reported.	[281]
Cauliflower residue, acorn, tomatoes residue, extracted acorn and hazelnut shell	600 °C, 35 MPa	Continuous	K_2CO_3, Trona	The catalyst resulted in a mixture of gases like H_2, CO_2, CH_4, CO, and a small amount of C_2 compounds. The H_2 yield (mol gas/kg C in feed) of acorn was 7 times more in the presence of Trona (53.5 mol H_2/kg C in feed) than that without catalyst. The use of Trona was realized as a more economical catalyst than commercial ones.	[282]
glucose	500 °C	batch	NaOH	An increase in H_2 yields of 135% with NaOH vs. non-catalytic process at a water-biomass ratio of 3.	[288]
Dewatered sewage sludge	400 °C, ~ 22.1 MP	batch	NaOH	NaOH not only promoted the water-gas shift reaction but also captured CO_2, driving the reaction with Ni	[289]

	a			catalyst towards more H_2.	
Acetic acid; phenol	600 °C, 40 MPa	tubular flow	NaOH	H_2 and CO_2 yields were highest at a 0.2 wt. % of NaOH; this can be attributed to the hydrogenation of phenol to benzene to cyclohexane.	[290]
Organics	600 -700 °C, 12 - 105 MPa	Micro-autoclave	NaOH	The process involved a novel H_2 generation method (HyPr-RING). A higher temperature and pressure increased H_2 yield, although the effect of temperature was greater.	[291]
Glucose; Molasses; rice bran	330 - 390 °C	---	NaOH	NaOH improved H_2 yield during the water-gas shift reaction by inhibiting tar/oil and char and promoting CO-intermediate compounds. H_2 yield increased with reaction temperature and time.	[292]
Glucose	200 °C, 2 MPa to 450 °C, 34 MPa	Batch	NaOH	Half the optimum H_2 gas yield was achieved at 350 °C and 21.5 MPa, and > 80 % (v) H_2 gas at 450 °C and 34 MPa. Apart from H_2, methane constituted (≥10 % (v)). The H_2 generation rate followed the order: glucose > cellulose, starch, rice straw > potato > rice husk.	[293]
Organosolv lignin	400 °C, 30 MPa	Batch type bomb	NaOH	The H_2 yield was four times higher than without catalysts due to partial oxidation and decomposition of lignin to H_2.	[294]
hard-shell nut residues	300 - 600 °C, 8.8 - 40.5 MPa	batch	Trona, dolomite, borax	Gaseous product (wt. %), H_2, and CH_4 yields followed the order: almond shell > walnut shell > hazelnut shell. Activities were in order: trona > borax > dolomite. The aqueous phase	[297]

	contained acetic acid for all biomass types and exhibited the highest yield with walnut shells.	

Table 7: Heterogeneous catalysts used for the hydrothermal gasification of model compounds or biomass

Model compounds /biomass	**Operating conditions**	**Reactor/ device /tubing**	**Catalysts (with/without support)**	**Key findings/remarks/observations**	**Ref.**
Glucose	750 ˚C, 30 MPa	Batch	Ni/Zr (Ce,Y) $O_{2-\delta}$	The highest H_2 yield of 22 mol kg^{-1} was obtained. The catalyst provided hydrothermal stability and had anti-carbon deposition properties. The addition of CeO_2 improved gasification efficiency.	[316]
Glucose	450-700 ˚C,	Parr type stirred vessel	Ni/MgO, Ni/ZnO, Ni/Al_2O_3, Ni/TiO_2	Ni/MgO had a superior effect on the gasification efficiency, attributed to the enhancement of the water-gas shift reaction.	[305]
Biocrude	500-700 ˚C	Continuous tubular	Dual metal (Ni, Ru)-dual support (Al_2O_3, ZrO_2)	The highest carbon gasification efficiency (92%) was obtained. High temperatures favored H_2 yield while high concentrations resulted in higher CH_4.	[359]

Plastics	450 ˚C, 10-38 MPa	Batch	RuO_2	20 wt% RuO_2 resulted in a carbon gasification efficiency of 99 wt% and a hydrogen gasification efficiency of over 100% . In the presence of the catalyst, the water-gas shift reaction and steam reforming occurred simultaneously.	[331]
Pine wood, wheat straw	300-500 ˚C, 23-25 MPa	Tubular batch	Ni	The catalyst accelerated methanation and water-gas shift reactions. The lower biomass concentration was easily hydrolyzable.	[306]
Glucose	500 ˚C, ~ 27.5 MPa	Continuous flow tubular	Ni Ru/γ-Al_2O_3	At 500 ˚C, the catalyst produced the maximum H_2 (0.68 mol mol^{-1} carbon-fed) and highest gasification efficiency (> 0.98 mol mol^{-1}). The catalyst showed good activity and stability.	[341]
Microalgae	385 ˚C, 26 MPa	Batch	Raney Ni, Nickel/α-alumina	The catalyst improved the yield asymptotically (80-90%) over time. The main gas products obtained followed the order: $CH_4 > CO_2 > H_2 > CO$	[342]
Valine	500-710 ˚C; 28 MPa	Fixed-bed	AC, Ni–Y/AC, Ni–Pt/AC, and Ni–Pd/AC	Ni-Y/AC achieved a carbon gasification efficiency of 98.1% at 600 ˚C, and the total gas yield increased with temperature. The catalyst disintegrated amines in the effluent.	[343]
Sugarcane bagasse	360 ˚C; 18 MPa	Micro-reactor	Cu with γ-Al_2O_3-MgO	The unpromoted catalyst resulted in the highest yields of H_2 (10 mmol g^{-1} of biomass) and	[354]

				gas (41 mmol g^{-1}).	
Glucose	400 °C		Ni/activated carbon (AC), Ni/MgO, $Ni/CeO_2/Al_2O_3$, Ni/Al_2O_3	An 81 % H_2 yield was reported with Ni/activated carbon (AC), 62% with Ni/MgO, 60% with $Ni/CeO_2/Al_2O_3$ and 52% with Ni/Al_2O_3. H_2 yield increased by 6.9% with AC and 36.9% with Ni/AC.	[288]
Glucose	500 °C, 30 MPa	autoclave	Raney nickel and K_2CO_3	Gaseous products were H_2, CO_2, CH_4, and C_2H_6. H_2 yield doubled with K_2CO_3. Ni improved CH_4 yield.	[295]
Corn, potato starch gels and wood sawdust	710 °C	Hastelloy C-276 tubing	Coconut shell AC	Gases like H_2, CO_2, CH_4, CO, and a little C_2H_6 were obtained Gas yield (>2 L/g) with 57 mol % H_2 was reported at the highest temperature.	[298]
Corn starch	650 °C, 28 MPa	Hastelloy C-276 tubing	Coconut shell AC	Gases such as H_2, CO_2, and CH_4 with little CO resulted from the reaction. The catalyst remained active over a 6 h period.	[299]
Chicken manure	700 ˚C 30 MPa	Fluidized bed	Activated carbon	The catalyst improved the H_2 yield of 25.2 mol kg^{-1} at 600 ˚C. The catalyst increased the carbon gasification efficiency at low temperatures.	[300]
Glycerol, glucose and cellobiose	600 °C, 34.5 MPa	Inconel 625 tubing	Spruce wood charcoal, macadamia shell charcoal,	Complete conversion of glucose (22% by wt. in water) to H_2 achieved at a weight hourly space velocity (WHSV) of 22.2 h^{-1}. The carbon catalyst was deactivated after < 4 h without	[41]

			coal activated carbon, and coconut shell AC	swirl in the entrance region of the reactor.	
Microcrystalline cellulose and organosolv lignin	400 - 600 °C	Quartz	Ni, Fe, Cu, Zn, Zirconium wires, ruthenium powder, and Raney nickel slurry	Exhibited highest H_2 yields (16.0 mmol/g) from Ni (surface area/biomass weight ratio of 240 mm^2/mg); H atom content in the product gas stream was 70%, with > 60% of C atoms gasified.	[304]
Cellulose and glucose	325 °C	batch	Ni	The maximum CH_4 yield of 73.8% was achieved in the presence of 0.1 mol of Zn and 1.0 g of porous Ni catalyst with at 325 °C for 2 h. A porous Ni catalyst was effective for the conversion of glucose into CH_4. Acetoin, hydroxyl-2-propanone, and 1,2-ethanediol acted as liquid intermediates for the formation of CH_4 during the reaction.	[309]
Glucose	350 - 410 °C	Batch	α-Al_2O_3, carbon nanotube (CNT), and MgO supports,	Highest carbon conversion was achieved from from α-Al_2O_3, carbon nanotube (CNT), and MgO supports; modest activities from SiO_2, Y_2O_3, hydrotalcite, YSZ, and TiO_2; and no activities	[310]

			SiO_2, Y_2O_3, hydrotalcite, yttria-stabilized zirconia (YSZ), and TiO_2	from zeolites were observed. The maximum hydrogen selectivity with 20% Ni/α-Al_2O_3 at 380 °C was found.	
Ethylene glycol	450 °C, 25 MPa	Continuous	Al_2O_3 supported Pt and Pt–Ni	Methanol, ethanol, and acetic acid were the main liquid by-products. The deactivation of Pt and Pt–Ni catalysts occurred due to the hydroxylation of the Al_2O_3 surface by acetic acid.	[311]
Glycerol	450 - 575 °C, 25 MPa	Inconel-625	Ni supported La_2O_3, α-Al_2O_3, γ-Al_2O_3, ZrO_2, and YSZ	Ni/YSZ was found to be effective for gasification but caused higher methanation. The maximum H_2 yield from Ni/La_2O_3 was reported. Reactions with moderate space velocities ($WHSV = 6.45\ h^{-1}$) and 5 % glycerol showed higher hydrogen selectivity and yield.	[312]
Sugarcane bagasse	400 °C	batch	Ni/CNTs and Ni–Cu/CNTs	The high internal surface of CNTs had a noticeable effect. Ni/CNT nanocatalysts improved the hydrogen yield by a factor of 5.84. The promoted Ni/CNT with 7.5 wt. % copper had 25.9 % reduction in CH_4.	[313]
Polyethylen	390 °C,	Inconel	Ni/ZrO_2	Gas yield and CGE increased	[314]

e glycol contaminated wastewater	24 MPa	625		with Ni loadings but decreased with PEG concentration.	
Glucose, organic waste and sludge hydrothermal liquefaction process	600 - 750 °C, 24 MPa	bench-scale continuous down-flow tubular	RuNi/γ-Al_2O_3 or RuNi/activated carbon (AC)	An γ- Al_2O_3-supported Ni catalyst was found to be effective in catalyzing the SCWG of a simulated aqueous waste feedstock. However, the catalyst showed deactivation during the SCWG of real waste. An AC-based catalyst exhibited higher stability and activity in the SCWG of real waste.	[315]
Composite refuse derived fuel (RDF)	650 ˚C, 45 MPa	Hastelloy	RuO_2/γ-Al_2O_3	The presence of a catalyst improved carbon gasification efficiency up to 99 wt%. In addition, H_2 and CH_4 yields increased.	[330]
Macroalgae	440 ˚C, 25 MPa	Batch microreactor	Fe-Ni-Ru/γ-Al_2O_3	The highest H_2 yield of 12.28 mmol g^{-1} was obtained with a 2 wt% catalyst. Hydrogen selectivity was 0.74.	[339]
Glucose	500 ˚C	Quartz capillaries (batch)	Ru/Al_2O_3	With a catalyst, the gas yield improved with longer reaction time. Phenols and arenes were found to be stable in supercritical water and thus showed little decomposition. The catalyst inhibited char formation.	[340]
Sugarcane bagasse	400 ˚C, 24 MPa	Batch micro-	γ-Al_2O_3 with	With increased Cu loading, CO, CO_2 and H_2 increased. However,	[352]

		reactor	Cu	the addition of potassium reduced gas yield. A catalyst with 20% Cu and 2.5% potassium on alumina was reported to be highly selective.	
Alkali lignin	400-600 ˚C	Batch	Ru/C	Higher temperature, longer reaction time, higher water density, and lower reactant concentration favored biomass gasification. A gasification efficiency and carbon conversion efficiency of 73.74 % and 56.34% were achieved.	[308]
Wood	300 - 410 °C, 12 - 34 MPa	Batch	Raney Nickel	The highest CH_4 yield of 0.33 g/g wood was observed. Complete gasification was achieved after 90 min.	[319]
Organosolv-lignin	400 °C, 37.1 MPa	tube bomb	Ru/TiO_2, Ru/C, $Ru/\gamma\text{-}Al_2O_3$	Ru/TiO_2 showed stable activities; Ru/C exhibited high lignin gasification; $Ru/\gamma\text{-}Al_2O_3$ lost its activity despite having higher activity initially.	[325]
Organosolv-lignin	250 - 400 °C	Tube bomb	Ru/TiO_2	Ru resulted in high CH_4 yield with no solid product; there was a rapid degradation of formaldehyde into gases such as CH_4, CO_2, and H_2.	[328]
Cellulose and sawdust	500 °C, 27 MPa	autoclave	Ru/C, Pd/C, CeO_2 particles, nano-CeO_2 and nano-$(CeZr)_xO_2$	The treatment of 10 wt.% cellulose or sawdust with CMC in the presence of Ru/C yielded 2-4 g H_2 and 11-15 g H_2/100 g feedstock.	[333]

Glucose	600 °C, 24 MPa	Continuous-flow tubular	(Ni, Ru, Cu and Co) and promoters (e.g., Na, K, Mg, or Ru) supported on(γ-Al_2O_3, ZrO_2, and AC)	A H_2 yield of 38.4 mol/kg glucose was obtained with Ni20/γ-Al_2O_3 (γ-Al_2O_3 with 20 wt% Ni); Mg and Ru were the effective promoters of the Ni/γ-Al_2O_3 catalyst and reduced deposits of coke and tar during reaction.	[335]
Glucose	650 °C, 28 MPa	Tubular flow	Ni/AC, Ni–Y/AC, Ni–Fe/AC and Ni–Co/AC	A Ni–Y/AC catalyst showed high gasification performance among the catalysts studied. Fe and Co loading into the Ni/AC did not improve H_2 yield; Y loading into the Ni/AC was presumed to prevent coke formation.	[337]
Glucose and cellulose	400 - 440 °C, 30 - 35 MPa	Batch	ZrO_2	Hydrogen yield almost doubled with the addition of ZrO_2.	[349]
Glucose, cellulose, heterocyclic compounds, paper sludge and sewage sludge	400 °C, ~30 MPa and 500°C, ~50 MPa	Inconel 625	RuO_2	Gases such as H_2, CH_4, and CO_2; were obtained. RuO_2 was not affected by nitrogen compounds; carbazole was gasified completely.	[350]
Cellulose, xylan and lignin	400 °C, 25 MPa	Batch	Ni	A decrease in gas production was observed from lignin mixtures; H_2 yield dropped from	[44]

				the reaction of cellulose intermediates with lignin	
Glycerol	700 - 800 °C	Tubular fixed-bed	Ru/Al_2O_3	A near-theoretical yield of 7 mol of H_2 was observed.	[307]
Microalgae	400 ˚C, 28 MPa	Continuous	Ru/C	A good catalytic activity persisted over 55 hours, after which sulphur poisoning deactivated the catalyst.	[347]
Industrial waste streams	300-375 ˚C	Batch	MnO_2, CuO and Co_3O_4	The catalytic activity followed the order: $Co_3O_4 > CuO > MnO_2$. High temperature (375 ˚C) and longer reaction time (45 min) favored H_2 production.	[351]
Fruit pulp	400-600 ˚C	Batch	Ru/C	With a biomass ratio of 2.5%, the highest H_2 yield was 54.8 mol kg^{-1} biomass. The gasification efficiency was 150.8 %.	[338]
Phenol water	350 ˚C, 20 MPa		Ni ($Ni/C/Al_2O_3$)	There was no deactivation of catalysts at 2 g L^{-1} of phenol concentration. Catalyst activity improved with time and the conversion of phenol reached 100%.	[344]
Black liquor	350-450 ˚C, 25 MPa	Batch	CeO_2	The catalyst decreased the production of carbonaceous solids; however, the H_2 yield was largely unaffected, as the catalyst was mainly involved in hydrogenation reactions.	[353]
Furfural	200-400 ˚C, 23-25	Batch	Cu+Zn, Co+Ni, Cu+Ni	Two elements with different combinations showed improved gasification efficiency compared	[358]

MPa	Zn+Ni	to single metal catalysts.

Table 8: Application of material from HTC in energy storage, conversion, and fuel cells

odel compounds/ Biomass	Applications	Ref.
lly pine wood chips	continuous HTC process through the fast HTC reactor with a retention time of 20-30 s. Hydrochar showed high energy densification and pelletization characteristics. At 290 ˚C, hydrochar yield was 85% based on dry feedstock.	
se from land plant (Grindelia)	erformed on plant after biocrude was extracted and hydrochars were pelletized. The HHV increased by up to 26 MJ kg^{-1} at 260 ˚C.	
y biomass and agro-residues	char pellets showed high mechanical strength and their moisture content decreased to < 2%. Pellets had increased mechanical durability and combustion characteristics, suggesting their suitability as solid fuels.	
a rhizome	ss hydrochar at 200 ˚C showed thermal characteristics similar to a low-rank coal with an HHV of 23.7 MJ kg^{-1}, suggesting its potential as a renewable fuel.	
o	mbustion characteristics of biomass increased along with its HHV. At 260 ˚C, the HHV increased from 17.1 MJ kg^{-1} (raw biomass) to 20.3 MJ kg^{-1}.	
ed husk	wave-assisted HTC resulted in a hydrochar HHV of 21.57 MJ kg^{-1}, suggesting its potential application as a solid fuel.	
l	HV from hydrochar produced from the HTC of bio-oil was 4.35-5.29 times higher than the initial feed, signifying a new approach to remove unstable components of bio-oil through the production of high energy-rich hydrochars.	
	dition of acetic acid as a catalyst improved the HTC reaction rates, thereby increasing the HHV of hydrochar to 20.2 MJ kg^{-1} on average. Other catalysts studied with this biomass	

	were borax and zeolite.	
yptus bark	er temperature improved the HTC of biomass, resulting in hydrochar with high fixed carbon and HHV as well as improved thermal stability. The HHV values for hydrochar lay in the range of 27-28.2 MJ kg^{-1}, showing potential for solid fuel application.	
stalk	stalk was transformed into hydrochar at a reaction severity of 5.05-8.29. As it increased to 7.11, the hydrochar had properties similar to those of coal. The hydrochar yield ranged from 71% to 36%.	
ose, xylan, lignin	ptimum temperature for greatest energy efficiency was 220 ˚C. Cellulose and hemicellulose had a significant impact on the properties of solid fuel. An increase in carbon contents and fixed carbon was reported following hydrothermal carbonization. The calculated calorific values of hydrochar were 23-26 MJ kg^{-1} at 220 ˚C.	
	acid was an effective catalyst for this biomass. Hydrothermal carbonization of mixtures of sewage, acetic acid, and cassava pulp had energy contents of 28.5 MJ kg^{-1}, which are comparable to natural coals, showing potential to use these mixtures as a fuel for combustion.	
residue	arbon content of hydrochar obtained had energy densification ratios of 1-1.5 and energy yields of 60-100%. At higher temperatures, solid yield dropped to ~40 %.	
ose, potato starch, and eucalyptus wood sawdust	d good capacitance retention ability (175 F/g).	
ose	anospheres were employed as anodes in Li^+ and Na^+ batteries	78]
ose	material was prepared by hydrothermal carbonization and the resulting PtRu/C anode electrocatalysts showed high performance for DMFC as opposed to Vulcan XC72 carbon.	

Glucose	Glucose in situ hydrothermal carbonization from carbon riveted PtRu/C catalyst showed application in methanol fuel cells.
ed sludge	Exhibited potential for solid fuel due to increased C and FC (fixed carbon) content. Reduced C-O and aliphatic C-H with an increase in aromatic C-H from CH_x functional group were observed.
e sludge	ing solid fuel showed higher FC and lower volatile matter, hydrochars with a fuel ratio up to 0.18, and HHVs of 0.98–1.03. The removal of 60% of the nitrogen and sulfur resulted in a cleaner fuel.
liquor	ved yield, HHV, C recovery, and total energy recovery efficiency of solid fuel at 265 °C.
an	ile carboxylated chitosan hydrothermal process resulted in N-doped carbon-coated $CoSnO_3$ composites with improved lithium storage properties and a reversible capacity of 650 mAh g^{-1} even after 50 cycles.
algae (*S. Platensis*) and glucose mixtures	sized microporous N-doped carbon materials (areas up to ~2200 m^2 g^{-1}) based on HTC and chemical activation processes. While working with neutral LiCl electrolyte, the porous carbons produced at 700–750 °C showed retention of 80% of the capacitance at a current density of 20 A g^{-1}.
ercial sugar	n microspheres (5–10 µm diameter) and uniform nanopores were synthesized by HTC-assisted microwave together with KOH activation. This process resulted in a superior specific capacitance (about 179.2 F/g) at a current density of 1 A/g and cycling performance over 1000 charging/discharging cycles with a KOH/C of 1:1 and a microwave irradiation level of 70%.
trafluoroethene waste	O_3-assisted template carbonization method was developed as a means of disposing PTFE waste and the resulting nanoporous carbon materials showed the potential for super capacitor application.

glucose	ical double layer capacitors were formed from the 1-ethyl-3-methylimidazolium tetrafluoroborate and carbon electrodes; they showed ideal polarizability ($\Delta V \leq 3.2$ V), a short charging/discharging time constant (2.7 s), and a high specific series capacitance (158 F g^{-1}).
se	phene/AC nanosheet composite was obtained by HTC together with KOH treatment. Nanosheet had specific capacitance of 210 F g^{-1} in aqueous electrolytes and 103 F g^{-1} in organic electrolytes.
ut shells	Nanoporous carbons behaved as anode materials for lithium ion batteries; the best cycling performance in Li cells was reported by HC-MA formed by MgO templating of hydrochar.